BOTSWANA UNIVERSITY OF AGRICULTURE AND NATURAL RESOURCES

DEPARTMENT OF AGRICULTURAL AND BIO-SYSTEMS ENGINEERING

WILDFIRE PREDICTION AND MONITORING IN THE RANGELAND AREAS OF BOTSWANA: A CASE STUDY OF KGALAGADI DISTRICT.

By

Issa Kaduyu

Student ID**: 202000794**

Main Supervisor**: Prof. R. Tsheko**

Co-Supervisors:

Prof. J.H Chepete

Ms. E. Kgosiesele

A Research Dissertation submitted to the Department of Agricultural and Bio-systems Engineering of the Botswana University of Agriculture and Natural Resources in Partial Fulfilment of the Award of a Master of Science Degree in Agricultural Engineering (LUP)

January 2023

DECLARATION

I hereby declare that to the best of my knowledge, the information presented in this report titled "WILDFIRE PREDICTION AND MONITORING IN THE RANGELAND AREAS OF BOTSWANA: A CASE STUDY OF KGALAGADI DISTRICT" is my original work and has not been presented for an academic award in any institution.

_____	_____	___/___/____
Author's Name	**Signature**	**Date**

APPROVAL

_____	_____	___/___/____
Main Supervisor's Name	**Signature**	**Date**
_____	_____	___/___/____
Co-supervisor's Name	**Signature**	**Date**
_____	_____	___/___/____
Co- supervisor's Name	**Signature**	**Date**
_____	_____	___/___/____
Head of Department's Name	**Signature**	**Date**
_____	_____	___/___/____
Faculty Dean's Name	**Signature**	**Date**

DEDICATION

I dedicate this piece of work to myself, for not giving up amidst all.

ACKNOWLEDGEMENT

I extend my heartfelt gratitude to the supervisory committee, Prof R. Tsheko, Prof J.H. Chepete and Ms E Kgosiesele. I appreciate your unwavering support, advice, guidance, and dedication throughout the journey of my MSc dissertation development and writing. Thanks to Prof R. Tsheko, for enriching the overall content of my study proposal and dissertation through your critical comments and questions and. I want to thank Mr John Isaac Molefe, whose valuable feedback, input and reviews improved my dissertation.

I also want to acknowledge my scholarship sponsors, the European Union and African Union. for providing financial support by awarding me the Mobility of African Scholars for Transformative Engineering Training (MASTET) scholarship. The financial support allowed me to pursue my MSc at the Botswana University of Agriculture and Natural Resources (BUAN). I am also grateful to the MASTET coordinator, Prof C. Patrick, for his parental and scholarly guidance and coordination during my stay at BUAN.

Last but not least, I'd like to express my gratitude to Ms O.G Mpatane of the Department of Forestry and Range Resources of the Botswana Ministry of Environment, Natural Resources Conservation and Tourism for providing data and guidance during my study.

Finally, my thanks go to all the Staff of the Department of Agricultural & Biosystems Engineering (ABE) and the Faculty of Agriculture for their knowledge and diverse skills that helped me to complete my study work. I'd also like to thank my friends and family, who have been there for me emotionally and intellectually as I worked on my coursework and dissertation.

MAY GOD BLESS YOU ALL!

TABLE CONTENTS

LIST OF FIGURES

LIST OF TABLES

LIST OF EQUATIONS

ACRONYMS

AVHRR	-	Advanced Very High Resolution Radiometer
BT	-	Brightness Temperature
CCES	-	Centre of Climate and Energy Solutions
CFFDRS	-	Canadian Forest Fire Danger Rating System
DFMC	-	Dead Fuel Moisture Content
DFRR	-	Department of Forestry and Range Resources
DMP	-	Dry Matter Productivity
dNBR	-	differenced Normalised Burn Ratio
FBP	-	Fire Behaviour Prediction
FMC	-	Fuel Moisture Content
FMT	-	Fire Mapping Tool
GWIS	-	Global Wildfire Information System
IUFRO	-	International Union of Forest Research Organizations
LFMC	-	Live Fuel Moisture Content
LST	-	Land Surface Temperature
MDA	-	Mean Decrease Accuracy
MDG	-	Mean Decrease Gini
ML	-	Machine Learning
MODIS	-	Moderate Resolution Imaging Spectroradiometer
NBR	-	Normalised Burn Ratio
NDVI	-	Normalised Difference Vegetation Index
NFDRS	-	National Fire Danger Rating System
NFFL	-	Northern Forest Fire Laboratory
NOAA	-	National Oceanic and Atmospheric Administration
RdNBR	-	Relative Differenced Normalised Burn Ratio
RS	-	Remote Sensing
SM	-	Soil Moisture
SMAP	-	Soil Moisture Active Passive
SMOS	-	Soil Moisture and Ocean Salinity
VI	-	Vegetation index

VIIRS	-	Visible Infrared Imaging Radiometer Suite

ABSTRACT

Fire is a critical tool for managing rangeland ecosystems, particularly in the savannah. However, the increasing wildfire occurrence poses a considerable danger to rangeland ecosystem continuity. Burned area extent and fire severity have been mapped over the years using different methods. There is a need to avail tools and techniques to reliably and accurately map burned areas and fire severity early enough for improved management of fires and restoration of rangeland burned areas. Thus, predicting fire occurrence and mapping wildfire danger is critical in managing savannah rangelands. This study developed a random forest (RF) prediction model using observed fire occurrence points and selected environmental variables in Kgalagadi District, Botswana. A wildfire probability map was also developed using a Logistic regression model (LR) applied to best-performing variables. The study used 107,883 active fire points from Visible Infrared Imaging Radiometer Suite (VIIRS) sensors from 2015 to 2021 and randomly created non-fire points. A dataset of remotely sensed predictor variables was developed using ArcMap 10.7. These are Dry matter productivity (DMP), Soil moisture Content (SM), Land surface temperature (LST), Live Fuel Moisture content (LFMC), and Dead Fuel Moisture content (DMFC). The selected RF model with an Out of Bag (OOB) error of 9.91% had an overall accuracy of 90.15% for classifying fires and non-fires for the test dataset. Results show a Kappa coefficient of 0.803, with 88.25% producer accuracy and 91.76% user accuracy for classifying fires. The DMP was the most important variable (MDA= 1,055.20 and MDG= 9.328.62), followed by SM (MDA= 828.39 and MDG= 15,745). The LR model indicated a relatively weak but significant ability to discriminate fires from non-fire points with an overall accuracy of 56.05% and an Area Under the Curve (AUC) of 56.05%. A probability map produced using the LR model indicates that more than 39.11% of the study area had a high and very high chance of fire ignition before the 2021 Kgalagadi Mega fire.

In this study, the burned area was estimated, and also fire severity assessed for the 2021 fires in the Kgalagadi District using the Monitoring Trends in Burn Severity (MTBS) Fire Mapping Tool (FMT) from Landsat 8 Operational Land Imager data. The burn area perimeter was delineated using the FMT tool and compared to aggregated Visible Infrared Imaging Radiometer Suite (VIIRS) active fires. Severity indices, including Normalized Burn Ratio (NBR), differenced NBR (dNBR), and Revitalised dNBR (RdNBR), were developed and assessed using sentinel-derived indices. The results from the FMT severity indices also showed significant ($P<0.05$)

agreement with the sentinel-generated indices. However, there was a slight variation in the severity thematic map when FMT threshold estimates were applied to sentinel dNBR values. Severity thematic maps indicated 39.7% and 35.1% low severity of the burn area extent for Landsat FMT and sentinel, respectively. Overall, results suggest that the 2021 Kgalagadi fire burned at Low burn severity. The results from this study demonstrated that FMT is a promising tool for rangeland wildfire and burn area management combined with existing burn area data. Therefore, field studies to measure severity thresholds are recommended to validate the burn area maps developed in this study.

CHAPTER 1: INTRODUCTION

1.1 Background

Wildfire outbreaks have become a significant occurrence globally, and their effects have caused large-scale environmental and economic losses (Brunson & Tanaka, 2011; Stavi, 2019; Wang & Zhang, 2020). Wildfires are estimated to affect over 400 million square kilometres of the Earth's surface each year, 50% of which occur in sub-Saharan Africa (ESA, 2021; Fayiah *et al*., 2021). Although a 24.3% decline in the global burned area has been reported between 1998 and 2015 (Andela *et al*., 2017), existing data show an increasing frequency and intensity of uncontrolled fire events resulting in adverse effects on livelihoods and human well-being, hydrology, soil, biodiversity, ecological services, and overall regional and national economies (Bowman *et al*., 2011). However, fire is an inherent feature of many global rangeland/grassland ecosystems particularly in the savannah, with several fauna species dependent on fire to extend their existence (Neary & Leonard, 2020). In fact, previous studies have indicated that the Savannah ecosystem of southern Africa owes its existence to fire (Ribeiro *et al*., 2019; Shekede *et al*., 2021; Smit *et al*., 2010). Although fire maintains ecosystem function, the extent, severity, and frequency of occurrence may result in negative effects such as deaths, damage to property, and loss of land value. In this regard, there is a need to evaluate the impacts of fire occurrence in space and time (IUFRO, 2018; Raiesi & Pejman, 2021).

The majority (75%) of the fires are anthropogenic, resulting from prescribed actions that go out of control or inappropriate use of fires by humans, while a significantly small number of fires result from lightning (IUFRO, 2018; Kimbrough, 2020). Fuel accumulation, especially in forested areas, has also been linked to increased fire occurrences (Gonsamo *et al*., 2017; Harden *et al*., 2000; Loehman *et al*., 2014; Stevens-Rumann *et al*., 2020). According to Loehman *et al*. (2014), the current climate variations are critical in controlling fuel accumulation and creating conditions that favour fire ignition. Climate change scenarios indicate hotter and drier fire seasons coupled with several environmental alterations as a result of population growth and inappropriate land management practices which are markedly contributing to the extreme wildfires experienced globally (Fayiah *et al*., 2021; IUFRO, 2018; Loehman *et al*., 2014; Maabong & Mphale, 2021).

The post-fire effects are often far-reaching and long-term despite the short-lived wildfire events. Ecological systems that experience profound wildfire effects may require extended periods to return to the pre-fire state (Turner, 2010). Although this is not the case for rangeland ecosystems,

the effect of fires can be direct or indirect, resulting in the loss of ecosystem services (Raiesi & Pejman, 2021). Direct/short-term fire effects in rangelands result from heating during the fire affecting the soil to a few centimetres (Girona-García *et al*., 2019; Snyman, 2015b). Indirect effects are often long-term, resulting from the loss of plant and litter biomass and alteration of the plant community structure and composition (Clark *et al*., 2016; Pereira *et al*., 2021; Snyman, 2015a). Several studies have reported the effect of wildfires on rangeland hydrology, vegetation structure, biodiversity and composition, soil quality, and climate (Clark *et al*., 2016; Fayiah *et al*., 2021; Girona-García *et al*., 2019; Hantson *et al*., 2015; Raiesi & Pejman, 2021; Stavi *et al*., 2017; Tacheba *et al*., 2009). Noteworthy, the impact of wildfires on rangelands depends on the fire intensity and other pre-fire conditions.

However, the prediction of fire occurrence, monitoring fire impacts, burned areas, and severities in sub-Saharan Africa remains relatively limited with only a handful of studies (D'Onofrio *et al*., 2020; Justino *et al*., 2013; Kahiu & Hanan, 2018; Yu *et al*., 2020) exploring wildfires in different environments. For example, Yu *et al*. (2020) applied the analytical framework of Stepwise Generalized Equilibrium Feedback Assessment (SGEFA) and machine learning techniques (MLTs) to assess the seasonal environmental drivers and predictability of African fires. The results of their study showed a skillful prediction of African fires using soil moisture, sea-surface temperature, and leaf area index that dominated the fire seasonal variability. D'Onofrio *et al*. (2020) assessed key ecological processes for a realistic representation of vegetation-climate-fire interactions using two state–of–the–art Dynamic global vegetation models (DGVMs) in sub-Saharan Africa. Results of the study indicate that the models perform well in simulating vegetation-fire feedback in open savannahs under varying precipitation conditions. Justino *et al*. (2013) applied the Potential Fire Index (PFI) to determine the environmental vulnerability to wildfire occurrence using climate anomalies and vegetation distribution. The study demonstrated that the PFI was able to reproduce critical fire risk areas under current climate and vegetation conditions in the Sahelian region and subtropical Africa regions. Kahiu & Hanan (2018) tested the relationship between aggregate fuel loads and partitioned woody and herbaceous fuel loads with fire activity in Sub-Saharan Africa (SSA) savannahs using the boosted regression tree analysis. Results of the study showed that herbaceous fuel load was consistently most influential with more explanatory power than overall biomass in fire activity. Although these studies highlight the relationships between climate, vegetation, and fire processes in African savannahs, no study attempts to develop an area-specific model and tool for wildfire prediction and burn area mapping. In

most studies, climate data is proposed for studying wildfires without considering the incosistance in meteorological data in many African countries. There remains insufficient wildfire data in developing countries, and many fire events in remote rangelands go undetected (Handmer *et al*., 2012). There is limited capacity to detect environmental occurrences and monitor disasters due to the little value attached to specific ecosystems (Handmer *et al*., 2012).

Nevertheless, there is overwhelming evidence that the intensity and frequency of wildfires in rangeland in arid areas may increase with escalating climate change effects. Several authors have attributed the increased wildfire in rangelands to climate change (Flannigan *et al*., 2009; Fox *et al*., 2017; Loehman *et al*., 2014; Mansoor *et al*., 2022). All other factors contributing to wildfires, including fuel, soil moisture, and temperature, are directly or indirectly linked to wildfire and Climate change (CCES, 2021). Abatzoglou & Williams (2016) estimated the contribution of anthropogenic climate change to the increase in fuel aridity and forest fire area across the western United States. The study revealed that anthropogenic climate change accounted for about 55% of observed increases in fuel aridity, underscoring both anthropogenic and natural climate variability as important contributors to the recent increase in wildfire risk. Liu & Wimberly (2016) assessed the effect of climate change and climate-driven vegetation change on future fire regimes. The study results revealed that climate-driven vegetation change can strongly affect fire occurrence and size resulting in the regional alteration of fire regimes. With the projected substantial effect of climate change on wildfire occurrence, frequency, and fire regimes, no single factor can give an accurate projection of fire risk. Therefore, various factors must be accurately assessed for their contribution to wildfire prediction and monitoring of wildfire impacts. However, only a few studies have incorporated such factors in wildfire prediction models (Bartsch *et al*., 2009; Chaparro, Vall-llossera, *et al*., 2016; Sungmin *et al*., 2020). Yet, integrating various fire-influencing factors in wildfire prediction models and tools is critical for achieving more accurate and reliable fire predictions

Several global, regional, and national studies have been conducted to predict wildfires using the different fire-driving factors. Many tools and models have been developed and are currently being used to predict wildfires, with the majority of the prediction methods based on fuel characteristics, especially fuel moisture content (FMC) (Arroyo *et al*., 2008; Dillon *et al*., 2015; Keane & Reeves, 2012; Srivas *et al*., 2017). Earlier models, including National Fire Danger Rating System (NFDRS), McArthur Forest Fire Danger Rating System, McArthur Grassland Fire Danger Rating System, the Canadian Forest Fire Danger Rating System (CFFDRS), and tools such as fire

behavior prediction and fuel modeling system (BEHAVE), Fire Area Simulator (FARSITE) were developed for wildfire prediction in North America, Australia and Canada (Finney, 1998; Lundgren *et al*., 1995; McArthur, 1967; Rothermel, 1972). Although these tools provide accurate fire risk maps for locations for which they are developed, the tools heavily depend on fuel information that is mapped using various fuel-based models. Therefore, to effectively utilize the tools, knowledge of existing fuel characteristics is needed (Chuvieco *et al*., 2004). Besides, significant variation in climate makes fuel characteristics complex, making them hard to map and describe (Keane *et al*., 2000). However, remotely sensed data provide a reliable alternative to mapping fuel characteristics even for remote locations that may be hard to access (Heisig *et al*., 2022; Keane *et al*., 2001). The recent increase in the availability of free satellite-based data has led to the development of remote-sensed tools and models for wildfire predictions (Arroyo *et al*., 2008; Chuvieco *et al*., 2020).

There is an increased effort to use remote sensing technology to predict, assess, and monitor wildfires, with several fire products being used in sub-Saharan Africa for wildfire monitoring (Flasse *et al*., 2004; Giglio *et al*., 2006; Williams *et al*., 2011). Remote sensing data from satellite missions such as Tera, Aqua, Landsat, SMOS, Sentinel, and Soil Moisture Active Passive (SMAP) is used in wildfire management (Hawbaker *et al*., 2017; Jia *et al*., 2019; Mondal *et al*., 2020; Pulvirenti *et al*., 2020). Despite the promising possibility of wildfire management using models and tools from remotely sensed data, few studies have been conducted in Africa (Kouassi *et al*., 2020; Moyo *et al*., 2020; Nhongo *et al*., 2019; Williams *et al*., 2011). These studies demonstrate how climate and environmental variables could be applied in fire prediction without considering fuel accumulation before fire season. For example, Verhegghen *et al*. (2016) demonstrated the potential use of Sentinel 2 and 1 supported with Moderate Resolution Imaging Spectroradiometer (MODIS) data to detect and map burned areas in Congo basin forests. In a similar study, Kouassi *et al*. (2020) developed a predictive model for wildfires in tropical west African savannah, while Nhongo *et al*. (2019) used logistic regression to model fire occurrences using Normalised Difference Vegetation Index (NDVI), climatic, topographic, and socioeconomic data of Niassa Reserve-Mozambique. Similarly, in Botswana, there has been an increased use of wildfire monitoring tools from earth-observing satellites such as MODIS. These satellites helped to monitor mega-fires, especially the Ghanzi fires, which have caused considerable economic losses and affected human livelihoods (Dube, 2013; Williams *et al*., 2011).

In recent years, the negative impact of wildfire in Botswana has been increasingly felt by communities, despite over BWP 40 million investment in wildfire management systems by Department of Forestry and Range Resources (DFRR). Large land expanses are being burnt annually, with 5,188,331 million hectares of land being burnt in 2021 alone (GWIS, 2022). According to the Botswana DFRR data, more than 80% of these fires occur in Kgalagadi, Ghanzi, and Ngamiland districts that house Botswana's rangelands, including the Central Kgalagadi Game Reserve causing substantial environmental, economic, and social impacts (DFRR, 2009). Most of the fires occurring in the rangelands could be put out before they become mega-fires (Maabong & Mphale, 2021); however, due to limited fire detection and early warning systems, most of these fires grow to become mega-fires.

Mega wildfire occurrences are common in Botswana, with an average of 1.8 million hectares being burnt annually between 2012 and 2021 (GWIS, 2022). There has been an overall increase in wildfire occurrences in the last decade (Figure 1), with the largest mega wildfire recorded in 2021, burning over 51,883 square kilometres of land (GWIS, 2022). Most wildfires occur between August and October when vegetation is dry in high temperatures and strong winds (Maabong & Mphale, 2021), causing considerable destruction of property and the environment. Therefore, it is evident that wildfire prediction and monitoring remain limited despite efforts to establish wildfire control measures countrywide. Moreover, drought-prone areas such as Kgalagadi are faced with increasing fire ignition probabilities, posing a great danger to humans, wildlife and livestock in the areas. The impacts of wildfires have been managed through community fire management plans to suppress fires, the use of prescribed fires, and legislation and law enforcement to prevent fires (Statistics Botswana, 2018b). In addition, fire breaks (strips of land cleared of inflammable matter to prevent the spread of fire) are increasingly being used in many parts of the country, with significant investment in fire control. The establishment of fire guards (firebreaks) in the country is legislated by the herbage preservation (fire prevention) Act of 1977 which provides for the establishment of herbage conservation committees and firebreaks between adjoining lands prone to fires (Government of Botswana, 1977). The Act also established guidelines for using prescribed fires by individuals to control wildfires (Government of Botswana, 1977). However, the program is constrained by limited funding resulting in less than 50% of the 10,000km firebreaks across the country being maintained by the DFRR for some financial years (Statistics Botswana, 2018b).

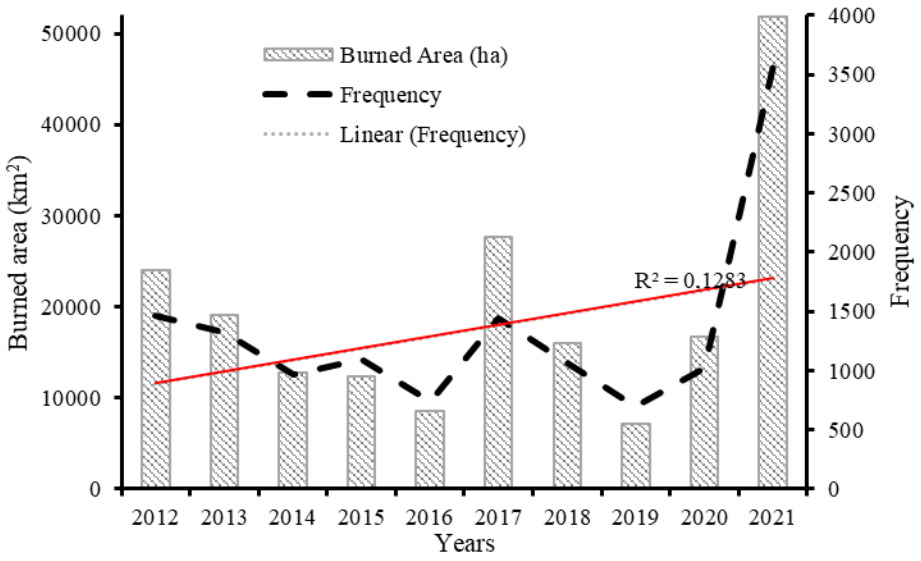

Figure 1: Burned area variation and wildfire frequency (Fires per year) between 2012 and 2021 in Botswana (Source: GWIS, 2022)

However, sustainable fire management requires area-specific approaches with percipient information to understand fires in line with accurate predictions for early warning systems, landscape-scale fuel or biomass management, burn severity, fire-regime restoration, active restoration landscapes, and population awareness and preparedness (IUFRO, 2018). Nevertheless, there is a significant gap in managing wildfires in the country, yet wildfire incidences continue to vary (Figure 1), indicating limited preparedness to reduce losses. This situation requires the development of reliable methods and tools for wildfire prediction and monitoring. Therefore, it is substantive that more effort is invested in developing accurate prediction methods for wildfire occurrences and monitoring burned areas and their impacts in different parts of the country.

1.2 Problem statement

Previous studies have explored various methods of wildfire prediction and burn area mapping (Çömert *et al*., 2019; Martín *et al*., 2019; Shang *et al*., 2020; Verhegghen *et al*., 2016). For example, Martín *et al*. (2019), applied the maximum entropy algorithm to analyze the intra-annual dimension of fire occurrence and fire-triggering factors in Spain using wildfire data (2008–2011), and GIS and remote sensing data. The study revealed that accessibility by road and human pressure coupled with land surface temperature strongly contributed to ignition probability. Shang *et al*. (2020) assessed the capacity of land cover, forest disturbance, and forest structure coupled with ancillary data to estimate burn probability in Saskatchewan, Canada. Results of the

study showed that forests composed of coniferous species had higher burn probabilities. Çömert *et al*. (2019) applied the object-based random forest algorithm for burned forest area mapping using Landsat 8 images. The study results showed a 99% overall accuracy making the approach important in mapping burned forest areas. Verhegghen *et al*. (2016) used Sentinel-2 (S2) optical satellite and the active radar Sentinel-1 (S1) satellite combined with MODIS active fire data to detect and monitor forest-burnt areas in the Congo Basin. The study results showed the S2 images provided a better estimation of fire propagation with a precise spatial extent to the point location of the MODIS active fire product. These studies demonstrate the potential and applicability of remotely sensed data and machine learning algorithms in fire prediction and burnt area mapping. However, forest fires are the focus of most of these studies, and spatial fuel accumulation is not included in prediction models despite its contribution to fire behaviour in the savannahs (Gomes *et al*., 2020). In addition, no single study proposes a unified tool or algorithm that could be applied by fire managers in arid savannahs.

In Botswana, there are no early warning systems to detect fires before they escalate into megafires. The situation is exacerbated by the wanting fire prediction tools and methods with scarce literature on fire prediction in Botswana (Dube, 2013). Most fire prediction models were developed for temperate and Mediterranean vegetation. They are less applicable to arid and semi-arid regions like Botswana as they can only be used for areas for which they were designed (Arroyo *et al*., 2008). This limitation creates a gap that restricts sustainable wildfire control in Botswana's rangelands which occupy over three-quarters of the country.

Natural and human activities shape the increasing frequency and extent of wildfires in Botswana's rangelands and require adequate preparation for their impacts (Maabong & Mphale, 2021). Fuel characteristics such as fuel types are extensively linked to wildfires globally and form most models for predicting wildfire occurrence (Arroyo *et al*., 2008). Few efforts characterize fuel types in sub-Sahara Africa, limiting their fire prediction application. In arid areas, biomass accumulation, soil moisture, and land surface temperature use in rangelands as wildfire prediction factors have not been largely explored. Existing efforts on soil moisture use have been limited to the prediction of Fuel Moisture Content (FMC). There is limited literature on its use as a wildfire prediction factor in different areas, with no study conducted in Botswana (Chaparro *et al*., 2016a; Chaparro *et al*., 2016b; Jensen *et al*., 2018; Rakhmatulina *et al*., 2021). Although not fully developed in Botswana, fire danger mapping is critical in wildfire management since it pro-

vides requisite information regarding fire spatial and temporal wildfire susceptibility and its expected impacts.

Accumulated biomass in rangelands is a critical resource for herbivores despite limited efforts to quantify the biomass lost during fires. The existing burn severity indexes provide no specific values of biomass lost. In Botswana, there is little effort to monitor and assess burned areas, with current burn area information having varying accuracy and not providing burn severity data. For instance, 312,974 ha of the burned area is not mapped by DFRR relative to that of GWIS (2022). It has become evident that there are possibly thousands of unregistered fires in Botswana that are yet to be mapped. Many fires in the wilderness seem undetected and unmapped, with no post-fire management practices, leading to rangeland degradation (Dougill *et al*., 2016). The lack of accurate and complete burned area and burn severity data limits the ability of rangeland managers to assess the impacts of fires and determine driving factors and their linkage and patterns to wildfires (Hawbaker *et al*., 2017). There is a need to develop and use new tools and methods to capture all burned areas effectively and independently demarcate perimeters and burn severity to reduce the incompleteness of the available wildfire datasets (Howard *et al*., 2014; Picotte, 2020). Incomplete and inaccurate wildfire burn area data trammels efforts by land-use planners and rangeland managers to efficiently plan for post-fire activities that require accurate burn severity information. This study demonstrates the use of moisture contents, land surface temperature, and biomass accumulation in wildfire prediction. The study also exhibits how the Fire Mapping Tool (MTBS) could be used to accurately map burned areas in Botswana.

1.3 Objectives

The main objective of this study was to model and predict wildfire occurrence using different variables in the Kgalagadi district as a way to enhance the sustainable management of rangeland resources.

1.3.1 Specific objectives

i. To predict the occurrence of rangeland wildfires using biomass (accumulation), moisture conditions and surface temperature; and
ii. To quantify the burned area.

1.4 Study hypothesis

i. Biomass accumulation in the rangeland is a potential predictor of wildfire occurrences under a changing climate;
ii. Low moisture contents are a predictor of wildfire occurrences;
iii. High surface temperature is a predictor of wildfire occurrences;
iv. The Fire mapping tool (FMT) provides accurate estimates of burn area extent and fire severity.

1.5 Significance of the study

Global ecosystems are increasingly becoming susceptible to wildfires and the increasing flammability of landscapes calls for more sustainable methods and tools for predicting and collecting information on fire occurrence to gain insight and develop management strategies (Bowman, 2018). This study contributes to available literature and fire prediction and monitoring methods. In addition, the information from this study may be used to inform rangeland managers regarding the extent and severity of burns from the fire incident. The availability of such information is critical in designing post-fire rangeland management strategies. Besides, reliable data is crucial for effective fire management as it forms a basis for appropriate management decisions and actions (Flasse *et al*., 2004). The study contributes to developing computationally effective and less costly prediction and monitoring methods applicable by decision-makers before and after fires. Overall, this study demonstrates remote sensing methods and tools for wildfire prediction and monitoring in Botswana that could contribute to more informed fire management decisions and policies for sustainable rangeland utilization.

1.6 Study scope

The primary focus of this research was to predict wildfire occurrence using biomass accumulation (Dry matter productivity), surface temperature, and moisture content in the rangelands of the Kgalagadi District of Botswana. The study was carried out in the arid conditions of Kgalagadi, which has experienced recurring wildfire events over the years. Wildfire prediction using biomass accumulation, moisture content, and surface temperature was achieved using remotely sensed data obtained from the National Aeronautics and Space Administration (NASA) websites, which were processed using ArcGIS software version 10.7. A random forest classification meth-

od was used to assess the accuracy of wild fire prediction using predictor variables. A logistic regression modelling method was used to map the probability of fire occurrence in the R statistical software. Burned area extent and burn severity indices were determined using the Fire mapping tool (FMT) and validated using the indices processed using Sentinel 2A images in ArcGis 10.7. Indices obtained from the FMT tool indicated biomass loss after the fire.

CHAPTER 2: LITERATURE REVIEW

2.1 Wildfire occurrence

Wildfires are unplanned ignitions that burn different vegetation types, including forests, grasslands, and shrubs (Jensen *et al*., 2018). The increasing frequency of wildfire occurrence globally has led to the development of fire science that deals with identifying fire causes and understanding prescribed and wildfire impacts and possible benefits to prevent and mitigate catastrophic events from large fires (USGS, 2022). Prescribed fires are purposely set and managed, while wildfires are uncontrolled fires that result from natural causes such as lightning and prescribed fire that go out of control. Several terms are used in fire science to describe different aspects of fires and fire management. Fire management starts with predicting the possibility of creating a fire based on the availability of fire-causing agents, termed 'Fire risk'.

The potential behaviour of a given fire related to fuel properties is referred to as a 'fire hazard' (Chuvieco *et al*., 2014). Fire science literature also refers to an index describing the factors affecting inception, ignition, spread, and difficulty controlling and preventing damage in a specific area as variable or constant "fire danger" (Chuvieco *et al*., 2014; S. Sharma & Dhakal, 2021). This definition, therefore, means that fire danger also referred to as fire hazard or probability, includes different factors that could be variables such as fuel moisture, temperature, or wind or constants such as fuel types and topography. In addition, burning material is characterized based on its ignitability which is the ease of igniting by glowing or flaming. Combustibility indicates the rate at which the fire burns or sustainability that reflects the extent a given fire will continue burning with no heat source (Quintiere, 2006). In fire prediction and monitoring, the fire vulnerability of an area (likely ecological and social effects) must be assessed to align it with fire danger. The magnitude of the impacts of fires on a given ecosystem depends on the fire intensity and severity. Keeley (2009) describes fire intensity as the amount of energy released during different fire phases and can be expressed using several metrics, including temperature, reaction intensity, heating duration, radiant energy, and fireline intensity. On the other hand, fire severity is the change or loss of above-ground or ground organic matter described using various indices based on the desired management levels (Keeley, 2009).

2.1.1 Factors responsible for wildfires

Different environmental and human-related factors drive the risk of wildfires in various areas. Although human activities are a crucial factor in fire ignition mainly due to the irresponsible use of fires (Guo, Su *et al*., 2016), climatic factors are a critical driver of the extent of burned area globally. Therefore, wildfire incidences could either be decreased by more responsible use of fires or increased through inappropriate land management practices. Other factors such as topography, the density of population, land cover, soil moisture and biomass were reported to significantly affect ignition density, and the extent of burnt area (Parente *et al*., 2019; Sungmin *et al*., 2020). This section elucidates the different factors that drive wildfire occurrences.

2.1.1.1 Climatic factors

In recent years, climate and weather conditions have become critical factors for wildfire occurrences in various areas (Lozano *et al*., 2017; Pereira *et al*., 2020). Wildfires are anticipated to be more frequent and extreme in many areas due to changes in climate and anthropogenic activities (Opitz *et al*., 2020). Climate variation enhances biomass drying, expected to increase drier conditions and temperature in the coming decades, contributing to wildfire risks (Huber, 2018). These changes will be experienced as prolonged fires over larger areas, including new areas where fires have never occurred (Hantson *et al*., 2015). Fire causal factors such as lightning are responsible for igniting many wildfires during fire seasons globally (Moris *et al*., 2020) and have also been linked to global warming. According to Romps *et al*. (2014), lightning is estimated to increase by 12% for every one-degree temperature rise.

Other climate change incidences, such as increased drought occurrences, affect the frequency and magnitude of fires. The increased frequency of droughts is due to reduced precipitation, temperature rise, higher wind speed, and reduced vapour pressure, all of which lead to more flammable fuels (Vicente-Serrano *et al*., 2020). Higher environmental temperatures and low precipitation are critical in wildfire ignitions and future prediction models based on simulated climate and burned area relationship projections (Halofsky *et al*., 2020; Mansoor *et al*., 2022). There are many reports of increased fire incidences due to increased drought. For example, Artés *et al*. (2019) indicate that the shared attributes in the most recent large fires in several regions globally were the high drought code (DC) and duff moisture code (DMC) values, which are components of the Fire weather index (FWI). Byer & Jin (2017) also call for the drought factor to be considered in wildfire prediction due to the known drought effects on vegetation and its

ease of being assessed from remotely sensed products. Parente *et al*. (2019) proved that drought impacts affect wildfire occurrences using the Standardized Precipitation Index (SPI) in Portugal, with 97 % and 98% of large wildfires and burnt areas evidenced during the drought from 1981 to 2017. According to Stavi (2019), fire behaviour is influenced by prevalent weather conditions such as air humidity, wind direction, and velocity throughout the fire. Evidence from their study indicates an increase in the possibility of wildfire with wind speed increase and decreasing relative air humidity. Guo *et al*. (2016) also reported a negative relationship between the daily precipitation and relative humidity with wildfire ignitions in southeast China.

Recent advances in soil moisture measurement especially using satellites and the establishment of soil moisture networks have resulted in the realization of the effect of soil moisture on wildfire occurrences and its use in wildfire prediction and danger applications (Sharma & Dhakal, 2021). Soil moisture effect on wildfire occurrence is linked to its complex relationship with other factors such as environmental temperature, vapour pressure, rainfall, and wind—a decrease in soil moisture results in higher wildfire risks (Sharma & Dhakal, 2021). Chaparro, Piles, *et al*. (2016) also indicated that most wildfires in the Iberian Peninsula occurred during warm and dry soil conditions. According to the authors, soil moisture and land surface temperature (SM-LST) are essential factors in predicting wildfires, although anomalies in SM-LST were observed during drought seasons. This is overwhelming evidence of the effect of climate and weather factors on increased wildfire occurrence. Therefore, there is a vicious rising cycle of wildfires and climate change with severe and catastrophic consequences on the environment, economy, livelihoods, and climate (IUFRO, 2018; Raviv *et al*., 2021).

2.1.1.2 Ecological factors

Fuel characteristics, including quantity and quality, affect wildfires' ignition, spread, and behaviour. Higher fuel quantities increase the potential of fires, while the low FMC resulting from long dry periods increases the flammability and risk of wildfires in a given ecosystem (Stavi, 2019). Although the quantity of fuels in rangelands is lower (10-50 mg ha^{-1}) than in forests (200-500 mg ha^{-1}), the available fuels tend to be drier with lower fire intensities and lower fire sustainability faster spread. Therefore, fire intensity in these lands is relatively low, but fires spread fast (Stavi *et al*., 2017). The fuel quantity and quality are affected by different factors such as the weather, soil moisture, and temperature. Several studies have been conducted to assess the effect of various factors on fuel characteristics and quantify the different fuel characteristics at different spatial and temporal scales. For instance, fuel accumulation and FMC have been indicated to vary

with soil moisture content (Rakhmatulina *et al*., 2021; Sungmin *et al*., 2020), while soil fertility and slope of the land affect the fuel arrangement, fuel continuity, and development of fire susceptible fuels within the system (Stratton, 2006; van Etten, 2010).

Fuel moisture content is an important factor in fire ignition, flammability, spread, and behaviour. Morvan (2013) highlighted that FMC reduced fire depth and buoyancy force depending on wind conditions. According to the author, fuel and oxygen-limited were the two regimes exhibited by the FMC effect; moisture in the fuel acts as a sink of burning heat as a proportion of the heat evaporates the water. Fire incidences predictions are also defined by the fuel moisture content (Turco *et al*., 2017). Similarly, Tihay-Felicelli *et al*. (2017) also highlighted that higher FMC decreases the rate of fuel consumption, smouldering time, and rate of heat release while increasing the time needed to propagate fire and its residence period. As in grasslands, drier biomass in an ecosystem increases all the previous fire parameters with higher fire hazards at low fuel moisture (Heisig *et al*., 2022).

Another environmental factor that influences wildfire occurrences is the topography of the land. Kane *et al*. (2015) state that fine environmental mosaics are created by mountainous topography with varying slope positions, precipitation, forest structure, moisture, and temperature. Water balance and topography (slope position, slope, and insolation) predicted 85-93% of the fire incidences in Yosemite National Park, California, North America (Kane *et al*., 2015). Heisig *et al*. (2022) also found fires occurring more frequently and faster on slopes with homogeneous stands. The redistribution explains the deference in fire behaviour across the slope in resources across the landscape, including wind, water, and nutrients, which profoundly influence fire behaviour. Nhongo *et al*. (2019) also reported many environmental factors that affected fire occurrences in the Niassa Reserve-Mozambique, mainly the NDVI, followed by temperature and elevation, slope, precipitation, and relative humidity. Jensen *et al*. (2018) also found a correlation between wildfire activity and soil moisture simulated by NASA's Gravity Recovery and Climate Experiment (GRACE) satellite compared with historical wildfire data in the U.S. from 2003 to 2012 obtained from the USDA Forest Service.

2.1.1.3 Human-induced factors

Human activities directly or indirectly cause the majority of wildfires occurring globally. The increasing practice of unsustainable land-use practices, such as the use of fires, has led to increased fire incidences. For example, the sprawling urban areas into wildlands due to rapid urban

population growth has increased the extent of the wildland-urban interface, increasing the wildfire risks that emanate from human ignitions (Radeloff *et al*., 2018; Weisshaupt *et al*., 2007). A study by Kolanek *et al*. (2021) reported that the built-up area and forest border's length and road density played a more significant role in fire density in Poland. Nunes *et al*. (2016) also reported that more than one-third of the fire ignitions are concentrated around the municipalities of Portugal, with a positive ignition trend over the last decade. The authors found significant effects of population on fire ignitions and burned areas. Guo *et al*. (2016) also found a higher likelihood of fire occurrences in areas with a higher frequency of human activities. Proximity to wildlands such as rangelands has increased fires, with more fire incidences occurring in areas closer to settlements than in areas with less population.

In addition, industrial activities such as exploiting wildland products through timber harvesting and logging have been reported to increase incidences of wildfires. According to McKenzie *et al*. (2004), logging activities tend to increase the rate of fuel drying due to increased temperatures, leading to higher fire severities and frequency. Timber harvesting activities leave the unwanted slash materials dry faster and increase the presence of dry fuels with higher wildfire potential. In Canada, Pew & Larsen (2001) reported that 29% of all logging fires resulted from burning unwanted slash materials left after logging operations. Studies by Miller *et al*. (2009) also reported increasing wildfire severity after timber harvesting. Their study indicated that higher burn severity was due to the increased forest fragmentation due to the creation of patches with different growth stages in a forest that exposes fuel to higher temperatures leading to drying (Miller *et al*., 2009).

2.1.2 Wildfire impacts

Fire occurrences in wildlands cause substantial damage and losses to humans and the environment. Fires have been reported to threaten human livelihoods and food security by damaging property and vegetation.

2.1.2.1 Environmental impacts

Wildfires have substantial effects on different environmental variables. In rangelands, it is estimated that about 5-95% of the existing biomass is destroyed during a prescribed or wildfire (Stavi, 2019). This effect, therefore, results in considerable changes in vegetation structure with short-term and sometimes prolonged changes in biomass productivity of pasture in rangelands.

Changes in vegetation structure result in habitat alterations; burned forests may be converted to grasslands after a fire (Mansoor *et al*., 2022; Nunes *et al*., 2016). Nevertheless, the changes in vegetation structure after the fires contribute to maintaining the competition between herbaceous and woody species in the savannah (Andela & van der Werf, 2014). Thus, fires are essential in preventing savannah grasslands from converting into forests.

Several studies have been conducted to characterize the impact of fires on different environmental aspects. For example, Stavi *et al*. (2017) studied the effect of fires in semi-arid Israeli Negev and reported a significant impact of fires on soil hydrophobicity. Their results showed a slight increase in mean Water Drop Penetration Time (WDPT) and a minimal reduction in average Critical Surface Tension (CST) in the burnt areas than in the unburnt areas. The study also found that soil organic carbon and ammonium nitrogen increase in burned areas more than in unburnt areas. The impact of fires on soils results in soil fertility and quality changes due to the deposition of ashes and partially burnt materials into the soils (Parson *et al*., 2010; Rau *et al*., 2008). In African savannahs, fires have improved grassland productivity by recycling nutrients (Andela & van der Werf, 2014). Improved grassland productivity after the fires plays a crucial role in attracting wildlife for hunting in hunting communities and other agricultural practices. However, in rangelands, fire impacts on soils are exacerbated by livestock and wildlife grazing actions on soil aggregate stability following a burn. After fires, the hoof action of livestock increases soil erodibility due to their shearing action resulting in accelerated land degradation (Stavi *et al*., 2017).

Wang & Zhang (2020) studied the Land surface phenology (LSP) that quantifies the timing and greenness of seasonal vegetation growth in satellite pixels. Their study indicated that wildfire causes significant land surface alterations leading to abrupt changes in the LSP magnitudes. According to them, the impact of fire on the LSP changes varied with burn severity, with the most noticeable impact on LSP timing and LSP greenness at moderate and high burn severity, respectively. Other studies have reported other environmental effects of wildfires varying with burn severity dependent on the intensity of fires. According to Stavi (2019), grasslands have low to moderate fuel loads that support moderate-intensity fires with moderate burn severity. Therefore, fuel management by selective grazing and thinning is recommended in rangelands to reduce burn severity with lower fuel quantities (Thomas, 2006).

In the recent decade, several gaseous emissions during burning have become a concern (Cruz Núñez et al., 2014; Liu et al., 2021; Loehman et al., 2014; Urbanski, 2014). The increasing wildfire occurrences have resulted in increased greenhouse gas and particulate matter emission of

pollutants into the atmosphere (Pettinari & Chuvieco, 2020). Higher quantities of these substances in the atmosphere are responsible for climate change with increased surface runoff, soil degradation, desertification, and decreased evapotranspiration. These fire consequences affect carbon budgets in burned areas, with large amounts of carbon released yearly (Cruz Núñez *et al*., 2014).

2.1.2.2 Social and economic impacts

Much as most impacts of fires highlighted in most of the literature is biophysical impacts, the effect of fires on social and economic aspects is considerably more extensive than the literature suggests. Moreover, all-natural resource management challenges are people challenges. Droughts, which are a significant driver of wildfires, have significant impacts on agricultural production; the occurrences of wildfires, therefore, aggravate the effects of droughts on the population by causing damage to property and posing a threat to life (Scasta *et al*., 2016; Turco *et al*., 2017). According to Meredith & Brunson (2021), wildfire occurrences affect community relationships, especially in need of collaborative management of wildfire effects since wildfires do not follow pre-established boundaries. Differences in goals/ missions, culture, limited resources, and mistrust could result in a lack of collaboration. The lack of cooperation during rehabilitation after fire results in a loss of landscape continuity that alters a community's human systems and ecological processes (Meredith & Brunson, 2021).

Economically, efforts to manage wildfires, fire detection, and extinguishing fires come with a high investment cost. National and regional governments incur high costs in fire suppression activities before and during the fire (Florec *et al*., 2019). In addition, the significant forage losses to rangeland farmers also result in considerable profit losses with higher costs invested in feeding livestock after the loss of available forage to fires. At the same time, grazing is restricted (Brunson & Tanaka, 2011). Wildfires have also been reported to have psychological or behavioural effects on individuals directly affected by fire damage to their property and personal health (Brunson & Tanaka, 2011; Grant & Runkle, 2022). Exposure to fire smoke and particle emissions during the burning results in long-term respiratory and cardiovascular complications (Grant & Runkle, 2022; Thomas, 2006). Communities experiencing fires also face visibility challenges due to thick smoke produced during the burning, which restricts visibility, especially for road users resulting in road accidents (Thomas, 2006).

Overall, wildfires remain an integral practice in the rangelands despite the challenges of uncontrolled fires. For example, many communities in the African savannahs apply frequent controlled fires as a protective measure to reduce the accumulated fuel (Shaffer, 2010). By shaping the availability of fuels, rural communities can protect their property from occasional uncontrolled large fires. Local communities in Africa continue to use controlled fires to reduce wildfire threats, control pests, clear land for cultivation, and remove bushes in rangelands. Therefore, it is essential to integrate such local knowledge when developing wildfire management strategies.

2.2 Wildfire prediction science, methodologies, and tools

Since fires considerably impact local and global scales, several models and tools have been developed to predict and map wildfire danger or probability of ignition to ensure early prevention and control of their occurrence. The increased fire incidences in the last few decades and the need to prevent or prepare for their event resulted in the development of a new science of fire prediction to develop more accurate fire prediction methods (Goode, 2019). Fire prediction methods are based on factors that must be understood for accurate wildfire prediction (Çolak & Sunar, 2020).

2.2.1 Remote sensing and machine learning methods

Many advanced statistical and Machine learning (ML) models have been proposed with remote sensing data from various satellites. The rapid development of ML (Bot & Borges, 2022; Koubarakis *et al*., 2017) has been used to predict spatial and temporal wildfire danger. ML and remote sensing methods derive values that indicate the danger index using input data (Bot & Borges, 2022; Zdeborová, 2017). On the other hand, remote sensing is a source of essential data from multiple sources of satellites like Landsat 8 & 9, Sentinel 1 and 2, VIIRS, and MODIS (Arevalo-Ramirez *et al*., 2021; Chuvieco *et al*., 2014; Mondal *et al*. 2020; Sá *et al*., 2017; Teodoro & Amaral, 2019). Remote sensed data has been instrumental in predicting wildfire locations and analysing wildfire-driving factors. Moreover, in their review of recent (2019-2022) studies, Bot & Borges (2022) concluded that machine learning techniques indicated a high potential for wildfire prediction and classification. These techniques support wildfire management decision-making despite the need for time-to-time improvement to achieve faster models and more accurate results interpretations.

Consequently, ML algorithms and remote sensing methods have been vital tools for predicting wildfire danger in the last decade, as indicated in several studies, such as Chuvieco *et al*. (2014) who integrated geospatial information and geographically weighted regression for forest fire assessment in Spain. The result showed a significant correlation ($R^2 = 0.7$) between the fire danger map and the fire occurrence. Le *et al*. (2021) proposed a deep neural computing method with a three-hidden layered structure to predict the spatial extent of wildfires in tropical areas. The method employed the Root Mean Square Propagation (RMSProp), Adaptive Moment Estimation (Adam), Adadelta, and Stochastic Gradient Descent (SGD) to optimise the model and produce a high prediction accuracy of 0.894 area under the curve and a kappa coefficient of 0.63.

Heisig *et al*. (2022) used ridge regression and random forest methods to predict surface fuel types, crown bulk density (CBD), and wildfire hazard using predictors derived from airborne LiDar (Light Detection and Ranging), Sentinel-l and Sentinel-2 data. Simulations from different scenarios indicated an overall accuracy (R^2) of 0.971 for fuel type classification and 0.73 for CBD. Similarly, Guo *et al*. (2016) used the binomial logistic regression method, and Ripley's K-function was analysed using geospatial information system (GIS) data to derive spatial wildfire patterns in China. The analysis models predicted between 80% and 90% of wildfires. A similar study by Tehrany *et al*. (2019) employed the Support vector machine (SVM), random forest (RF), Kernel logistic regression (KLR), and LogitBoost ensemble-based decision tree (LEDT) machine learning method to predict wildfires in Vietnam using multisource spatial data. Their results indicated higher accuracy (90%) on predicting wildfires obtained using LogitBoost ensemble-based decision tree (LEDT).

Other studies, including Chaparro *et al*. (2016a), used remotely sensed soil moisture derived from Soil Moisture and Ocean Salinity (SMOS), land cover, and ERA-interim land surface temperature reanalysis to predict fires in the Iberian Peninsula from 2010 to 2014. Wildfire predictions using the model were 83.3% accurate with significant coherency with wildfire behaviour in the study area, making it a promising model. Nhongo *et al*. (2019) used a logistic regression model to map wildfire probability in Niassa Reserve-Mozambique using the normalised difference vegetation index (NDVI), topographic factors, climatic variables, and socioeconomic data which produced high precision of wildfire ignition probability with an area under the curve of 74%. Naderpour *et al*. (2019) reviewed recent studies (2000-2018) on wildfire prediction methods. They concluded that machine learning and ensemble algorithms could make more accurate predictions of wildfires than other methods, such as multi-criteria and statistical methods. Many

remote sensing and machine learning methods for wildfire prediction offer promising potential, especially in developing countries. However, few studies have been conducted on wildfire prediction in Africa and Sub-Saharan Africa, presenting a need for further investigation on the possibility of ML and RS application in wildfire prediction under African conditions.

2.2.2 Fuel-based prediction methods and systems

Fuel and fuel characteristics are essential factors in fire ignition, spread, intensity, and burn severity; they are critical in wildfire prediction and modelling. Using fuel models, previous studies on fire prediction dealt with characterising fuel types in different fire-prone areas. According to Merrill & Alexander (1987), a fuel type could be described as a recognisable association of fuel elements of distinctive form, species, arrangement, size, and continuity that will exhibit specific fire behaviour under defined conditions of burning. The fuel model is a numerical description of physical parameters that define each fuel heap (Arroyo *et al*., 2008). Many earlier fire prediction models and tools were developed using fuel type characterisations in the United States, Australia, Canada, and Europe.

For example, Rothermel (1972) developed Rothermel's fire spread model that simulates surface fuel fire spread following plans for a complete fire danger rating system in North America. These efforts resulted in the National Fire Danger Rating System (NFDRS). The NFDRS is a fuel model that provides daily or seasonal fire danger and potential for large areas (Arroyo *et al*., 2008). This model was later incorporated into several fire support systems and tools in North America, such as the fire behaviour prediction and fuel modelling system (BEHAVE), fire area simulation system(FARSITE), FlamMap program for fire behaviour mapping and analysis, and the National Fire Management Analysis System for economic planning (NFMAS) (Andrews & Queen, 2001; Finney, 1998; Lundgren *et al*., 1995). McArthur (1967) also proposed the McArthur Grassland Fire Danger Rating System and the McArthur Forest Fire Danger Rating System for fire behaviour prediction in Australian Eucalyptus Forests. Fire prediction studies by Van Wagner & Pickett (1985) developed the Canadian Fire Weather Index (FWI) and the Canadian Fire Behaviour Prediction (FBP), which make the Canadian Forest Fire Danger Rating System (CFFDRS). The Prometheus system was also developed in Europe, adopting the Northern Forest Fire Laboratory fuel (NFFL) type classification for Mediterranean ecosystems (Arroyo *et al*., 2008).

The fuel-based models are packaged in different tools based on fire management needs. However, to effectively apply these models and tools, knowledge of existing fuel characteristics is vital;

because fuel conditions form part of the fire (Chuvieco *et al*., 2004). Noteworthy, fuel characteristics are complex, making them hard to map and describe. For instance, according to Keane *et al*. (2000), fuel types may be characterised as live woody, herbaceous or dead woody with differing sizes, which may vary for different areas. Fuel characterisation has received significant effort (Ottmar *et al*., 2007; Won *et al*., 2006). Many fuel type classifications have been developed and used for fire management globally, such as the Fuel characteristic Classification system and the Prometheus fuel classification system (Ferraz *et al*., 2009; Ottmar *et al*., 2007). Accurate fire prediction for fire management strategy development using fuel models requires explicit knowledge of the spatial distribution of fuel conditions.

2.2.3 Fire prediction accuracy and uncertainty

An important component of fire prediction approaches is the accuracy and uncertainty associated with their application in different environments. Many elements of wildfire prediction approaches have resulted in unforeseen discrepancies between simulated and actual wildfires, including insufficient knowledge, inaccurate models, and parameter inaccuracies. Most possible variations in simulated fires arise from input variables used in the prediction models (Benali *et al*., 2016). Input variables have been cited as crucial sources of uncertainties in fire predictions. Beven (2002) also points out that ignoring the non-linear sub-grid process could result in inaccuracies despite contradicting evidence from Clark *et al*. (2008). They indicate the negligible effect of spatial resolution of fire predictions.

According to Benali *et al*. (2016), uncertainty in fire modelling is categorised into three: vegetation, ignitions, and weather. For example, the assumption by fire prediction models of uniform weather conditions such as wind speed, relative humidity over a grid cell, and wind prediction discrepancies may result in significant changes in prediction accuracy (Anderson *et al*., 2007; Clark *et al*., 2008; Hilton *et al*., 2015; Palmer *et al*., 2005). The complex interactions between fuel load and existing weather conditions and topography also affect the accuracy of wildfire predictions arising from ignition uncertainty (Parisien *et al*., 2010). Other authors have also indicated considerable variations between observed and simulated wildfires due to minor differences in the fuel structure (Fernandes *et al*., 2004). The differences in fuel structure could arise from the prominent temporal and spatial variations in fuels with significant heterogeneity across landscapes that are difficult and expensive to map. The low ability of remote sensing techniques to

record surface fuels, lack of robust fuel mapping systems, and highly subjective fuel classification systems may explain the variations (Keane & Reeves, 2012).

Benali *et al*. (2016) investigated the impact of uncertainty in input variables on prediction accuracy by determining the discrepancy between satellite-observed and simulated fire progression data in Portugal. The study results indicated that wildfire prediction accuracy was affected by uncertainties in fuel model assignment, wind direction, and speed, fuel typology, timing, and location of fire ignitions. Therefore, it is essential to account for the different sources of uncertainty in wildfire prediction modelling, such as fuel structure, homogeneity assumptions, scale effects, and model parametrisation (Hilton *et al*., 2015; Salvador *et al*., 2001). Different authors have proposed and used several optimisation algorithms in machine learning methods to improve prediction accuracies. Models include Stochastic Gradient Descent (SGD) presented by Kim (2017), Root Mean Square Propagation (RMSProp), Adaptive Moment Estimation (Adam) (Kingma & Ba, 2015), and Adadelta (Zeiler, 2012). Therefore, assessing the different sources of inaccuracy and using various techniques to improve fire prediction accuracy should be applied during modelling to lead to more reliable fire predictions.

2.3 Wildfire prediction variables

Many factors have been proposed for use as variables in fire prediction, including climate, weather, fuels, fuel properties, soil moisture, population, settlements, and other economic and social factors that have been incorporated into fire simulation and fire probability models (Benali *et al*., 2017; Le *et al*., 2021; Parisien *et al*., 2010).

2.3.1 Fuel moisture content (FMC)

Fuel moisture content (FMC) is the most utilised fuel condition in fire ignition and behaviour prediction and modelling and development of most fire flammability/danger rating systems (Dimitrakopoulos & Papaioannou, 2001). FMC can be described as live (Live Fuel Moisture content, LFMC) or dead (Dead Fuel Moisture Content, DFMC). The fire ignition probability has been reported to be inversely proportional to the FMC of the existing fuel. The inverse relationship is attributed to heat energy loss through the evaporating moisture before burning starts and flammability by humid materials that reduce ignition chances (Dimitrakopoulos & Papaioannou, 2001). The determination of FMC for wildfire prediction is conducted using several methods such as meteorological indices, remote sensing techniques, and field sampling. Field sampling is

the most accurate FMC determination method. However, its applicability for the larger spatial area (global or regional scales) is restricted and costly, making meteorological indices such as Keetch–Byram Drought Index that use atmospheric characteristics the most used in fire danger rating systems. Such indices are better estimators of dead FMC since they are dependent on the atmospheric conditions (Yebra *et al*., 2007).

The development and availability of remote sensing data on different characteristics, such as surface temperature and reflectance, have increased the use of remote sensing methods to estimate FMC. However, remote sensing methods provide better estimates of LFMC than DFMC since they depend on existing vegetation conditions (Yebra *et al*., 2007). Several authors have proposed numerous methods for estimating FMC for fire ignition prediction. For instance, soil moisture content to assess FMC is growing due to the availability of soil moisture networks in many parts of the world at different scales (Dennison *et al*., 2009). In addition, the growing availability of remote sensed soil moisture products from various satellites, such as Soil Moisture Active Passive (SMAP), have been reported to be accurate LFMC estimate predictors in the Southern California Mediterranean ecosystem, North America (Jia *et al*., 2019). Vinodkumar & Dharssi (2019) and Vinodkumar *et al*. (2021) also reported a 0.74 correlation between LFMC and soil moisture with a time lag of 14 days over Australia. Lu & Wei (2021) also found a correlation between LFMC and microwave soil moisture data, with more significant correlations observed for soil moisture obtained within 60 days to LFMC sampling in North America. The primary fuel types with a high response to soil moisture include pine, red cedar, sagebrush, oak, manzanita, chamise, mesquite, and juniper (Lu & Wei, 2021).

Danson & Bowyer (2004) examined the FMC relationship with leaf equivalent water thickness (EWT) and a range of spectral vegetation indices (VI) using Leaf Optical Properties Experiment (LOPEX) spectral reflectance data and modelled data from the Prospect leaf reflectance model. Their study indicated a significant correlation between FMC and Normalised difference water index, NDVI, Water index, moisture stress index, and global vegetation moisture index. They observed stronger relationships between FMC and leaf EWT and the strongest correlation for the Water index (WI). In a similar study by Quan *et al*. (2017), two Radioactive Transfer Models (RTMs) (PROSAIL- which modelled the spectra of the continuous lower grass canopy layer and PRO-GeoSail- which modelled the spectra of the discontinuous upper tree canopy layer) were coupled to retrieve fuel moisture content of a forestry structure. Their results indicated more accurate FMC retrieved from the coupled model than FMC retrieved using the PRO-GeoSail model

alone. Similarly, Slijepcevic *et al*. (2015) evaluated daily FMC predicted using three models based on modifications of the Canadian Fine Fuel Moisture Code and the process-based model with and without changes to fit the data better. Their results showed better predictions from the modified Canadian model, while most false conditions were obtained from the modified process-based model.

2.3.2 Estimation of fuel moisture content

Unlike other continents where FMC is measured at weather stations, Africa's lack of a dense network of weather stations limits the availability of field-based fuel moisture content for wild-fire management. Nevertheless, wildfire prediction models require quality input data of both LFMC and DFMC for accurate predictions. Earlier, the field-based sampling method was used to estimate FMC accurately; however, this method is restricted when studying large-scale areas with significant spatial variation in the landscape (Sharma & Dhakal, 2021). Similarly, the sparse network of weather stations, especially in developing countries, makes FMC estimates prone to errors, uncertainty, and bias (Sharma & Dhakal, 2021). Earlier efforts to model FMC, especially LFMC, depended on drought indices and meteorological variables (Ruffault *et al*., 2018). Mete-orological estimates and drought indices in FMC estimation showed significant potential despite considerable variations across sites, even with limited spatial variations (Ruffault *et al*., 2018).

2.3.2.1 Live fuel moisture content

Several studies have proposed numerous models for estimating LFMC using remotely sensed measurements. Retrieval of vegetation moisture content using remotely sensed measurements, especially in the visible region, depends on the leaves' optical properties (Chuvieco *et al*., 2004). Remote sensing literature uses equivalent water thickness (EWT) to express the water content/ mass of water in the leaf tissue per unit area of the leaf. EWT is defined as (Equation 1):

$$EWT = \frac{M_f - M_d}{A} \qquad \text{Equation 1}$$

where M_f is the field-measured mass of the fresh leaf, M_d is the oven-dried weight mass of the same leaf, and A denotes the leaf area. Studies have reported significant sensitivity of EWT to the shortwave infrared (SWIR) range of the spectrum (1.1-2.5) since solar radiation absorption from compact leave can be approximated by an equivalent water layer (Ceccato *et al*., 2002a). However, additional bands may be required to counter the uncertainty arising from the effect of

other variables affecting SWIR reflectance (Chuvieco *et al*., 2004). Canopy EWT (EWT_c) can then be determined by multiplying EWT by the Leaf area index (LAI), which indicates the amount of water in the canopy per unit of ground area (Ceccato *et al*., 2002a; Ceccato *et al*., 2002b). Although EWT is the most used in remote sensing studies due to its optical properties of vegetation, it differs from LFMC, which quantifies the percentage of water relative to the leaf dry matter mass (Chuvieco *et al*., 2004). LFMC is derived using Equation 112;

$$LFMC = \frac{M_f - M_d}{M_d} \times 100 \qquad \text{Equation 2}$$

Unlike DFMC, a broad body of literature attests to remote sensing measurements to retrieve the moisture content of fuels, either directly or indirectly (Yebra *et al*., 2013; Yool, 2009). The use of remotely sensed measurements depends on the leaves' spectral properties, which vary with water content and stress (Yebra *et al*., 2013, 2018). Fire behaviour and the spread of woody vegetation are influenced by leaves and small twigs whose water content is strongly correlated (Saura-Mas & Lloret, 2007; Viegas *et al*., 2001). Some models have been proposed to estimate LFMC. Overall, two approaches to LFMC estimation exist; simulation methods using radiative transfer models (RTM) and empirical relations between VIs and LFM (Yebra *et al*., 2008). comparing the two approaches of LFMC estimation in Mediterranean grassland/shrub land in Spain, Yebra *et al*. (2008) found that superiority was exhibited by Regression models over RTM for the exact calibration dataset. However, the two methods performed similarly when validation and calibration datasets were used. The superiority was attributed to the difficulty of parameterising RTM relative to the empirical approach. According to the authors, the accuracy of empirical and RTM models used for grasslands was higher (R^2 = 0.914 and 0.927) than for shrub land (R^2=0.723 and 0.703). Jia *et al*. (2019) used Soil Moisture Active Passive (SMAP) L-band radiometer soil moisture (SMAP SM). They proposed a multi-variant regression model for LFMC in the Mediterranean ecosystem of Southern California, USA. The weighted accumulative SMAP SM and Cumulative growing degree days (CGDDs) model yielded the best results (R^2 of 0.529 and an RMSE of 19.876) than the MODIS VARI reference model.

Other methods involve using radiance values derived from airborne hyperspectral imagery (Al-Moustafa *et al*., 2012). While others involve radiative transfer model inversion with MODIS reflectance data (Yebra *et al*., 2018), neural network deep learning model using microwave backscatter (from Sentinel-1) and Landsat-8 optical reflectance (Rao *et al*., 2020). Chuvieco *et*

al. (2004) proposed an empirical method for determining the FMC of Mediterranean grassland using NOAA-AVHRR data of normalised difference vegetation index (NDVI) and surface temperature (ST). The study found that the proposed empirical model avails FMC estimations with high accuracy observed for all sites and species. The temporal convolutional neural network for determining LFMC (Temp CNN-LFMC) presented by Zhu *et al*. (2021) achieved a correlation coefficient of 0.74 with an overall RMSE of 25.57%. LFMC model consisted of three 1-D convolutional layers that learn the specific multi-scale temporal dynamics (features) of one-year MODIS time series. Overall, accurate determination of FMC is necessary for fire prediction models with methods that separate Live Fuel moisture content from dead fuel moisture content, achieving better accuracy. Therefore, choosing an efficient and reliable model for FMC estimation is necessary for more accurate wildfire predictions.

2.3.2.2 Dead fuel moisture content

Although less used in fire prediction models, Dead fuel moisture content (DFMC) estimation broadly uses meteorological measurements. However, empirical and process-based models could also provide a significant degree of accuracy for acceptable fuel moisture content (Matthews, 2014). The sparse and sometimes missing measurement network, especially in developing countries, indicates that fire predictions depend on empirical models to estimate DFMC (Matthews, 2014; Rakhmatulina *et al*., 2021). Noteworthy, dead fuel moisture content DFMC estimation from remotely sensed measurements is limited by the inability to observe dead fuels covered by a canopy from optical and thermal remote sensors. Unlike optical and thermal sensors, radar sensors have been reported to have the ability to sense litter moisture. The radar sensor penetrates the cloud cover and is sensitive to radar backscatter from litter, providing an opportunity for direct DFMC estimation (Leblon *et al*., 2016). The sensor can retrieve measurements in different vegetation covers under varying weather conditions, and radar backscatter has been reported to correlate significantly with various indices of the Fire Weather Index System related to DFMC (Abbott *et al*., 2007). However, vegetation structure, biomass, and water content have affected radar backscatter (Leblon *et al*., 2016).

Thus, indirect methods of DFMC estimation using empirical or process-based models are required to separate canopy components from dead fuel components in optical remote sensed measurements to determine fuel moisture content or the corresponding value of DFM indices (Merzouki & Leblon, 2011; Yang *et al*., 2018). Existing models have been site-specific, yet pro-

cess-based approaches tend to provide biased DFMC values, especially in low vegetation density areas (Nolan *et al*., 2016). The Nelson Dead Fuel Moisture Model is the most familiar DFMC model (Nelson Jr, 2000). The model has been applied in different fire danger systems, including the NFDRS fire behaviour, FlamMap, BEHAVEPlus, and other fire management models utilized in the USA. The model uses various inputs, including the volume of precipitation received and time from the rainfall and other environmental variables, to describe the moisture and heat transfer (Nelson Jr, 2000). Although the model has been reported to perform well in different environmental conditions, there are reports of over estimation, especially in wet conditions (Estes *et al*., 2012). Such errors in FMC estimates could have considerable consequences, especially in predicted fire behaviour, affecting management strategies.

According to Rakhmatulina *et al*. (2021), errors and biases observed in wet conditions could result from excluding soil moisture from the prediction (Hiers *et al*., 2019). Using precipitation in FMC models to account for wetness may provide a poor representation of SM in complex landscapes (Rakhmatulina *et al*., 2021). Moreover, linear relations have been reported between vegetation and soil moisture indices (Hunt *et al*., 2011). According to Zhao *et al*. (2021), soil moisture models perform better during wet conditions than models that exclude SM. According to Samran *et al*. (1995), 41-59% of fuel bed moisture content is explained by soil moisture and precipitation in direct contact with soil. Rakhmatulina *et al*. (2021) further reported that soil moisture content was the most critical factor of all environmental variables used in their study for wet soil conditions, with a 0.6% increase in FMC for every 1% soil moisture increase observed. Other models have been suggested for the estimation of DFMC from automated fuel moisture sticks (Cawson *et al*., 2020), while Nolan *et al*. (2016) used a model for the prediction of DFMC using MODIS-derived vapour pressure deficit and gridded weather data in Australia and realized between 3.9 and 6.0% absolute errors. Zormpas *et al*. (2017) developed regression models for DFMC prediction from Landsat-based NDVI, LST, and BT, and the BT model produced a more acceptable DFMC prediction (R^2=0.733) than NDVI and LST-based models. Therefore, it is vital to consider the interactions between dead fuel moisture content with other environmental variables to retrieve accurate DFMC variables from remotely sensed measurements (Hiers *et al*., 2019).

2.3.2.3 Limitations of fuel-based methods for fire prediction

Although fuel models are widely used for fire prediction, their application seems limited. Existing fuel-based methods, fire danger mapping, and prediction tools are based on models developed for specific areas. According to Arroyo *et al*. (2008), fuel models tend to be site-specific, with their use restricted only to the regions for which they were developed. Using such fuel prediction tools for other areas may result in inaccurate predictions and misinforming land managers and planners. Furthermore, the fire prediction models are also limited to the aims for which it was developed (Arroyo *et al*., 2008). For example, a fire behaviour prediction model cannot be used for fuel classification for a different area. Moreover, fuel characterises vary significantly both spatially and temporarily, making mapping fuels and their characteristics hard to map. Yet, the other fuel classification systems create confusion due to the complexity of describing all the fuel characteristics.

2.3.3 Surface temperature

Land Surface Temperature (LST), also known as skin temperature, is the temperature of the earth's surface. Several studies have indicated that Land Surface temperature (LST) and its anomalies significantly correlate with wildfire severity and frequency in different regions (Vlassova *et al*., 2014; Yang, 2021; Yang, 2021). However, the land surface temperature use in wildfire prediction studies is limited. LST and LST anomaly estimates have been used to assess plant water stress conditions, energy budgets, heat energy available before fire occurrence, and to predict wildfire occurrence (Bisquert *et al*., 2012; Nolan *et al*., 2016). In addition, LST estimates have also been reported to be a potential predictor of fuel moisture content (Chuvieco *et al*., 2004). The significant relationship between temperature and FMC indicates a strong association between LST and fire ignition, spread, and behaviour. According to Huh & Lee (2017), areas with higher evapotranspiration levels have minor LST differences. The difference results from the loss of energy as latent heat to the atmosphere during evapotranspiration from soil and plants. Thus, areas with higher LST differences tend to be more fire-prone due to lower fuel moisture content. However, there remains a lack of literature relating LST and LST anomalies to wildfire occurrence.

For example, Bisquert *et al*. (2012) used combined LST and EVI to develop a fire danger model using LR and ANNs. They expected LST would be the critical factor in predicting fire danger due to the high temperatures linked to low moisture conditions that increase the risk of ignition.

Logistic regression and ANNs were used to obtain a fire danger model. The developed ANN model achieved an accuracy of 76% compared to regression. Yang (2021) evaluated the relationship between LST anomaly and fire frequency in the Caribbean region using daily LST anomalies derived from MODIS observations. Results indicated significant growth in LST anomaly before the fire incidence. According to the author, 1.4 degrees higher than the average temperatures increase fire occurrence chances (Yang, 2021). The study also analysed the relationship between LST anomaly and fuel types, but it was insignificant (Yang, 2021).

The successful use of LST in fire prediction depends on the availability of accurate and continuous estimates of LST. Satellite thermal infrared (TIR) data is linked to LST through the radiative transfer equation (RTE), and this has attracted attention to developing algorithms for retrieving LST from satellite TIR (Li & Duan, 2018). Several algorithms have been developed over the years to retrieve LST from TIR measurements by different sensors about satellites. The commonly used method is Landsat TIR measurements to retrieve LST, as presented in (Dahiru & Hashim, 2020). Landsat data offers the potential for recovering continuous and accurate LST estimates and has been used in several environmental studies (Chuvieco, Riaño, *et al*., 2002; Vlassova *et al*., 2014). The method uses the split-window algorithm (SWA) to retrieve temperature estimates from brightness temperature (BT), as indicated in Equation 3 below. The split-window LST algorithm was also developed for Moderate Resolution Imaging Spectroradiometer (MODIS) to retrieve LST from land surface reflectance. These have been used to analyse vegetation stress conditions (Wan, 2013; Wang *et al*., 2019; Yang, 2021). Other LST products derived from TIR data obtained by ASTER, Along-Track Scanning Radiometer (ATSR) aboard European Remote Sensing Satellite (ERS-1), AVHRR, and SEVIRI data (Li & Duan, 2018).

$$LST = \left(\frac{BT}{1 + \left(0.00115 \times \frac{BT}{14388} \right) \times \ln(\varepsilon)} \right) \qquad \text{Equation 3}$$

Where BT is the brightness temperature and ε is the emissivity

2.3.4 Fuel quantity/biomass accumulation

The quantity of fuel accumulated during a wildfire is an essential factor influencing fire ignition, behaviour, spread, and severity. Despite the criticality of fuel quantity in wildfire behaviour, most wildfire danger rating systems and prediction models focus on fuel moisture content (Chu-

vieco *et al*., 2004; Martín *et al*., 2019; Rakhmatulina *et al*., 2021; Yebra *et al*., 2013, 2018). A lack of literature explicitly uses fuel quantity to model wildfire risks. Available literature incorporating vegetation quantity tends to rely on vegetation indices, especially NDVI (Cao *et al*., 2013; Karimi *et al*., 2021; Le *et al*., 2021; Leblon, 2005; Michael *et al*., 2021; Nhongo *et al*., 2019). Although solid relationships have been reported between NDVI and biomass estimates (Filella *et al*., 2004; Gómez *et al*., 2014; Shoshany & Karnibad, 2011), only weak relationships, have been reported for scrublands (Calvão & Palmeirim, 2004; Gómez *et al*., 2014). NDVI's ability to estimate fuel quantity is limited. The limitation of NDVI estimates is that they indicate vegetation greenness rather than vegetation quantity and structure (Leblon, 2005). Moreover, green, healthy vegetation has a higher NDVI value than dry, dead, leafless vegetation and bare ground since the green vegetation absorbs the visible light reflecting the infrared, leading to high NDVI values.

Estimating fuel/biomass accumulation in rangelands remains a challenge, especially in an arid area where vegetation is senescent and not easily discernible by remote sensing techniques for the most significant portion of the year (Marsett *et al*., 2006). Therefore, the inability of remote sensing techniques limits NDVI in quantifying biomass accumulated in rangeland areas. Alternative ecosystem productivity indicators (such as Dry Matter Productivity (DMP), Net Primary Productivity (NPP), Gross Primary Productivity (GPP), and Net Ecosystem Productivity (NEP)) are proposed for use in wildfire prediction. Ecosystem productivity has been reported to be a promising indicator of the current condition of the land surface area with application in different ecological systems and processes (Gower *et al*., 2001). According to Running *et al*. (2009), ecosystem productivity indicators integrate geochemical, climatic, and anthropogenic influences, giving them universal applicability and suitability even for agricultural analyses. The commonly used ecosystem productivity variables include the GPP, NPP, and DMP due to the high uncertainties in model results associated with NEP, limiting their accuracy and application (Luyssaert *et al*., 2010). DMP indicates the vegetation growth rate or the biomass increase and quantifies the Net Primary Productivity of an ecosystem in kgDM/ha/day (Swinnen *et al*., 2021a). Therefore, using the time series of DMP enables identifying high and low biomass production locations, making it a critical factor in wildfire warning systems. DMP can be derived from Gross Dry Matter Productivity (GDMP) using an algorithm (Equation 5) that was developed based on the Montieth model (Monteith, 1972; Swinnen *et al*., 2021a).

The DMP algorithm (Equation 5) uses some inputs derived from different remote-sensed products. Algorithm inputs include the Global meteorological data of temperature and incoming Radiation (R) as per the Monteith model (Monteith, 1972), the fraction of photo-synthetically active radiation absorbed by the green elements of the canopy (fAPAR), Light Use Efficiency (ε_{LUE}) values of different land cover types, Normalized temperature effect (ε_T), Normalized CO_2 fertilization effect (ε_{CO2}), autotrophic respiration (ε_{RES}) and autotrophic respiration (ε_{AR}) (Swinnen *et al*., 2021a). The inputs are combined as indicated in the equation. High-accuracy-free DMP data at a spatial resolution of 300m are available for environmental and agricultural studies (Swinnen *et al*., 2021b). The DMP product was assessed by comparison with other products and had R^2 ranging from 0.55 to 0.96 (Swinnen *et al*., 2021b).

$$GDMP = R.\varepsilon_c . fAPAR.\varepsilon_{LEUE_c} .\varepsilon_T .\varepsilon_{CO_2} (.\varepsilon_{RES}) \quad \text{Equation 4}$$

$$DMP = R.\varepsilon_c . fAPAR.\varepsilon_{LEUE_c} .\varepsilon_T .\varepsilon_{CO_2} .\varepsilon_{AR} (.\varepsilon_{RES}) = GDMP \times \varepsilon_{AR} = GDMP \times 0.5 \quad \text{Equation 5}$$

3.3.5 Soil moisture

Using soil moisture in wildfire prediction was uncommon in earlier fire prediction models and fire danger rating systems. However, recent advancements in wildfire predictions have increased soil moisture use, realising its link to FMC. Over the years, the improved accuracy of SM estimates derived from dense SM networks has increased the use of SM information in environmental and prediction studies (Sharma & Dhakal, 2021). These field-based soil moisture data have become critical parameters in wildfire prediction models. These, in addition to the available remotely sensed data, have improved the modelling and monitoring of wildfires in different ecosystems. Despite dense soil moisture networks in developed countries, field-based soil moisture data is lacking in developing countries, especially in Africa, limiting its use in wildfire monitoring and prediction.

Therefore, significant resources have been committed to developing missions devoted to soil moisture sensing (Ochsner *et al*., 2013). The recently launched satellite missions, the ESA's Soil Moisture and Ocean Salinity (SMOS) and NASA's Soil Moisture Active Passive (SMAP), devoted to assessing surface soil moisture, provide quantitative SM estimates (Entekhabi *et al*., 2010; Kerr *et al*., 2010). Since their launch, the two missions have provided continuous and accurate information that is now used in wildfire prediction and monitoring. The missions operate at a microwave-protected L-band (1.4 GHz), an optimal frequency for SM retrievals (Kerr *et al*.,

2010). The SMOS mission launched in November 2009 has provided three-day interval global surface (0-5cm) SM estimates with a 40 km spatial resolution and 0.04 $m^3 \cdot m^{-3}$ accuracy (Sánchez-Ruiz *et al*., 2014). The product is currently being used for high-accuracy environmental and agricultural applications due to the near real-time availability of the dataset despite its limitations of high spatial resolution that restrict its use at a regional scale (Chaparro *et al*., 2016a). Downscaling algorithms have been developed using surface temperature and NDVI products to produce more refined products requiring high-resolution applications (Piles *et al*., 2014). On the other hand, the SMAP mission launched in January 2015 retrieves SM estimates from the SMAP radiometer descending and ascending half obit passes and sentinel -1A and -1B radar (Das *et al*., 2020). The mission provides 12 days intervals of 3km and 1km resolution global soil moisture estimates with an accuracy ranging between $0.02 m^3/m^3$ to $-0.6 m^3/m^3$ (Das *et al*., 2019).

The presence of data from these missions has created potential use for SM applications in wildfire danger warning systems. Nonetheless, there is limited literature on the use of SM in wildfire prediction. A recent study by Chaparro *et al*. (2016b) employed SMOS-derived soil moisture data in a forest fire study in the Iberian Peninsula. According to Chaparro *et al*. (2016b), combining SMOS soil moisture and LST provides more accurate estimates of wildfire risk, as evidenced in their study area. Moreover, Chaparro *et al*. (2016a) reported higher wildfire risk estimated when anomalies of SM and LST were used. Earlier studies employed the SM dataset from Earth Observation Satellites (ERS-1 and 2) to assess pre-fire conditions in Siberia (Bartsch *et al*., 2009). Their results indicated limited fires and burned areas in wet soil conditions, with over 80% of recorded fires occurring during dry soil conditions in summer (Bartsch *et al*., 2009). Forkel *et al*. (2012) also used SM data obtained from the Advanced Microwave Scanning Radiometer—Earth Observing System (AMSR-E) and identified surface soil moisture as a critical factor in the propagation of extreme fire events in Siberia. However, according to Kerr *et al*. (2010), SM estimates derived from ERS and AMSRE were restricted by lacking penetration through thick vegetation and eminent exposure to radiofrequency interference. These limitations have throttled their use in wildfire monitoring.

2.4 Wildfire monitoring systems & tools

Wildfire monitoring aims to reduce the possible risk and ensure wildfire damage to the ecosystem is well assessed. The considerable environmental, human, and economic losses caused by

wildfires create the need to monitor the occurrence of wildfires and their impact using different tools to develop prevention, recovery, and response plans. Therefore, wildfire monitoring could be in fire detection systems or burnt area monitoring tools.

2.4.1 Fire detection and early warning systems

Wildfires continue to occur annually, burning millions of hectares of land globally and affecting human and animal lives. Despite the substantial progress in developing fire prediction technologies worldwide, fire forecasts remain inefficient. Therefore, many communities and regions adopt well-coordinated systems and tools for wildfire detection and early warning to reduce wildfire impacts on nature. Most wildfires go through four development stages; incipient fire growth, fully developed fire and decay, but fire detection and early warning tools aim to detect fires in the early stages (Barmpoutis *et al*., 2020). Several systems are being used for wildfire detection; Barmpoutis *et al*. (2020) categorise them into three, namely, airborne (aircraft), space-borne-based systems (satellites, Unmanned Aerial Vehicles), and terrestrial (fixed camera, sensor systems). These systems are supported by several wildfire danger predictions that are being studied for different environments.

Numerous wildfire detection and early warning systems and tools are being used worldwide and proposed by different authors. Although earlier wildfire detection systems depended on images, photos, and videos recorded by cameras to detect wildfire features, recent developments have improved the speed of fire detection and confirmation depending on the technology used. The Fire sensor networks have become a standard wildfire detection method; in their study, Lutakamale & Kaijage (2017) proposed using a wireless sensor network for wildfire monitoring and detection based on the environmental humidity, smoke, and temperature. Although earlier sensors had no communications means (Barmpoutis *et al*., 2020), newly developed sensors and sensor networks are connected to a cloud. The sensors can send warning messages about of location of the fire to people living within the neighbouring community, who can then notify responsible authorities (Lutakamale & Kaijage, 2017). A project by Müller *et al*. (2015) also developed fire sensors that use hydrogen molecules, a particular pyrolytic product, to detect fires to a distance of 105m from the sensor, making it suitable to detect fires. Sharma *et al*. (2019) also proposed a generic sensor network for fire detection in remote and inaccessible areas with the ability to visually represent sensor nodes in real-time using a web map system. This natural time fire detec-

tion system covering up to 4sq kilometres was proven effective in tracking fire incidents to facilitate the whole fire management system.

Recent remote sensing fire detection methods have also been proposed and applied in fire detection in different areas. Mazzeo *et al*. (2022) recently presented the Integrated Satellite System (ISS) for fire detection and prioritization in Italy. The system depends on the Fire Danger Dynamic Index (FDDI) and Robust Satellite Techniques (RST). The ISS uses data obtained from MODIS, AVHRR, and Spinning Enhanced Visible and InfraRed Imager (SEVIRI) to avail near real-time integrated fire presence and danger information over the affected area (Mazzeo *et al*., 2022). Li (2019) presented an autonomous early warning system that used Unmanned Aerial Vehicle (UAV) that regularly flies over forests following predetermined routes to collect data (containing forest temperature and humidity) from sensors deployed on trees. The data from the sensors to the aircraft is collected using Bluetooth Low Energy (BLE) for wildfire monitoring and prediction; data is then used to provide early warnings before a fire eruption.

2.4.2 Burned area monitoring

Accurate data on burned area location and extent is crucial in sustainable fire management applications. This information is applicable in determining future wildfire patterns, assessing the trends in fire occurrence, identifying drivers for wildfires, and evaluating the environmental, social, and economic damage of a given wildfire incident. This final section elucidates the different burned monitoring tools, indices, and methods used and employed in various studies.

2.4.2.1 Burned area monitoring tools and methods

Burned area data in many countries is lacking and inconsistent relative to other burned area data, especially in Africa, with very little progress in monitoring and managing burned areas after wildfires. However, the need for complete, accurate records of the geospatial wildfire occurrences is essential in assessing the post-fire effects such as biomass loss, emissions, and hazards (Sharma & Dhakal, 2021). Burn severity indices are commonly used to evaluate fire impacts across a burned area. Several indices have been proposed to map burned areas: the Composite Burn Index (CBI) and Normalized Burn Ratio (NBR). The NBR has been modified over time for the delta Normalised Burn Ratio (dNBR, Equation 6), relative dNBR (RdNBR, Equation 8), and the Relativized Burn Ratio (RBR) (Key & Benson, 2006; Miller & Thode, 2007; Parks *et al*., 2014). The CBI, with typical values ranging from 0.0 to 3.0, was proposed by Key & Benson

(2006) to indicate the magnitude of fire effects. The index incorporates community factors such as the quantity of vegetation/fuel consumed, soil colour, blackened/ scorched trees, new species colonisations, and re-sprouting plants after-burn.

The commonly used burn severity index, the normalised burn ratio (NBR), is estimated using Equation 6, representing burn severity using post-fire imagery, isolating burned areas from un-burned areas (Escuin *et al*., 2008; García & Caselles, 1991). The determination of NBR capitalises on the fact that near-infrared (NIR) reflectance reduces the shortwave infrared (SWIR) reflectance increases after the fire due to fire damage to vegetation. However, it was found that NBR does not provide the extent of change, which resulted in the development of the differenced NBR (dNBR) derived by subtracting post-fire NBR from pre-fire NBR as in Equation 7 with typical values ranging between −2000 and 2000. The obtained difference is assumed to correlate to the measure of environmental change caused by the fire (Key & Benson, 2006). Over the years, the scientific community has preferred the dNBR over NBR due to its ability to separate signals directly related to wildfires (Key & Benson, 2006; Kolden & Rogan, 2013; Veraverbeke *et al*., 2011).

Several authors have assessed the efficiency of dNBR; for example, Allen *et al*. (2008) used ten fires in Alaska and found a 0.74 positive correlation between CBI and dNBR. Boucher *et al*. (2017) indicate an excellent consistency for the dNBR-CBI relationship assessed using boreal forests of eastern Canada despite better non-linear models showing the relationship better than linear models. Tran *et al*. (2018) also found that dNBR produced the most accurate burn severity mapping for severity in re-sprouting open forests and woodlands. The RBR index, a Landsat-based burn severity metric, was also proposed as a robust alternative to NBR-based dNBR and RdNBR, which are sensitive to fire caused changes in vegetation (Chen *et al*., 2021; Parks *et al*., 2014). Equations 6-7 indicate the expression for deriving NBR, dNBR, RdNBR and RBR.

$$NBR = \frac{(NIR - SWIR_{2.2\mu m})}{(NIR + SWIR_{2.2\mu m})}$$ Equation 6

$$dNBR = NBR_{pre-fire} - NBR_{post-fire}$$ Equation 7

$$RdNBR = \frac{dNBR}{\left|(NBR_{pre-fire})\right|^{0.5}}$$ Equation 8

$$RBR = \frac{dNBR}{NBR_{pre-fire} + 1.001}$$ Equation 9

Many tools have been developed for mapping burn severity using the different burn severity indices. Remote sensing remains a primary tool in mapping burned areas and estimating the impact of wildfires due to its ability to consistently cover large spatial areas, even in remote regions (Chuvieco *et al*., 2020). Most fires in the remote wilderness make manual burn area mapping methods ineffective, rendering remote sensing a promising alternative. Burn severity indices are estimated using most remote sensing applications in fire management and Landsat products research (French *et al*., 2008). The USGS has also invested efforts in combining satellite data from MODIS, AVHRR, GEOS and Landsat to derive freshly burned area perimeters indicating the date and time of burned area detection to determine undocumented fires (Howard *et al*., 2014). Several other multispectral Very Near Infrared (VNIR) fire severity indices have been proposed for mapping burn severity, including the Normalized Difference Vegetation Index (NDVI, Equation 10, Tucker, 1979), the Soil-Adjusted Vegetation Index (SAVI, Huete, 1988), the Modified SAVI (MSAVI, Qi *et al*., 1994) the Green NDVI (GNDVI, Gitelson & Merzlyak, 1998), Burned Area Index (BAI) (Chuvieco *et al*. 2002) and the Global Environmental Monitoring Index (GEMI, Pinty & Verstraete, 1992). These indices use the property of decreased NIR observed for burned areas to assist in discriminating burned areas from unburned areas. However, according to Chuvieco *et al*. (2002b), NDVI, GEMI and BAI indices tend to classify albedo surfaces such as water and cultivated soil as burned areas, while SAVI may also classify sparsely vegetated areas as burned areas.

Earlier efforts to map wildfires by the USGS led to the development of the Burned Area Essential Climate Variable (BAECV). This product maps burned areas larger than four hectares by combining models of burn probability with a region-growing algorithm (Hawbaker *et al*., 2017). The BAECV products provide information about patterns of wildfire occurrences that may not have been recorded in the fire databases, especially in the grassland ecosystems of the United

States. The USGS also developed the Monitoring Trends in Burn Severity (MTBS) that maps burned areas from prescribed fires of size thresholds of 500 and 1,000 acres in the Eastern and Western United States Respectively (Picotte, 2020). However, the project misses many burned areas, especially smaller fires (Howard *et al*., 2014). The FMT QGIS tools have now been developed to map smaller fires not mapped by the MTBS project (Picotte, 2020). The FMT tool uses Landsat imagery to examine the Normalised Difference Vegetation Index (NDVI) curves to determine the differences between Landsat scenes and produce NBR, burned area perimeters, and determine dNBR and RdNBR images. The FMT tools also can establish thresholds and metadata after examining imagery (Picotte, 2020).

2.4.2.2 Burned area and severity studies

Many studies have been conducted to map burn severity using different burn severity indices globally. To name but a few, Teodoro & Amaral (2019) analysed affected areas by the fire of 2016 for two municipalities in Portugal using NVI and NBR derived from Landsat OLI and Sentinel 2A MSI before and after fire data. Their study indicated a significant reduction in NDVI after the fire, with the highest differenced NDVI, observed for burned areas. According to the authors, Sentinel 2A data provided a better estimate of burned area (less than 7.8% error) than Landsat data (13% error) when compared to the filed data due to the higher spatial resolution (Teodoro & Amaral, 2019).

Chen *et al*. (2020) found that the Global Environmental Monitoring Index (GEMI) index had closer predictions (R^2 = 0.77 and 0.85 for uni-temporal and bi-temporal, respectively) of burn severity. The GEMI index was less affected by the differences in vegetation than CBI and NBR in the Arctic Tundra Ecosystems, making it a promising index with the capability to map fire severity for heterogeneous vegetation types, seasons, and ecological regions. Their results also agree with Tran *et al*. (2018), who concluded that the optimal spectral index for fire severity mapping varies with forest types in Australian Temperate Forests. Hawbaker *et al*. (2017) presented a burned area detection algorithm of Landsat Burned Area Essential Climate Variable (BAECV) products derived from dense Landsat time series. The burn classifications for the algorithm are derived from burn probability surfaces using pixel-level and were found to map over 30% more fires than Global Fire Emissions Database (GFED) and MTBs.

2.5 Conclusion

A review of the literature has shown that limited studies on wildfire occurrence in Africa and sub-Saharan Africa have been conducted. Yet, wildfire occurrences remain a critical challenge affecting African savannahs. Although controlled fires in the rangelands play a crucial role in maintaining the vegetation structure, the impact of large uncontrolled fires is evident. Therefore, it is essential to have in place early warning systems and tools such as fire prediction models to help communities prepare for and manage wildfires. Moreover, there is growing evidence of the potential of remote sensing and machine learning tools and models in wildfire prediction. Many studies applied meteorological variables for wildfire prediction. However, their use in the sparse meteorological networks of Sub-Saharan Africa is limited. Environmental variables such as Land surface temperature, Dry matter productivity, and soil moisture offer a promising alternative for wildfire prediction that must be explored. In addition, new tools for monitoring burned areas and burn severities must be evaluated for their applicability in different environments.

CHAPTER 3: MATERIALS AND METHODS

3.1 Study Area

The study was conducted in Kgalagadi District (135287.8 Km^2) located southwest of Botswana, about 400km west of Gaborone city, lying between latitudes $20^0$54' and $21^0$20'S longitudes -$23^0$16' and -$26^0$46'E (Figure 2). The district lies in the Kalahari/ Okavango basin and is characterised by a large portion of rangeland housing large numbers of wildlife and livestock. Kgalagadi is a semiarid district with a relatively higher fire susceptibility to wildfires since fuels are dry most of the year due to dry conditions.

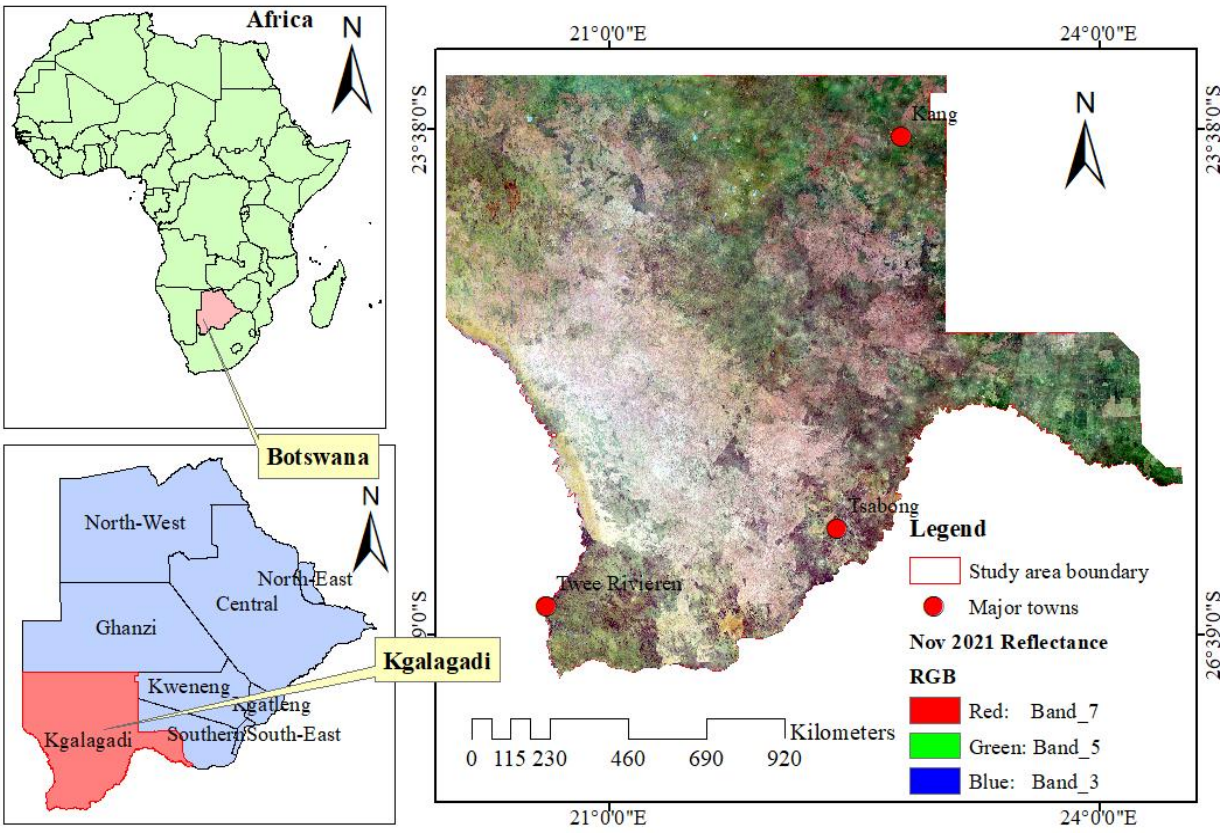

Figure 2: Location of the study area indicating the burn scar of the 2021 mega fire, inset map indicating the location of Botswana in Africa.

3.1.2 Climate, soils, and vegetation

The climate of the Kgalagadi district is characterised by a tropical or subtropical climate (Cantymedia, 2022). There has been a significant variation in the area's climate over the last two 10-day decadal, with the driest years being 2007, 2013, 2017, and 2019 (Figure 3). The region is prone to droughts with less than 300mm of annual precipitation in the past years and relatively low average temperatures (Figure 3, Kgosikoma & Batisani, 2014). The region experiences two significant winter and summer seasons and has an average temperature of 20.2°C, with the highest (27.2^0C) temperatures experienced in January. The lowest temperatures occur in June, with an average temperature of 11.7°C. The average annual precipitation in the area ranges between 300mm and 350mm. The highest (58.4mm) rainfall is received in February, while the driest month (2.5mm) is in July, with very low or no precipitation in most districts. Overall, the area experiences scanty rainfall, with the majority of the days in the year being dry and only 42 days of rain, with February having the highest precipitation days.

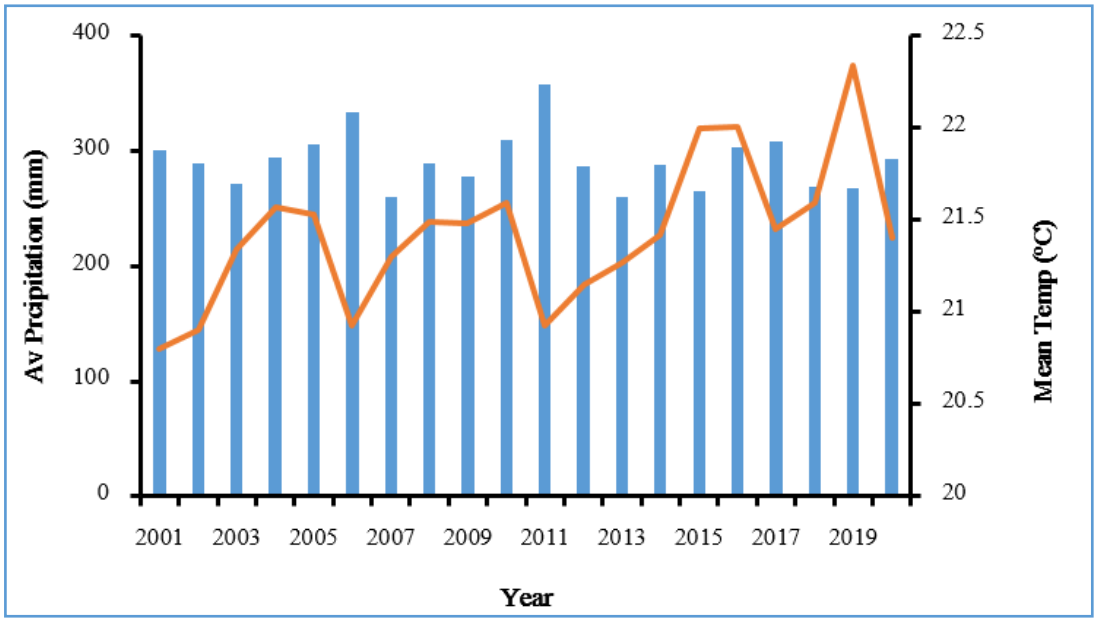

Figure 3: Climate of Kgalagadi District (2001 and 2022) indicating the average annual precipitation (Bar graph) and mean annual temperatures (Line graph) (Source: World Bank Group, 2022)

The vegetation of the Kgalagadi district is a savannah grassland interspersed with trees. Generally, the landscape comprises sand veld bare rolling dunes enshrouded by varying vegetation ranging from grasslands to low shrubland and shrub savannah, especially along the Nossop and Molopo rivers (Kgosikoma & Batisani, 2014). The vegetation of the district is characterised by species such as *Stipagrostis ciliata* and *Cymbopogon schoenanthus* with other grass species, includ-

ing *Aristida meridionalis* and *Centropodia glanca,* and tree species like *Vachellia reficiens,* and *Boscia albitrunca*. The vegetation grows fast when rains are received in the area during the summer season and is a source of herbage to various wildlife, especially in the Kgalagadi Transfrontier park, with large wildlife populations, including giraffes, pangolins, lions, hyenas, leopards, and wildebeest. Vegetation in the area has become tolerant to fire, with the ability to regenerate after successive wildfire incidents occurring. The vegetation re-sprouts immediately after the site receives rains months after the fire season. Kalahari sandy soils are the dominant soil texture in the district, with Arenosols forming the predominant soil type of the area. Other soil types in the region include the luvisols, gleysols, and regosols in the southern part of the district, while small areas of calcisols are in the eastern parts of the study area.

3.1.3 Topography

The topography is generally characterised by plain terrain with an average elevation of 1,065m above sea level. Locations in the northern part of the district are at higher altitudes than the southern area, with a gentle slope of the land to the south (Figure 4).

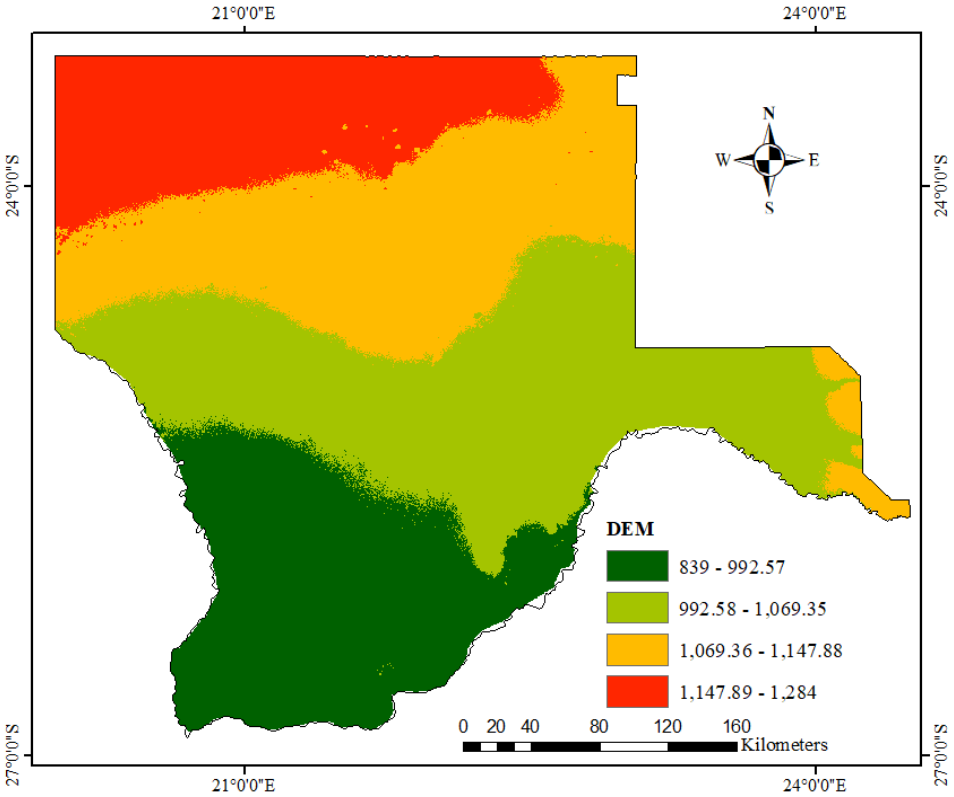

Figure 4: Elevation (meters above sea level) of Kgalagadi district (Source: NASA, 2020)

3.1.3 Land use and land cover

The area is predominantly a wildlife conservation area, with most of the land area being covered by the national park, the Kgalagadi Transfrontier Game Park (Figure 5). Pastoral farming and ranching are also prominent in the district, with many ranches in the Eastern part of the district (Kgosikoma & Batisani, 2014). The low rainfall and poor soil fertility inhibit successful arable farming; hence livestock production is the mainstay of the area. Pastures in the rangelands of Kgalagadi are grazed continuously by cattle, goats, and sheep, especially on communally owned land (Kgosikoma & Batisani, 2014). The district is sparsely populated, with an average population of 57,673 people majority of whom live in the southern part of the district (Statistics Botswana, 2018a). The central administrative town of the district is Tsabong, with the most government offices in the town.

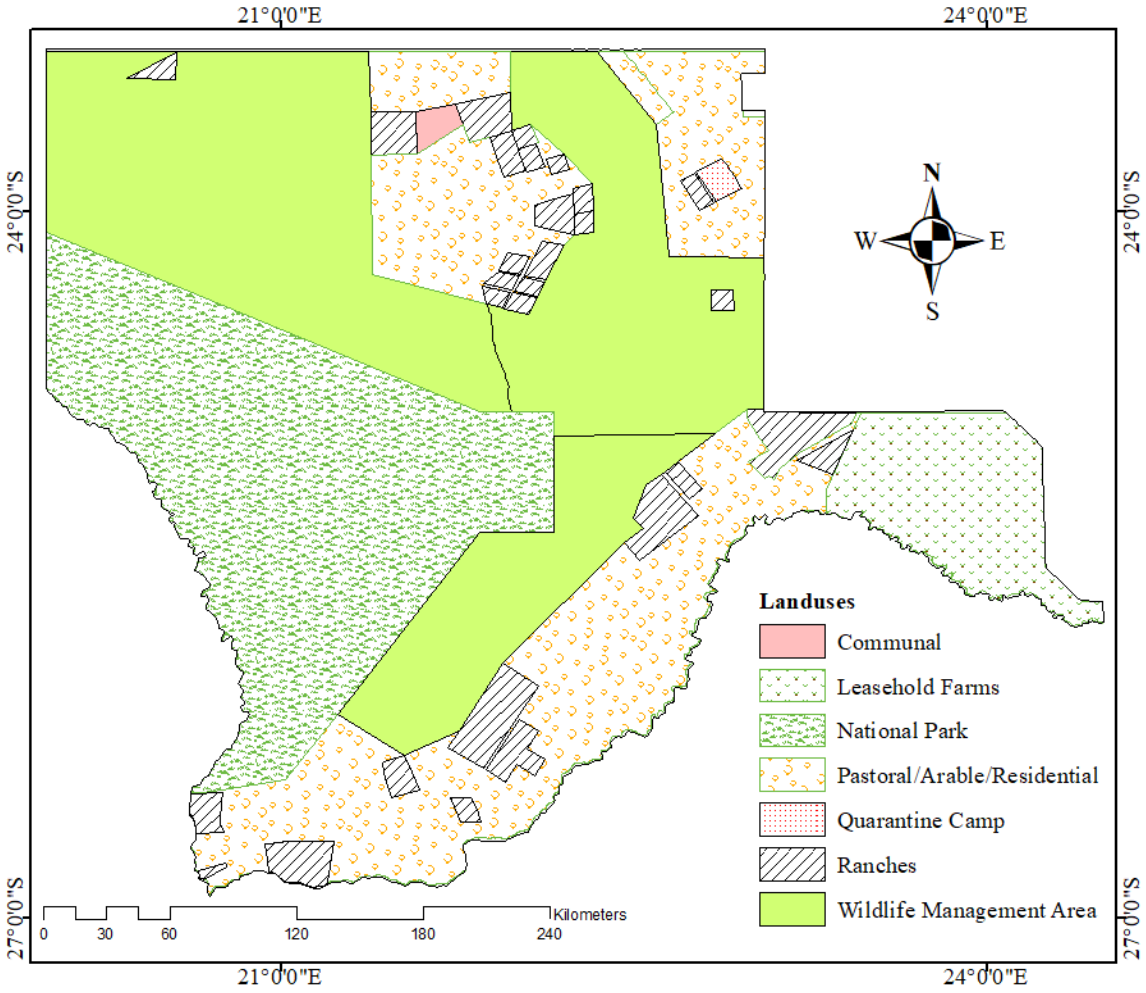

Figure 5: Land use types of Kgalagadi district (Source: Botswana Department of Surveying and Mapping, 2019)

Figure 6 shows the distribution of land cover types in the Kgalagadi district developed by the ESA World Cover project 2020 with an overall accuracy of 94.0% and a Kapa coefficient of 93% (Zanaga *et al*., 2021). Grasslands form the primary land cover type in the district, covering 54.4% of the district's land area. Shrub land includes the second-largest land cover covering 45.3% of the land area. About 0.264% of the land is bare or with sparse vegetation, while 0.004% is built-up and 0.011% is water bodies and herbaceous wetlands.

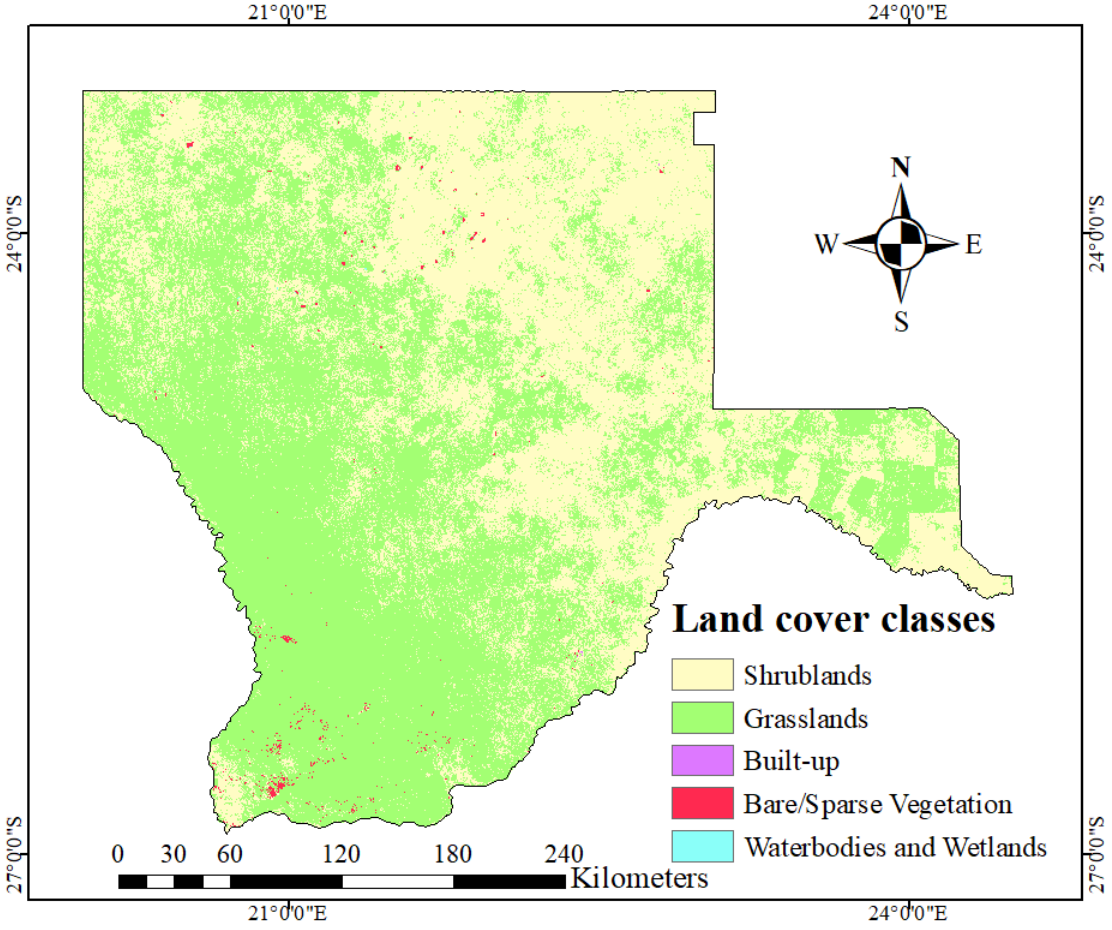

Figure 6: Land cover types of Kgalagadi District (Sources: Zanaga *et al*. (2021))

3.2 Prediction of the occurrence of rangeland wildfires

The study developed a wildfire prediction model using live fuel moisture content, surface temperature, soil moisture content, dry matter productivity, and dead fuel moisture content. Active fire points recorded between 2015 and 2021 were used to develop and validate a wildfire prediction model. Figure 7 shows the step-by-step workflow followed for developing the prediction model.

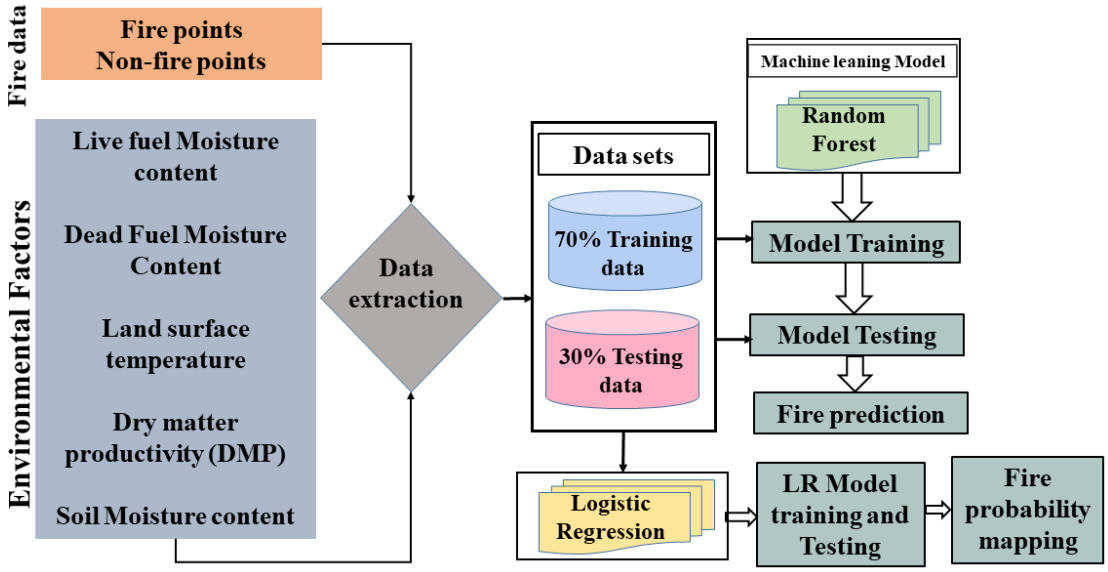

Figure 7: Workflow for wildfire prediction using remotely sensed products

3.2.1 Random forest

The Random Forest (RF) classification algorithm in R-project software was used to predict wildfire occurrence in the study area. The RF algorithm has been reported to give accurate wildfire predictions relative to other algorithms with the capacity to estimate missing data and work with large datasets (Shahdeo *et al*., 2020). Random Forest (RF) is an algorithm developed by Breiman and Cutler in 2001 that can be used for classification and regression. Unlike logistic regression, RF has become the most applied machine learning algorithm due to its ability to give accurate predictions using large datasets with a negligible effect of missing values and overfitting. It is an ensemble learning method that operates by constructing many decision trees (*ntree*) using bootstrap samples from the original dataset producing a classification or regression tree (Shahdeo *et al*., 2020; Su *et al*., 2018). In this study, the bootstrap samples were drawn with replacement. By training each tree using different samples, the overall forest variance is lower despite having a high variance amongst trees while at the same time minimizing the bias (Shahdeo *et al*., 2020). During testing, predictions are calculated as the average of predictions of each decision tree. The model output is the average of all trees, that is, the different classes in the case of classification or means prediction in RF regression.

The algorithm is designed to retain about one-third of the samples for validation, referred to as the Out-Of-bag (OOB). In addition, at each node in the tree, the RF algorithm randomly samples some of the predictor variables referred to as '*mtry*' to produce the best split for each predictor variable. The number of trees (*mtree*) and the number of variables at the nodes (*mtry*) are hyper-

parameters. However, it is recommended that the mtry be the square root of the number of variables ($\sqrt{P}$ where P is the number of variables) (Probst *et al*., 2019).

The number of trees and variables at the nodes affects the overall OOB; as it tends to stabilise with the increase in the number of trees until the RF converges (Probst *et al*., 2019; Probst & Boulesteix, 2017). Overall, the number of trees should be large enough to ensure a lower error rate. For this study, increasing or decreasing the number of trees beyond 700 did not change the results for the better. RF can also be used to rank the importance of variables. RF also calculates the variable importance (VI) of the predictor variables by calculating the OOB error for each tree (t) and permuting each variable (X^j). In contrast, the other variables in the OOB data are left unchanged, and the OOB error (errOOB) is calculated in the permuted dataset (Grömping, 2009; Su *et al*., 2018). The variable importance is calculated as:

$$VI(X^j) = \frac{1}{ntree}\sum_t (err' OOB_t^j - errOOB_t) \qquad \text{Equation 10}$$

Where *ntree* is the number of trees in the forest and $\sum$ indicates the sum of all trees, for this study, RF classification was used; thus, the OOB error suggests the rate of misclassification by the forest. The aim is, therefore, to minimise the OOB by the RF algorithm. The RF can then be used to select contributing variables in the model.

3.2.2 Dependent variable

Wildfires obtained using Visible Infrared Imaging Radiometer Suite (VIIRS) sensors at 375km resolution were obtained from the NASA Fire Information and Resource Management System (FIRMS). The fire points were used as an indicator of success. The data is processed by the University of Maryland using the standard quality Thermal Anomalies/Fire locations. The wildfire data presented as point data containing the location (x and y coordinates), date of capture, and time of capture is supplied by FIRMs. For the study period, a total of 99,651 fires were recorded by VIIRS (

Table 1) in the study area.

Table 1: Number of fires recorded in Kgalagadi between 2015 and 2021 (Source: FIRMS website)

Year	Number of fire points
2015	1210
2016	715
2017	17,154
2018	6,679
2019	382
2020	7,666
2021	65,845
Total	99651

Data for Botswana were downloaded from the FIRMS website (*https://firms.modaps.eosdis.nasa.gov/*) and clipped to the study area using ArcGIS software to remove fires outside the study area. The location of the wildfire record for the study area is indicated in Figure 8 below.

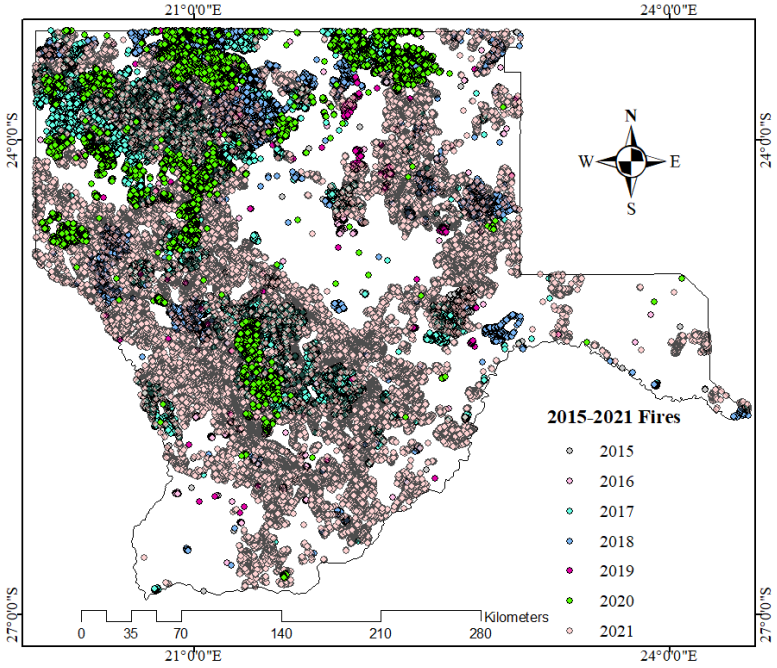

Figure 8: Recorded wildfires in Kgalagadi district 2015-2021 (Source: FIRMS website)

Since both random forest classification and logistic regression require binary variables as the prediction variables (Guo *et al*., 2017; Su *et al*., 2018), random points of the same number as fire points were generated using the create random points tool in Arcmap (10.7) as control for the study. A buffer zone of a 1000m radius was created around fire points for each year to avoid non-fire points from being created very close to the fire points, and points that fell in the buffer

zone were later excluded. The study applied the double random principle of time and space and randomly assigned dates and times of occurrence from the fire seasons to the randomly created fire points (Guo *et al*., 2017; Su *et al*., 2018).

The study excluded all points with missing values from the final dataset used for the study. The overall dataset contained actual fire points (n=80,860) and non-fire points (n=76,965). For analysis purposes, the study assigned 1 and 0 to the fire points and non-fire points, respectively. The final dependent variable for RF and LR analysis contained 107,883 points. The data was split into 70% training dataset, and 30% testing dataset as applied in most machine learning studies.

3.2.3 Independent and dependent variables

The independent variables used in this study included soil moisture content (SM), Dry matter productivity (DMP), Land surface temperature (LST), and two fuel characteristic variables, including the dead fuel moisture content (DFMC) and Live fuel moisture content (LFMC). This study resampled all variables to 1000m spatial resolution to ensure accurate comparisons of the variables. Values of the independent variables for the day/10-days decadal before the fires were extracted to the fire points and non-fire points and then exported to Excel sheets. Details and descriptions of the independent/ predictor variables follow are provided in the following section.

3.2.3.1 Soil moisture/ surface moisture

This study used the SMAP surface soil moisture (0-0.05m) for fire prediction. Soil moisture products were acquired from NASA National Snow and Ice Data Centre Distributed Active Archive Centre. The SMAP/Sentinel-1 L2 Radiometer/Radar 30-Second Scene 3 km EASE-Grid Soil Moisture V003 was used for the study. The product provides land surface conditions estimates for agricultural and environmental applications requiring high-resolution data. This soil moisture product is retrieved from SMAP radiometer descending and ascending half obit passes and sentinel -1A and -1B radar (Das *et al*., 2020). The daily data were downloaded from the online repository and then resampled to 1000m resolution using the resample tool in ArcGISver 10.7. The mean soil moisture was then estimated for each 10-day decadal using the daily data. The soil moisture values for the study area from the SMAP range between $0.02cm^3/cm^3$ to $-0.5cm^3/cm^3$ align with those indicated for SMAP-sentinel1 active-passive soil moisture retrievals (Das *et al*., 2019). Figure 9 shows the spatial distribution of soil moisture in the study area.

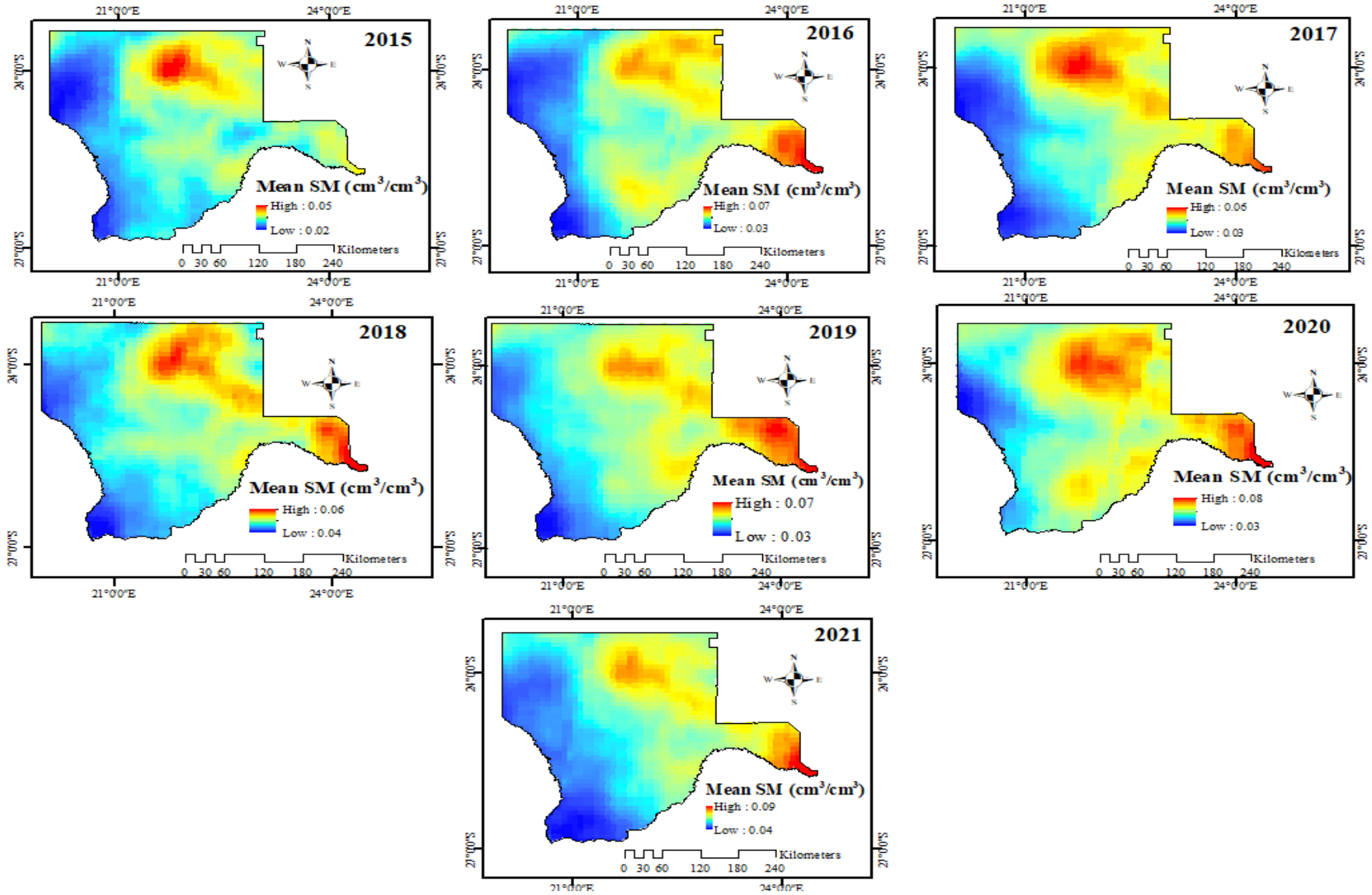

Figure 9: Thematic maps for the study area indicating the mean soil moisture content during the study period

3.2.3.2 Land surface temperature

This study used the MODIS daily Land Surface Temperature/Emissivity (MOD11A1 v61) data obtained from the NASA MODIS site (*https://modis.gsfc.nasa.gov/data/dataprod/mod11.php*). The study retrieved MODIS Terra LST day data at a spatial resolution of 1km using the generalized split-window algorithm and 6 km grids by the day/night algorithm (Wan *et al*., 2021). The Terra day data was preferred to Aqua due to the 10:30 am overpass with clear sky compared to Aqua with 1:30 pm overpass time (Butt *et al*., 2021; Wan *et al*., 2021). The MOD11A1 has been applied in several other fire-related studies (Butt *et al*., 2021; Freeborn *et al*., 2022) and other environmental studies(Roznik *et al*., 2019; Xie *et al*., 2022). LST datasets were downloaded for the study period using the Nasa Application for Extracting and Exploring Analysis Ready Samples (AρρEEARS). Obtained datasets were converted to degrees Celsius from digital numbers that range from 7,500 to 75,000 by applying the scale factor and addition offset and then deducting -273.15 to convert the form Kelvin to Celsius using the raster calculator spatial analysis tool in ArcMap (Figure 10). The MODIS-derived LST has been reported to correlate significantly with Landsat 8-derived LST with an RMSE of 1.19K (Zhang & He, 2013). Similarly, an RMSE of 2.44K and bias of 1.43K were indicated for MODIS LST collection 6 data compared with in-situ station data in the Kalahari Desert (Duan *et al*., 2019).

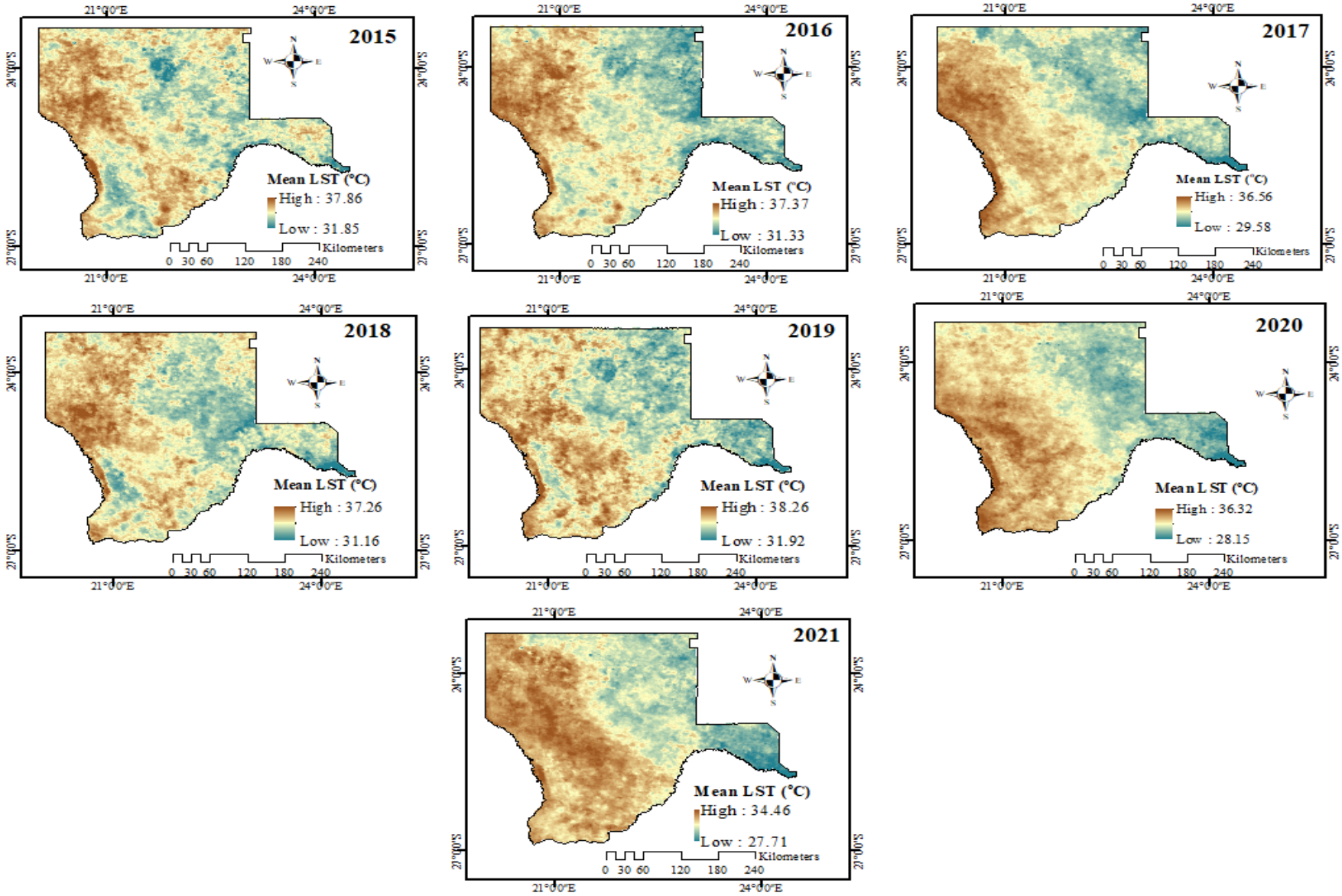

Figure 10: Mean Surface temperature during the study period (2015-2020)

3.2.3.3 Biomass accumulation

The biomass/ fuel accumulation during fire occurrence was assessed using the Dry Matter Productivity (DMP) data in ecosystem productivity monitoring. The data is freely available from the Copernicus Global Land Service site (*https://land.copernicus.eu/global/*) at a temporal resolution of 10 days and spatial resolution of 300m. The data downloaded contained digital numbers converted to physical values by multiplying by a scaling factor and adding the offset provided for the downloaded products using the raster calculator spatial analysis tool in ArcMap. DMP values range from 0 kg/ha/day to 327 kg/ha/day. After rescaling, the data were resampled to 1000m to match other products used in the study using the resample tool in ArcMap. The study compared the products with the land cover data obtained from the ESA World Cover project 2020 at a 10m resolution (Zanaga *et al*., 2021). The data agreed with the land cover classes with the lowest DMP values in bare areas, while the shrub land indicated the highest DMP for the study period (Figure 11). The DMP was prepared for the study period (2015-2021).

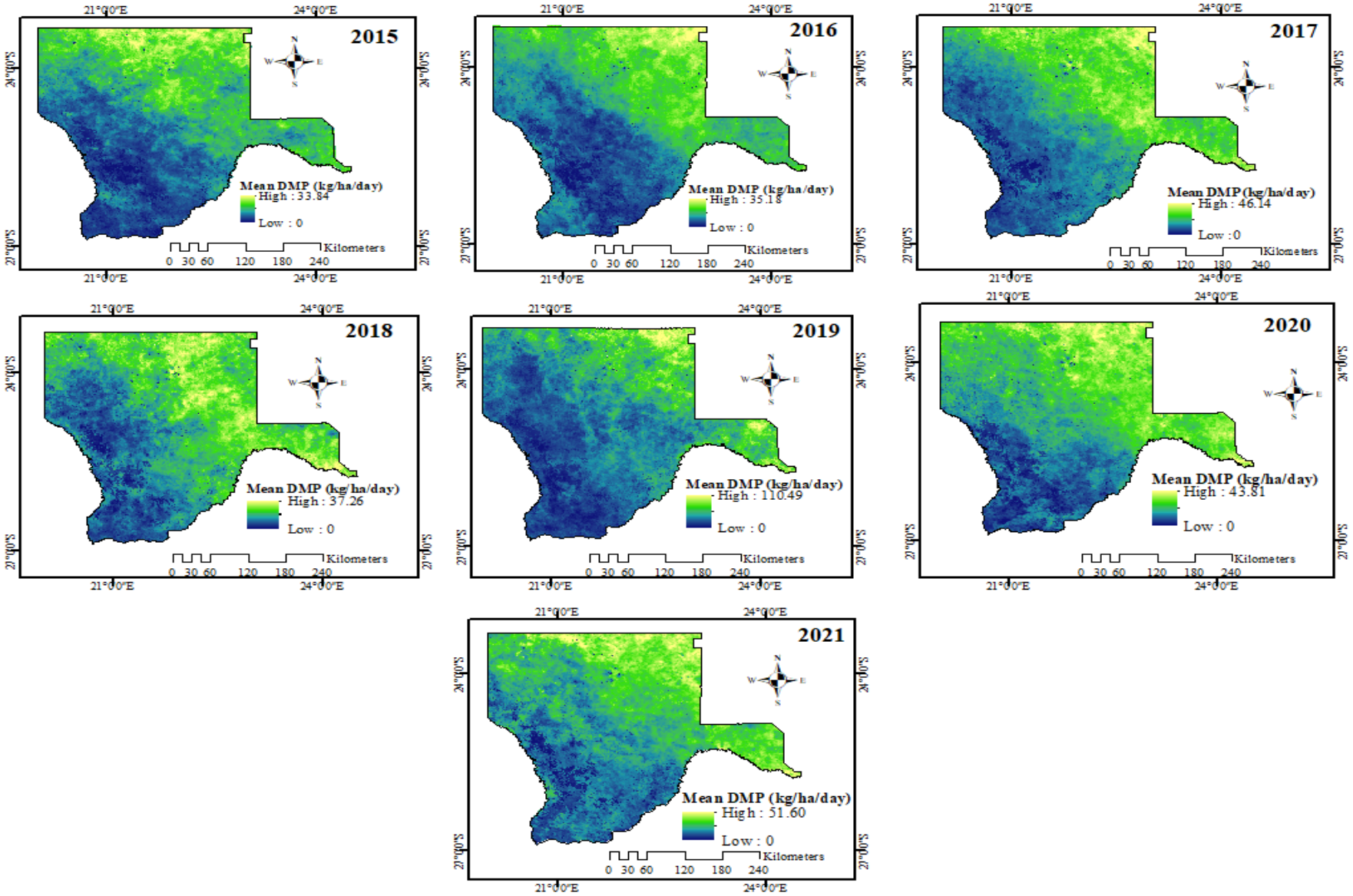

Figure 11: Dry matter productivity (kg/ha/day) variation for the study period 2015 to 2020

NDVI has previously been used to quantify the fuel load available when the fire occurred (Cao *et al*., 2013; Karimi *et al*., 2021; Nhongo *et al*., 2019). However, due to the inability of other vegetation indices to indicate the quantity of available fuel (Calvão & Palmeirim, 2004; Gómez *et al*., 2014), this study utilized DMP and calculated the cumulative DMP for each 10-day decadal using the raster calculator spatial analysis tool in ArcMap. For this study, the cumulative values were computed starting with the January first 10-day decadal when the highest rainfall amounts are received in the study area (Figure 12). Figure 12 indicates that the dry matter productivity increases significantly from January until April when the study area gets lower rainfall with a high positive correlation (r=0.998) between rainfall and DMP variation in the study area. Although some rains were received from October and December, the quantities were meagre, and many fire incidences occurred during that period. The DMP values were extracted to the fire and non-fire points for the 10-day decadal before fire occurrence.

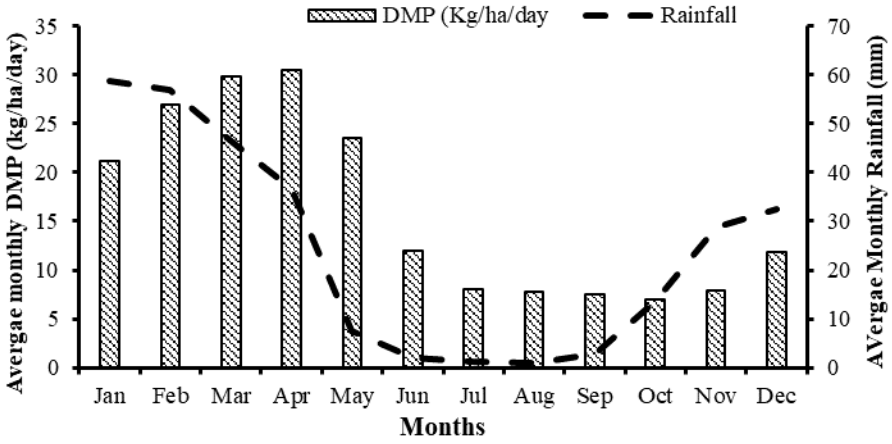

Figure 12: Average monthly variation in dry matter productivity (kg/ha/day) against rainfall average for the study period (2019-2021).

3.2.3.4 Live fuel moisture content

This study applied the empirical model proposed by Chuvieco *et al*. (2004) to compute live fuel moisture content (Equation 11). The LFMC estimates were derived using the NDVI and LST from an empirical equation developed by multiple linear regression. The model incorporates the day of the year (FD) function to account for the seasonal FMC variations (Equation 12, Castro *et al*., 2003; Chuvieco *et al*., 2004). The model developed for grasslands was used for the study since the most extensive areas are made of savannah grassland cover, where most of the fires in the study area occur.

$$LFMC_g = -57.103 + 284.808 \times NDVI - 0.089 \times LST + 136.75 \times FD_g \quad \text{Equation 11}$$

The function of the day was derived from Equation 12 (Chuvieco *et al*., 2004);

$$FD_g = \left(\sin\left(1.5 \times \pi \times \frac{Dy + Dy^{\frac{1}{3}}}{365} \right) \right)^4 \times 1.3 \quad \text{Equation 12}$$

Where; D_y is the day of the year.

The NDVI data at 300m spatial and ten days temporal resolution was obtained from the Copernicus Global Land service website (*https://land.copernicus.eu/global/products/ndvi*). The NDVI data were derived using Sentinel-3 OLCI TOA and PROBA-V using algorithms that utilise the NIR and red bands (Swinnen & Toté, 2022). FMC was estimated using the raster calculator spatial analysis tool in ArcMap l values obtained ranged between -50 to 350%, with most of the values falling between 0 and 200% (Figure 13). The negative FMC values obtained are due to the very low NDVI for the study area, with NDVI values below 0.1 (Chuvieco *et al*., 2004). Although the model was developed in temperate regions, it shows significant potential in predicting LFMC tropical areas with a similar variation in fuel moisture content which was the basis for the derivation of the year's day (FD).

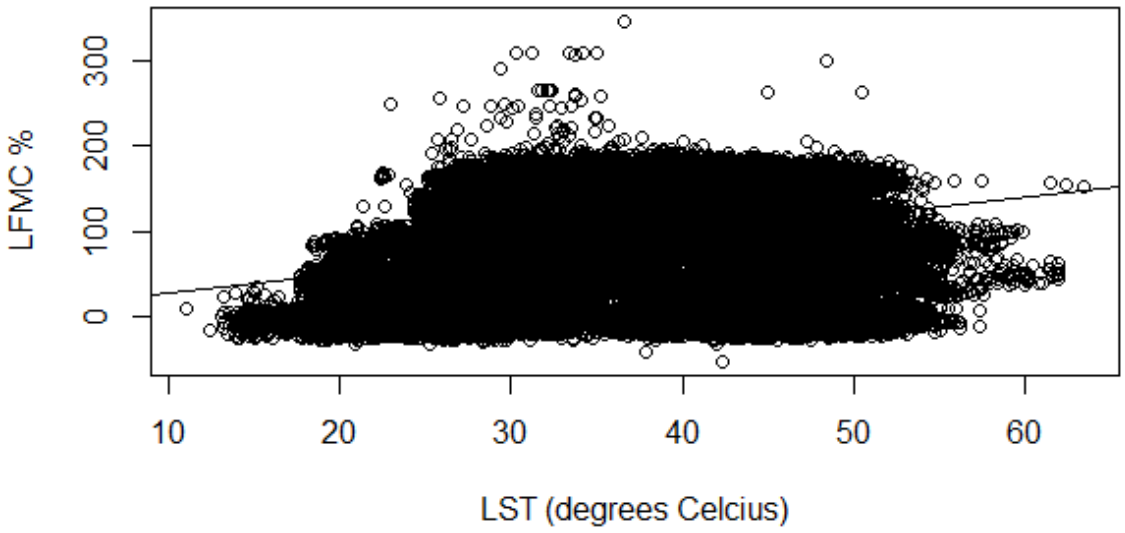

Figure 13: Distribution of LFMC values with varying LST (^{0}C) for the study period in the Kgalagadi District.

3.2.3.5 Dead fuel moisture content

DFMC estimates were derived using the regression model proposed by Zormpas *et al*. (2017). The model was developed using Landsat 8 derived Brightness Temperature (BT) estimates with validation results indicating a 73% accuracy for a complex Mediterranean ecosystem. MODIS

band 20 brightness temperature data were obtained from the USGS Earth data site (*https://appeears.earthdatacloud.nasa.gov/).* The daily BT data was derived from Tera MODIS thermal band 20 at a spatial resolution of 1 kilometre (Boschetti *et al.*, 2015). The data was clipped to the study area and then converted to Celsius degrees using the raster calculator spatial analysis tool before applying the proposed equation. DFMC values were then estimated using the proposed equation (Equation 13). The DFMC values were overlaid on the fire points using the value to point tool in ArcGIS. Areas covered with shrubs in the northeastern part of the district had the highest DFMC, up to 7.6% in 2020. The South western part of the district with bare lands had the lowest DFMC, with negative values due to the high BT, especially during summer.

$$DFMC = 19.832 - 0.4 \times BT \qquad \text{Equation 13}$$

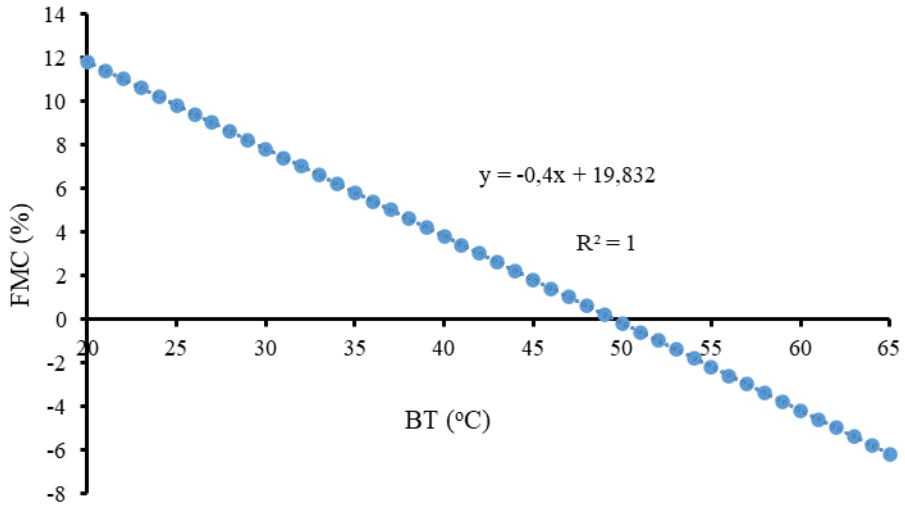

Figure 14: DFMC (%) Variation with Brightness temperature values (Zormpas *et al*., 2017)

3.2.2 Data analysis

The R package *randomForest* was used for implementing the random forest algorithm classification in R studio. The analysis applied the *caTools* package to split the data into training (70%, 107,883 fire and control points), testing datasets (30%, 53,942 fire, and non-fire points), and the *caret package* was used to streamline the training process. In this study, to determine the optimal number of trees, several trials were conducted with varying numbers of trees, and the optimal number of trees (ntree) was set at 900 with a mtry of 3 (Figure 15).

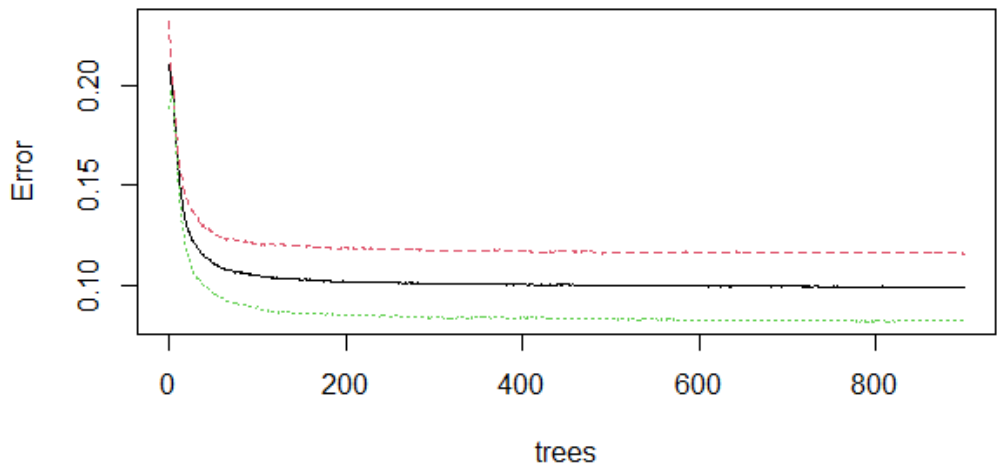

Figure 15: RF plot for the number of trees against the error rate. The black line is the OOB error rate, the green line is the error rate of 0.075, and the red line is the 0.125 error rate.

The model was then tested using the training and test dataset, and the variable importance was obtained for each variable used. The overall accuracy of the model, kappa coefficient, and user's and producer's accuracy were also calculated using results from the testing of the RF model. Mcnemar's Test P-Value was used to determine if the performance of the actual fire and non-fire point prediction models are equal.

3.2.3 Wildfire probability mapping using Logistic regression

Since RF is a tree-based model with the final output being variable importance and no functional equivalent representation that can be applied in the future, this study applied logistic regression to develop fire probability maps. The logistic regression (LR) method has been widely used in wildfire studies in different areas (Chang *et al*., 2013; Su *et al*., 2016; Rodrigues *et al*., 2014; Saefuddin *et al*., 2012). LR models are often used to test hypotheses and describe relationships between categorical outcomes (Fire and non-fire) and one or more predictors that may be categorical or continuous variables (Peng *et al*., 2002). This study used the LR model to develop fire probability maps. LR applies the logit (natural logarithm (ln)) transformation to the dependent variable (Fire and non-fire) and predicts the logit of the dependent variable from the independent variables (DMP, SM, and LFMC) (Equation 14). The LR model takes on the simplest form (Peng *et al*., 2002);

$$\log it(Y) = natural\log(odds) = \ln\left(\frac{\pi}{1-\pi}\right) = \alpha + BX \qquad \text{Equation 14}$$

Where π = wildfire probability (Y= Outcome of Interest = x, a specific value X) $= \frac{e^{x+Bx}}{1+e^{\alpha+Bx}}$, B is the regression coefficient and e base of the system of natural logarithms. For this study, it was assumed that the probability of fire occurrence (Y=1) was P while the likelihood of no fire (Y=0) was (1-P). The same dataset for the RF classification was used for running the LR model analysis. The dependent variable for the study consisted of fire points assigned one and non-fire points assigned the value of zero. Regression model's independent variables, including the most important predictors with variable importance,>300 for classifying fires in the RF model; that is, dry matter productivity (DMP), soil moisture (SM), and Land surface temperature (LST). Regression was performed between non-fire and fire points. DFMC and LFMC were excluded from the model due to their negative effect on the prediction accuracy resulting in lower model accuracy. In addition, results from the multi-collinearity test indicated high collinearity between LST, LFMC, and DFMC, resulting in unreliable statistical conclusions (Appendix 1).

This study used the Area under the curve method to evaluate the performance of the LR model in predicting the wildfire occurrence in the study area. Other authors have also used this method for assessing the model (Chang *et al*., 2013; Guo, Su *et al*., 2016). Typical values of the AUC range from 0.5 and 1, with higher AUC values (0.9-1) indicating stronger goodness of fit for wildfire prediction, while lower values (0.5-0.7) indicate weak goodness of fit. This method established the cut-off points for fire occurrence for the study area, with values above the cut-off indicating fire occurrence while values below indicate no fires. The accuracy of predicting the test data was also estimated.

After the LR analysis, the obtained model was applied to the predictor variables for the 10-day decadal before the 2021 mega-fire in Kgalagadi District. The wildfire probability was determined using the variables derived from the raster calculator tool in ArcMap. The burn probabilities were classified into four classes that are low, moderate, high, and very high. Predicted fire probabilities by the model were compared to the burned area by the mega fire of 2021. The fire prediction maps were characterised based on the likelihood of fire occurrence using the cut-off values obtained from model calibration.

3.3 Burned area mapping and impact monitoring

This study used the QGIS- Fire Mapping tool (FMT) to assess and map burned areas in Kgalagadi District during the 2021 fire season (August 7, 2021, to October 25, 2021). The fires resulted from lightning ignition in August in the Kgalagadi Trans-frontier Park in the Kgalagadi South sub-district, destroying property and biomass. Analysis was conducted using Landsat 8 scenes and validated using VIIRS aggregated active fire points and indices from sentinel scenes following a step-by-step process indicated in Figure 16.

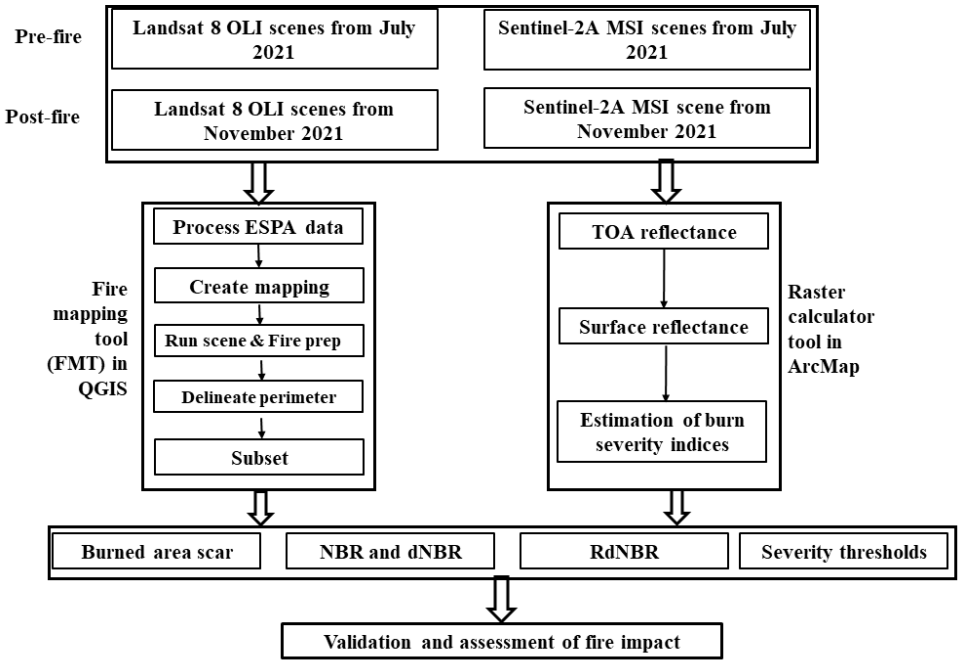

Figure 16: Burn area extent and severity mapping workflow

3.3.1 Image acquisition

Landsat-8 OLI images were obtained from EROS Science Processing Architecture (ESPA) website (https://espa.cr.usgs.gov/). Pre-fire and post-fire images were considered in this study. Post-fire images for November 2021, after the fire before the burned area, becomes unrecognisable due to the rapid regeneration of grasses soon as the rains start. The USGS (2018) recommends using post-fire images in the peak green period when the burned vegetation begins recovery. NDVI curve (Figure 17) for 2021 indicates NDVI values start increasing from November 2021. The NDVI values for the study area increase with the rapid growth of grasses immediately after rains are received (Dube, 2013).

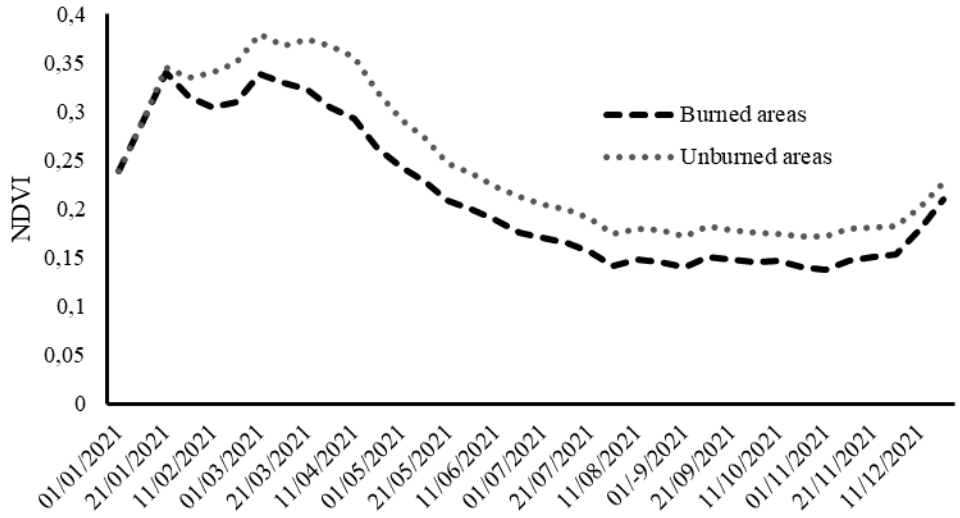

Figure 17: NDVI variation for burned and unburned areas for 2021. NDVI data at 300m spatial and ten days temporal resolution was obtained from the Copernicus Global Land service website (https://land.copernicus.eu/global/products/ndvi).

Landsat 8 Collection 1, level 1 scenes were identified using the Earth Explorer website and the scene list prepared (Table 2). The scenes projected to the coordinate system of the study area (UTM zone 34S) were then ordered and downloaded from the ESPA site. The files were then added to the FMT tool for the fire analysis. Sentinel 2A level 1C scenes were obtained from the USGS' Earth Explorer website (https://earthexplorer.usgs.gov/). The study obtained the Pre-fire (July 2021) and post-fire (November 2021) scenes for the study area for the same period as the Landsat images. Table 2 illustrates the data that was used in this study.

Table 2: Pre and post-fire scenes description and date of acquisition

Sensor	Scene	Event	Acquisition date
Landsat-8 OLI	173078, 173077, 174076, 174077, 174078, 174079, 175076, 175077,175078,175079, 176076, 176077	Pre-fire	1st to 31/07/2021
		Post-fire	1st to 30/11/2021
Sentinel 2A	T35JKM, T34KGU, T34KFV, T34KFU, T34KEU, T34KEV, T34KDV, T34KDU, T34KCV, T34KCU, T34JHT, T34JHS, T34JGT, T34JGS, T34JFT, T34JFS, T34JFR, T34JET, T34JES, T34JER, T34JDT, T34JDS, T34JDR, T34JCT	Pre-fire	1st to 31/07/2021
		Post-fire	1st to 30/11/2021

3.3.2 Image processing

Top of atmosphere reflectance Landsat scenes and NBR were obtained and added to the FMT scene folder. The study processed scenes using the process ESPA function in the FMT plugin in QGIS to create an NBR image. After the ESPA image processing, the fire assessment was then carried out. The obtained sentinel 2A top-of-atmosphere (TOA) reflectance images were processed using the dark object subtraction (DOS) technique to get surface reflectance values before analysis (Chavez, 1988). The DOS method is widely used in remote sensing studies since it does not require *in-situ* measurements. The DOS technique assumes very few objects on the earth's surface are absolute black. Thus, a one percent reflectance is better than zero. Surface reflectance (ρ_{sur}) is estimated by Equation 15 (Teodoro & Amaral, 2019).

$$\rho_{sur} = \frac{\pi\left(L_{sat} - L_p\right) \times d^2}{ESUN_{\lambda} \times Cos\theta_s \times T_z} \qquad \text{Equation 15}$$

Where L_{sat} is the radiance at the sensor, $ESUN_{\lambda}$ is the mean solar exo-atmospheric irradiances, θ_s the solar zenith angle, and L_p radiance as produced from the interaction of the electromagnetic radiance with the atmospheric components, and Tz is for the atmospheric transmissivity between the earth's surface and the sun. The DOS technique in this study was implemented using the QGIS semi-automatic classification plugin (SCP) to obtain the sentinel surface reflectance. The images were then mosaicked in ArcMap 7.0 using the Mosaic to new raster tool and clipped to the study area with projection to the study areas' coordinate system (UTM zone 34S) before calculating burn severity indices.

3.3.3 Data analysis

3.3.3.1 FMT analysis of Landsat-8 images

The FMT generated burned area and severity indices to assess the fire damage in the study area. Kgalagadi fire event was created in the FMT plugin, indicating the location (Latitude and longitude), the scene in which the fire occurred, the date of fire occurrence, and other information about the fire event. The created fire event was opened, and a new map was created; each scene in the study area was analysed as a separate map. The initial assessment method was selected in the create map menu. As is the case for this study, grasses regenerate immediately after the fire event; hence this requires the analysis of post-fire event images to be acquired immediately after

the fire event (USGS, 2018). For each mapping session, the pre- and post-fire scenes corresponding to the time of the fire were selected for the assessment. The selection of the scenes was followed by the Run scene prep step that creates the dNBR image and then the Run fire prep that establishes a mapping folder for each mapping session. The fire perimeter was then delineated manually using the burned area boundary template. The image registration accuracy for the pre-fire and post-fire images was assessed by comparing how far the images extend in the x and y direction. The study observed that the pre and post-fire images aligned well with no further adjustment required. Then the fire perimeter was delineated with the assistance of the QGIS display and create feature tools. By alternating between the NBR, reflectance and dNBR images in the QGIS display, the burned area perimeter was accurately delineated and saved to the boundary shape file template.

The reflectance images, NBR and dNBR were then clipped to the burned area perimeter with a three kilometres buffer using the subset option in the FMT. The subset option also estimates the low, moderate and high severity thresholds based on a random sample of dNBR pixels. Table 3 shows the values estimated by the FMT. The Relative dNBR (RdNBR) image was then created using the dNBR offset values, which account for the absolute difference between the pre- and post-fire NBR. This step was followed by developing the burn severity thematic map using the dNBR thresholds (Table 3). The threshold values obtained from the FMT fall within the range proposed by the USGS.

Table 3: Severity thresholds estimated by the FMT and threshold values proposed by the USGS

Thresholds	**dNBR threshold value**	**USGS values**
Enhanced regrowth	<-150	-500-101
Unburned	-150-69	-100 to 99
Low severity	70-315	100-269
Moderate	316-535	270-659
High severity	>536	660-1300

3.3.3.2 Sentinel burn severity indices

The NBR, dNBR and RdNBR were computed for the study area using the sentinel images to assess the indices generated using the FMT. Equation 16 calculated NBR values using the raster calculator tool in ArcMap from sentinel images using bands 8 and 12 (Mallinis *et al*., 2018). The calculated NBR was then used to estimate the dNBR and RdNBR.

$$NBR = \frac{Band8 - Band12}{Band8 + Band12}$$ Equation 16

NBR was computed for both the pre-fire and post-fire images, and dNBR was determined. The difference between the post-fire and pre-fire NBR images represents the fire's environmental impact. A severity map was then developed using the dNBR values estimated using sentinel images by applying the USGS dNBR ranges as indicated in Table 3.

3.3.4 Validation

Since there were no field-based burned area data from the Botswana Department of Forest and Range Resources (DFRR), the obtained FMT burned area perimeter boundary was validated by overlaying and comparing the VIIR burned area for the study period. The active fire points derived from the VIIRS sensors were obtained from the FIRMS website (*https://firms.modaps.eosdis.nasa.gov/*). The fire points were aggregated using a 1500m aggregation distance to estimate the burn area for the August-October Kgalagadi fires. The aggregation distance of 1500m was reported to give the best fit (R^2= 0.9) for arid shrublands and grasslands compared with MODIS MCD64A1 burned area (Briones-Herrera *et al*., 2022). The FMT and VIIRS burned areas were overlaid to compare the mapping accuracy. VIIRS 375m active fires were reported to accurately detect smaller fires with low related omission error (ROE) and related commission error (RCE) (Oliva & Schroeder, 2015; Santos *et al*., 2020). The differences between the FMT burned area perimeter and VIIRS burned area perimeter were determined.

The severity indices (NBR, DNBR and RdNBR) obtained using the FMT were assessed by comparing them with those estimated using the Sentinel images. The relationship between the sentinel severity indices and FMT Landsat indices was assessed using correlation analysis in R statistical software. The hypothesis tested in this case was that the correlation is not equal to zero at a 95% confidence level. Similarly, by applying the severity thresholds from the FMT (Table 3) a thematic map of burn severity was developed using the Sentinel 2A dNBR values. The thematic map from the FMT tool and sentinel map were then compared to assess the severity of the fire in question.

CHAPTER 4: RESULTS AND DISCUSSION

4.1 Prediction of the occurrence of rangeland wildfires using predictor variables

The rising global wildfire incidences have necessitated the development of more accurate wildfire prediction methods to prevent fire damage which has ecological, social and economic effects. This study explored the contribution of fuel parameters such as dry matter productivity (DMP), Dead fuel moisture content (DFMC), Live Fuel Moisture content (LFMC) and environmental variables such as Land surface temperature (LST) and Soil moisture (SM) on the prediction of rangeland fires in Botswana. The confusion matrix and accuracy matrices in Table 4 indicate the model predictions and actual outcome of the training dataset used for training the model. Overall results showed an OOB accuracy rate of 90.09%, which means a reasonably good model for predicting wildfires in the study area. The model was tested using a randomly selected testing dataset, and the different statistics from the testing are indicated in Table 4 and 5.

Table 4: Confusion matrix for RF classification model training and testing, the class errors, accuracy statistics and overall error of the RF classification model

		Training		Testing	
	Event	Fires	Non-fires	Fires	Non-fires
Reference	Fires	53 905	0	24 816	2 137
	Non-fires	0	53 978	3 177	23 812
Accuracy Metrics	Producer's Accuracy	1.0000	1.0000	0.8823	0.9207
	User's Accuracy	1.0000	1.0000	0.9176	0.8865
	Overall accuracy	1.0000		0.9015	
	Kappa	1.0000		0.8030	
	Overall OOB error	9.91			

Results indicate an agreement between the fire and non-fire observers with an overall kappa statistic of 0.803, which is lower than when the model is tested using the training dataset (Table 4). Although the RF model correctly classified 92.07% of the reference non-fires, only 88.65% were identified as non-fire points by the classification model. In addition, the model achieved a user accuracy of 91.76% for points classified as fires despite a lower producer's accuracy of 88.23% with 11.77% for fire points classified as non-fire points (Table 4). There was a significant difference (P-value<0.05) between the prediction of fires and non-fires by the model, indicating that it performs differently for the two classes (Table 5). The study observed a Detection prevalence of 50.03% of the total predictions, which shows the number of positive events (correctly and incor-

rectly classified fires). The study found the detection rate to be 44.14% of the predictions, which indicates the fraction of points classified as real fires.

Table 5: Statistics calculated from testing the RF model using the testing dataset

Statistic	Value
P-Value [Acc>NIR]	<0.001
Mcnemar's Test P-Value	<0.001
Detection rate	0.4414
Detection Prevalence	0.5003
Balanced Accuracy	0.9021

The RF model showed a balanced fire prediction accuracy of 90.21%. The high balanced accuracy indicates the high sensitivity and specificity of the classifier. The performance of the RF model agrees with earlier studies that also showed high accuracies of the RF model in wildfire studies Çömert *et al*., 2019; Latifah *et al*., 2019; Leuenberger *et al*., 2013; Su *et al*., 2018). The model accurately predicted fires and non-fires (Producer's accuracy of 83.72% and 86.43%, and User's accuracy of 86.93% and 83.12%, respectively). The results indicate the high reliability and accuracy of the RF model in predicting fire occurrences using the predictor variables. The accuracy is in the range reported by other authors for predicting fires by using different variables. For example, Karimi *et al*. (2021) reported more than 80% accuracy when they used six vegetation indices derived from MODIS data to predict fire hazards in Golestan forests.

Moreover, the model exhibited a high probability of correctly predicting fires as real fires, indicated by the high User accuracy (Table 4). Tonini *et al*. (2020) attribute the power of the Random Forest models to discriminate burned areas in 75% of their study period in Greece to the good generalization capabilities of the models. Furthermore, the Kappa statistic of 0.803 obtained in this study is almost in perfect agreement and is comparable to and higher than earlier fire prediction studies. dos Santos *et al*. (2020) reported a substantial Kappa value of 0.65 for an RF fire prediction model of Minas Gerais, Brazil. Le *et al*. (2021) also found a 0.63 kappa value for their proposed deep neural computing model for predicting wildfires in tropical Vietnam. The results from this study indicate a promising and reliable RF model for predicting wildfires in the rangelands of Botswana. Accurate and reliable wildfire prediction models such as RF are important considering the increasing climate change impacts that have resulted in changes in fire regimes with more frequent and highly severe fires (Clarke & Evans, 2019; McColl-Gausden et al., 2022) making fire mitigation complex. Accurate models are especially relevant in the savan-

nahs considering the high speed at which grassland fires spread after ignition than in other vegetation types. Combined with other existing wildfire management methods, reliable prediction models contribute to the development of more effective and efficient fire mitigation and community adaptation measures (Dube, 2013; Yu et al., 2022).

4.1. 2 Variable importance in classification

This study used validated remote-sensed global products such as DMP, SM, LFMC, DFMC, and LST to predict wildfires in Kgalagadi District. The RF analysis outcome was the relative importance of the wildfire prediction factors used in training the model. The variable importance increases with the magnitude of the values indicated in Figure 18 and Table 6. DMP and surface SM were the essential variables in predicting wildfires in the study area, with MDA and MDG greater than 800, respectively (Figure 18). LFMC and DFMC were the least important factors in wildfire prediction, with MDA and MDG of 600.28 and 9,208.96 and 478.43 and 9480.72, respectively. Noteworthy, despite the higher MDA (1055.20) observed for DMP, SM has a significantly higher MDG (15745.69) than all predictor variables, followed by LST (10169.40). Overall, all variables were more important in predicting fires than fires, with DMP and SM having higher variable importance for classifying fires. The overall order predictor variable significance in predicting wildfires was DMP> SM> LST> LFMC> DFMC.

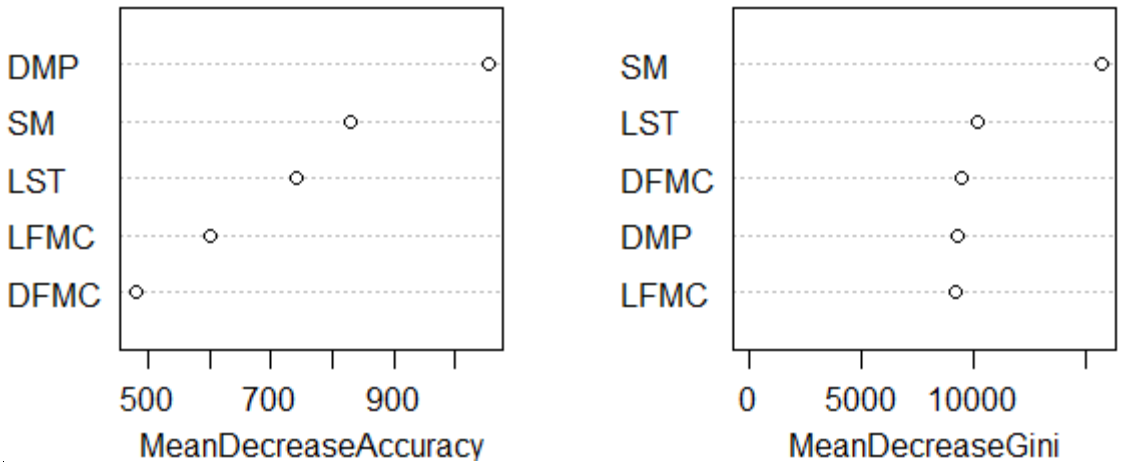

Figure 18: Relative predictor variable importance calculated by the RF model using the MDA and MDG plots. (DMP-Dry Matter Productivity, SM-soil moisture, LFMC-Live Fuel Moisture Content, LST-Land Surface temperature, and DFMC-Dead fuel moisture content).

Wildfire prediction studies have primarily been conducted using meteorological and climatic parameters such as humidity, wind speed, temperature, and human factors that are directly or indi-

rectly related to fire ignition (Anderson *et al*., 2007; Bergonse *et al*., 2021; Latifah *et al*., 2019; Su *et al*., 2018; Valdez *et al*., 2017). The lack of dense meteorological stations or networks in sub-Saharan African countries limits the meteorological factors' use in wildfire prediction studies. On the other hand, using forest and vegetation composition maps, as suggested in the earlier studies (Shang *et al*., 2020), is not possible in Botswana due to the lack of fuel maps.

Table 6: Variable importance from the RF model for prediction of both fire and non-fire points

	Non-fires	Fires	Mean Decrease Accuracy	Mean Decrease Gini
DMP	282.732	999.744	1 055.1978	9 328.616
LFMC	165.318	503.436	600.2813	9 208.956
LST	212.724	634.351	740.1304	10 169.398
SM	163.969	753.415	828.39	15 745.69
DFMC	282.584	484.285	478.4341	9 480.715

Fuel quantities available to burn at any time are fundamental in successful wildfire prediction studies, yet quantifying fuels remains entirely labour-intensive. This study employed the DMP product from Copernicus Global Land Service developed from Sentinel-3/OLCI, PROBA-V data. These results indicate that 1055.1978 additional points would be misclassified by the model with a reduction of 9328.616 in the purity of the decision tree nodes if DMP is removed (Table 6). In the arid Kgalagadi district, most of the fuel produced during the summer rains becomes dry immediately after the end of the rainy season, increasing ignition potential. The quantification of dry matter available to burn during the August to November fire season explains the higher contribution of DMP to wildfire prediction by the RF model. Despite the limited use of the DMP product in wildfire prediction, the results indicate considerable potential for its use and application for mapping wildfire danger. Evidence from earlier long-term field studies and satellite sensors-based studies also bespeak the substantial contribution of fuel availability to fires in the southern African dry grassland savannahs (Lehsten *et al*., 2009). The cumulative dry matter productivity could also be used to assist in identifying areas with significant fuel accumulation before the fire season for timely fire management activities to be carried out to prevent the effects of severe and mega-fires.

The availability of large quantities of dry matter produced during the rainy season and low soil moisture content seems to be a good recipe for wildfire ignition in the study area. The use of SM

content in wildfire prediction has been suggested by several studies (Bartsch *et al*., 2009; Sharma & Dhakal, 2021; Vinodkumar & Dharssi, 2019). Results from this study agree with earlier studies that suggest the use of soil moisture content in wildfire prediction, with soil moisture having the highest (15,745.69) MDG of all parameters (Table 6). The high MDG indicates that SM has the highest contribution to the leaf nodes' purity at the decision tree's end. The substantial contribution of SM to prediction in the model is attributed to its effect on the fuel moisture contents, as shown in earlier studies (Rakhmatulina *et al*., 2021; Vinodkumar *et al*., 2021). Rakhmatulina *et al*. (2021) found that soil moisture content was the most critical environmental parameter in wildfire prediction in the Sierra Nevada. According to the authors, every 1% increase in soil moisture resulted in a 0.6% increase in fuel moisture content. The increasing availability of remotely sensed soil moisture data had increased the possibility of using soil moisture as a wildfire danger prediction variable. However, there is a lack of remote sensors capable of capturing soil moisture data across large spatiotemporal domains (Sharma & Dhakal, 2021). This study used the 3km SMAP soil moisture data for the fire prediction. Improving the availability of higher-resolution soil moisture data could help improve the prediction accuracy of wildfire danger.

Land surface temperature was the third most important variable in predicting wildfires, with variable importance of 634.35 (Table 6). The results from the RF model agree with those found by Bisquert *et al*. (2012), indicating LST to be an essential factor in forest fire danger prediction using Artificial Neural networks (ANN) and LR. Adding the day of the year improved the performance of LST in fire prediction by separating high summer temperatures from winter (Bisquert *et al*., 2011). Other studies have also applied the LST and LST anomalies in wildfire studies, arguing that higher LST and LST anomalies could indicate vegetation stress, with is a crucial indicator of fire danger and ignition (Chaparro *et al*., 2016a; Yang, 2021; Yang, 2021). The strong performance of LST in this study could be attributed to the fact that most fires occur after winter with increasing temperatures in the spring and summer seasons while, at the same time, the vegetation is generally dry. The high surface temperature during fire season could account for the increase in the purity of the decision tree nodes (MDG= 10,169.40) when LST is added. Additionally, there is a correlation between the number of fire incidences and LST, with lower fires recorded between winter, May and July when LST values are relatively low.

Results from the RF model also indicated that Live fuel moisture content was the fourth important variable with a mean decrease accuracy of 600.28, showing a lower increase in misclassification if LFMC is removed. On the other hand, DFMC had a minor contribution to fire predic-

tion by the RF model, with the lowest MDA of 478.43 (Table 6). Fuel moisture content is the most used fuel characteristic in wildfire danger rating systems and studies (Chuvieco *et al*., 2009; Jurdao *et al*., 2011). It is the most studied fire danger prediction variable, with several methods proposed for its estimation ranging from the use of meteorological factors (Viegas *et al*., 2001) to the use of drought indices (Ruffault *et al*., 2018) and the application of remote sensing methods to estimate FMC (Al-Moustafa *et al*., 2012; Chuvieco, Riaño, *et al*., 2002; Rao *et al*., 2020; Yebra *et al*., 2013; Zhu *et al*., 2021). This study applied the model proposed by Chuvieco *et al*. (2004) to estimate LFMC using LST and NDVI. The low contribution of LFMC compared to DMP and SM could be attributed to the fact that the faction of the day of the year in the proposed model is specific to Mediterranean areas which somehow vary differently in the FMC across the year.

On the other hand, the DFMC values were estimated by an equation proposed by Zormpas *et al*. (2017) for DFMC estimation in Greece using brightness temperature. Earlier studies suggested using meteorological variables and field-based sensors (Cawson *et al*., 2020; Nolan *et al*., 2016). However, the use of these methods is limited by the lacking meteorological stations and equipment in the study area.

4.1.3 Wildfire probability mapping using logistic regression

The variables that exhibited the highest contribution (DMP, SM and LST) in the RF model classification and demonstrated low multi-collinearity were used to develop a logistic regression model for wildfire prediction for the study area. DFMC and LFMC were excluded from the model since their addition reduced the model's accuracy. The logistic regression model for fire prediction in the study area indicated that SM is the most significant ($P<0.05$) contributor to wildfire prediction (

Table 7), which explains the spatial distribution of wildfire likelihood in the study period. DMP is the second most significant ($P<0.05$), while LFMC was the minor contributor to wildfire prediction in the study area. The goodness of fit test showed a significant ($P=0.05$) fit of the model to the data with an accuracy of 56.05% for the testing dataset, indicating a weak model fit. The LR results showed a weak fit of the model to the data.

Table 7: Results of the Logistic regression model for wildfire occurrence

	Estimate	Std.	Error	Pr(>|z|)
(Intercept)	5.01E-01	3.23E-02	15.54	<2e-16***
DMP	-8.39E-04	2.55E-05	-32.877	<2e-16***
SM	-1.45E+00	4.12E-01	-3.512	0.000445***
LST	1.95E-03	8.56E-04	2.273	0.023019*

Significance codes: 0 '***' 0.001 '**' 0.01 '*' 0.05 '.' 0.1 ' ' 1

The ROC-AUC was used to indicate the accuracy and ability of the LR model to predict wildfires in the study area (Figure 19). The ROC curve revealed an AUC of 56.05% with a kappa value of 0.121, indicating a slight agreement of the model. The low AUC means that the model has weak discrimination of fire points from non-fire points (Figure 18). These results are of lower accuracy than that reported in other studies that applied logistic regression models in predicting wildfires (Bisquert *et al*., 2012; Cao *et al*., 2013; Chang *et al*., 2013; Nhongo *et al*., 2019). The model's poor fit could be attributed to the low ability of the predictor variables to discriminate between fire and non-fire points when training the LR model. Unlike Bisquert *et al*. (2011) and Nhongo *et al*. (2019), which obtained higher AUC by utilizing vegetation indices, climate and topographic variables with a clear relationship with fire occurrence, this study employed environmental variables for predicting fire events. The low performance of the ecological variables could be due to no significant variations in the variables between fire and non-fire points. Comparing the LR prediction and RF classification accuracies, the RF model appears more robust in classifying fire and non-fires points using the predictor variables than the LR model in predicting fire and non-fire occurrences.

Table 8: LR prediction confusion matrix and accuracy values

Prediction	Fires	Non Fires	Producer's Accuracy	User's Accuracy
Fires	16 225	10 728	0.5556	0.6020
Non Fires	12 980	14 009	0.5663	0.5191
Overall Accuracy			0.5605	
Kappa			0.1210	

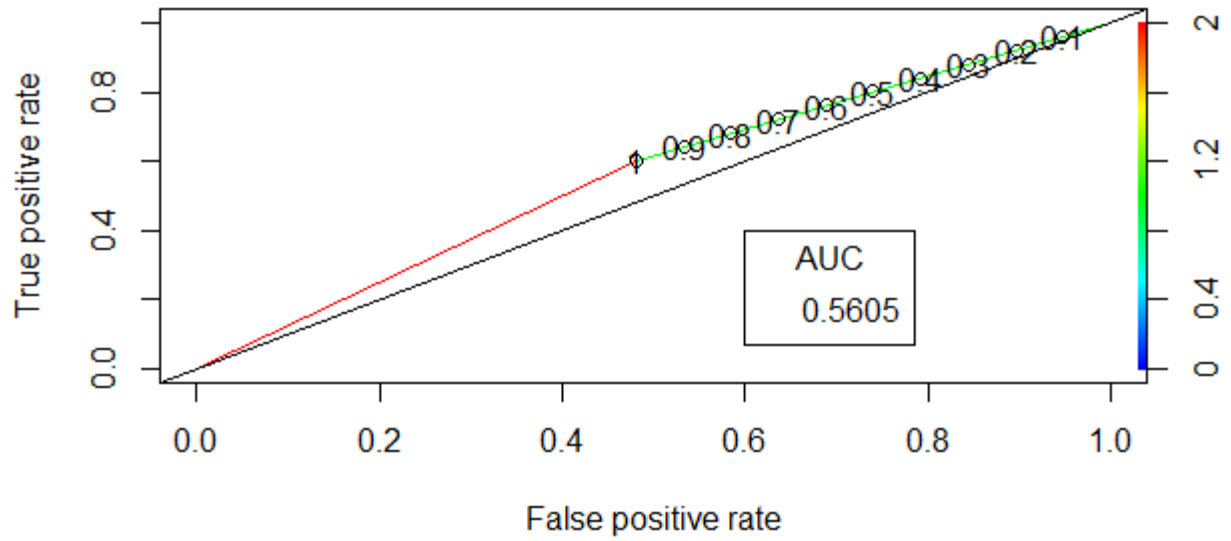

Figure 19: The receiver operating characteristic (ROC) curve from the LR-Logistic regression model classification in-set with the Area Under the Curve (AUC).

The wildfire probability distribution map for August 2021 before the 2021 Kgalagadi mega-fire that intensely burned large areas in the study area (Figure 20). The probability map was developed using the Raster calculator in the ArcGIS 10.7 environment. The likelihood of fire occurrence was split into three classes using natural breaks. The cut–off points were established at 0.5 for low probability as established during testing of the model, 0.513 for moderate, and greater than 0.514 for high probability (Chang *et al*., 2013, Figure 20). The results indicate that areas covered by grassland in the southern part of the study area had a higher chance of fire occurrence. The low fire occurrence probability class covered the northeastern shrubland of the study area (Figure 20). The high fire probability area in the study area covered 39.11% of the study area, while the moderate probability area covered only 4.5%. The low probability of fire occurrence classes occupied 56.39% of the study area.

The fire points recorded after August 2021 were compared to the fire prediction probability map; the results are indicated in Table 9. Results show that 57.35% of the fire points were in the high fire probability classes in the southern parts of the study area. Only 36.47% of the fire points occurred in low fire probability areas. Only 6.181% of the fire points were recorded in the moderate probability areas.

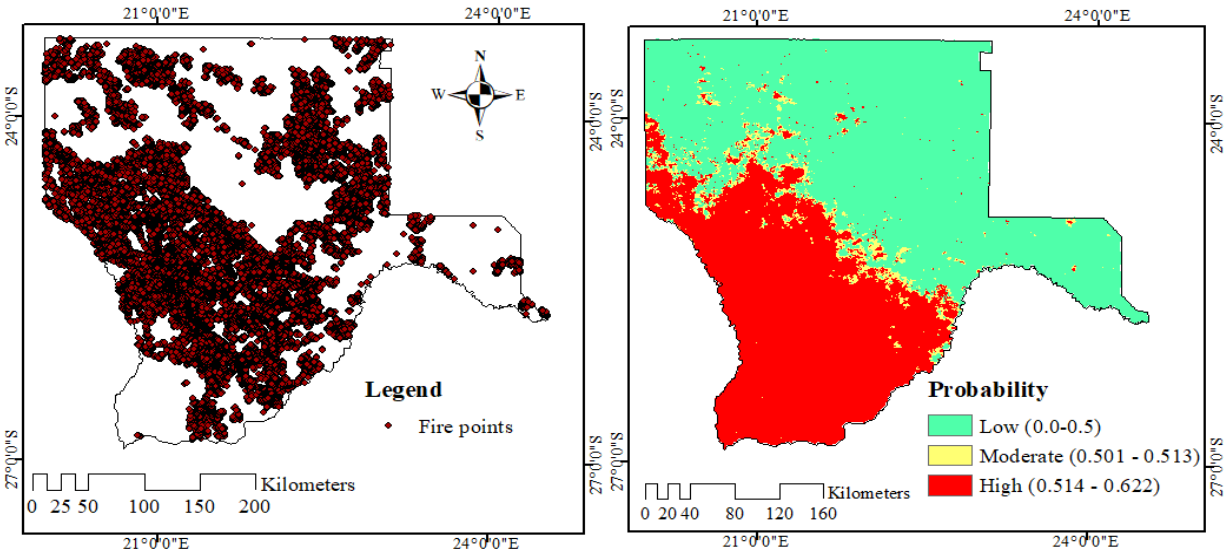

Figure 20: Fire points distribution after August 2021 (Left) and Wildfire probability of occurrence before the August-November 2021 mega-fire (Right)

In addition, the area with high fire probability experiences deficient soil moisture levels with increased surface temperature, which could potentially increase the ignition potential of the dry fuel significantly. The results of this study suggest that fire managers should invest more effort in controlling fires in the Southern areas of the Kgalagadi district, which have a high potential for mega-fires, to prevent losses due to the fire. The sites have higher dry fuel loads coupled with higher temperatures. The lower fire ignition probability in the Eastern part of the district could be due to the presence of fuel with high FMC since the area is covered by shrubland. In addition, the availability of dry fuel with lowe soil moisture (Figure 9) in the south western region could be due to lower free-range wildlife densities compared to the Eastern areas used for livestock grazing. Besides, the periodical rainfall received during the summer results in a significant accumulation of biomass that are readily available to burn during the fire season if not consumed by herbivores (Bond et al., 2003). The fact that areas with higher wildfire potential were identified implies the need to map wildfire probability in the area. The study results could support approaches to building a fire potential index for the study area to minimise fire disturbances and optimise resources for potentially dangerous fires (Sharma & Pant, 2017). The results from the fire occurrence probability mapping show that the model has the potential to predict rangeland fires in the study area, with 57.346% of the fires occurring within the high-probability areas. Thirty-six percent of the fire happened with low fire probability, which indicates the model's low miss classification accuracy.

Table 9: Distribution of fire points across probability classes between August and December 2021.

Probability class	Number of fire points	Percentage
Low	22 370	36.47
Moderate	3 791	6.181
High	35 172	57.346
Total	61333	100

4.2 Burned area mapping and burn severity

Figure 21 represents the burn area derived using the QGIS FMT tool and the VIIRS-based burn area aggregated from active fire points to an aggregation distance of 1500m. Using the FMT to delineate burned area size requires effort and field knowledge of burned areas. Practical delineation of the burned area seems to accurately map the burned area using the reflectance, NBR, and dNBR images generated by the FMT. The Landsat FMT burned area mapped was estimated as (50,297.9 km^2) while the VIIRS burned area was 11,428 km^2 (Table 10:). The burned area perimeter derived from the FMT is significantly larger than the aggregated burned area perimeter of VIIRS active fire points.

Table 10: FMT Landsat Burned area and aggregated VIIRS burned area

	Area (Km^2)	% of the study area
FMT Landsat burned area	50 279.909	37.165
VIIRS 375m burned area	11 428.929	8.448

The higher burned area mapped using the FMT could be attributed to the high sensitivity of Landsat 8 OLI bands reported by several authors (Mallinis *et al*., 2018; Teodoro & Amaral, 2019). According to Teodoro & Amaral. (2019), Landsat 8 bands recorded a slightly higher sensitivity in the reflectance of ash deposition from burning and leaf pigments, which accounts for their efficient discrimination of burned and unburned areas. Earlier studies accurately mapped burned areas by aggregating active fire data from remote sensors such as VIIRS, MODIS, and NOAA-AVHRR (Briones-Herrera et al., 2020; Chuvieco et al., 2008; F. L. M. Santos et al., 2020). Similarly, results from this study indicate that high spatial resolution satellite imagery enhances accurate burned area mapping in rangelands.

Results from the aggregation of the VIIRS active fires produced a smaller burned area than the FMT burned area (Figure 21). The difference in the burned area from VIIRS active fires could be

attributed to the fact that grassland fires in the study area burn at a fast speed with low residence time and some may go undetected due to temporal sampling problems (Dwyer et al., 2000; Neary & Leonard, 2020; Pereira, 2003). In addition, the savannah cloudiness and smoke from active fires may hinder the VIIRS sensor from detecting active fire locations (Pereira, 2003). Besides, Landsat-8 images may not have a visible change in spectral data for some small fires detected by the VIIRS 375m product, especially for active night fires (Schroeder *et al*., 2014). Moreover, due to the low spatial resolution, active fire data products such as MODIS and VIIRS are not ideal for mapping burned areas. Burned area maps from active fire data have also reported high omission errors from cloud cover and low temporal resolution (Oliva & Schroeder, 2015). Overall, results from mapping using the FMT indicate high accuracy in mapping even small fires that lower-resolution sensors may not capture. The high resolution of the Landsat data and the possibility of mapping the area based on field data make the QGIS FMT plugin promising for mapping rangeland fires that are complex to map from low-resolution data.

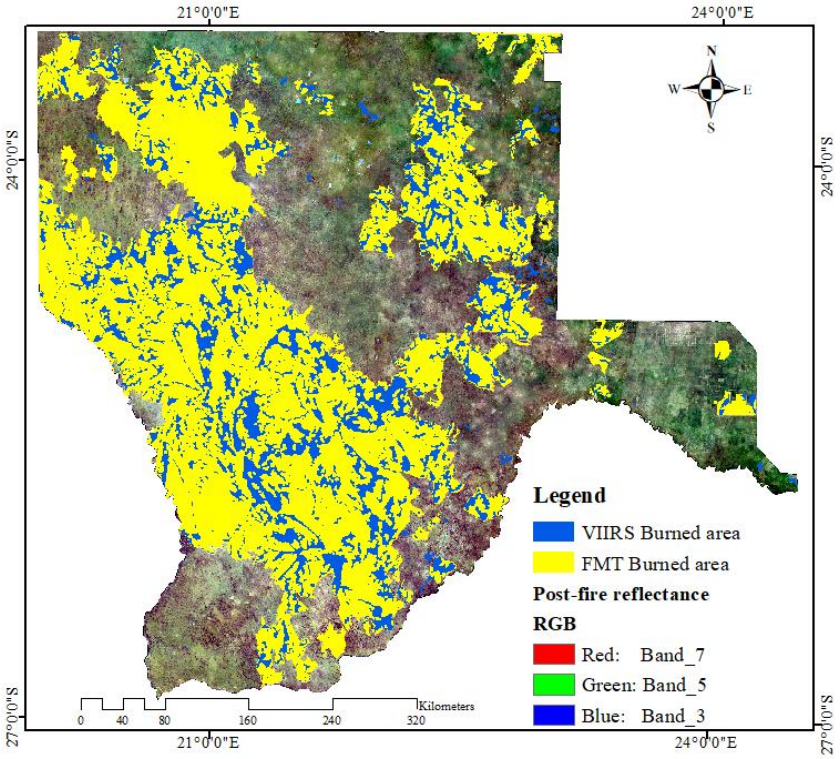

Figure 21: FMT Burned area perimeter (yellow) overlaid by VIIRS burned area perimeter (blue) derived by aggregating active fire points to an aggregation distance of 1500m

4.2.1 Burn severity indices

Assessment of the resulting burnt area maps can be accomplished by visual inspection; the comparison between FMT and Sentinel NBR and dNBR is shown in Figure 22 and Figure 23 respectively. Comparing the images in Figure 22, it is evident that NBR values were lower in burned areas in the post-fire image (Figure 22 b and d) than in pre-fire images. Results from correlation analysis indicate a significant ($P<0.05$) correlation between FMT and sentinel pre-fire ($r=0.30$) and post-fire ($r=0.68$) values (

Table 11). Comparing images in Figure 23, high dNBR values (white) in both Sentinel and FMT images fall in the burned areas while negative values in the north eastern part of the area are the regrowth area. The correlation analysis results also indicate a significant ($P<0.05$) correlation ($r=0.39$).

Several studies have applied various severity indices derived from Landsat bands in mapping burn severity. In this study, the FMT computed the normalized burn ratio (NBR), the dNBR and RdNBR using the Landsat images for the study area. Figure 22 (a) and (b) represent the NBR derived from Landsat images taken before and after the 2021 fire incidents. An analysis of the results of the NBR, a trend between pre- and post-fire images can be detected. There was an increase in the area with low NBR values, while regions with high NBR values were reduced. The increase in areas with low NBR values (green and light green areas) indicates an increase in bare areas after the fire than before the fire. Burned areas have been reported to have lower NBR values due to the destruction of vegetation by the fire (Alcaras *et al*., 2022). The reduction in NBR values is attributed to the relative decrease of reflectivity in the NIR band and the increase in SWIR band reflectance after the fire event (Pepe & Parente, 2018).

Similarly, values obtained from Sentinel images indicate more areas with low NBR in the post-fire image than in the pre-fire image (Figure 22 c and d). The similarity in the values confirms the strength of the FMT in mapping burn severities. However,

Table 11 indicates a significant (P<0.05) positive correlation between Landsat FMT NBR and sentinel NBR for both pre-fire and post-fire data. The high positive correlation between the FMT-derived and sentinel post-fire NBR indicates the potential of both sentinel and Landsat images for mapping burn severity due to their high resolution.

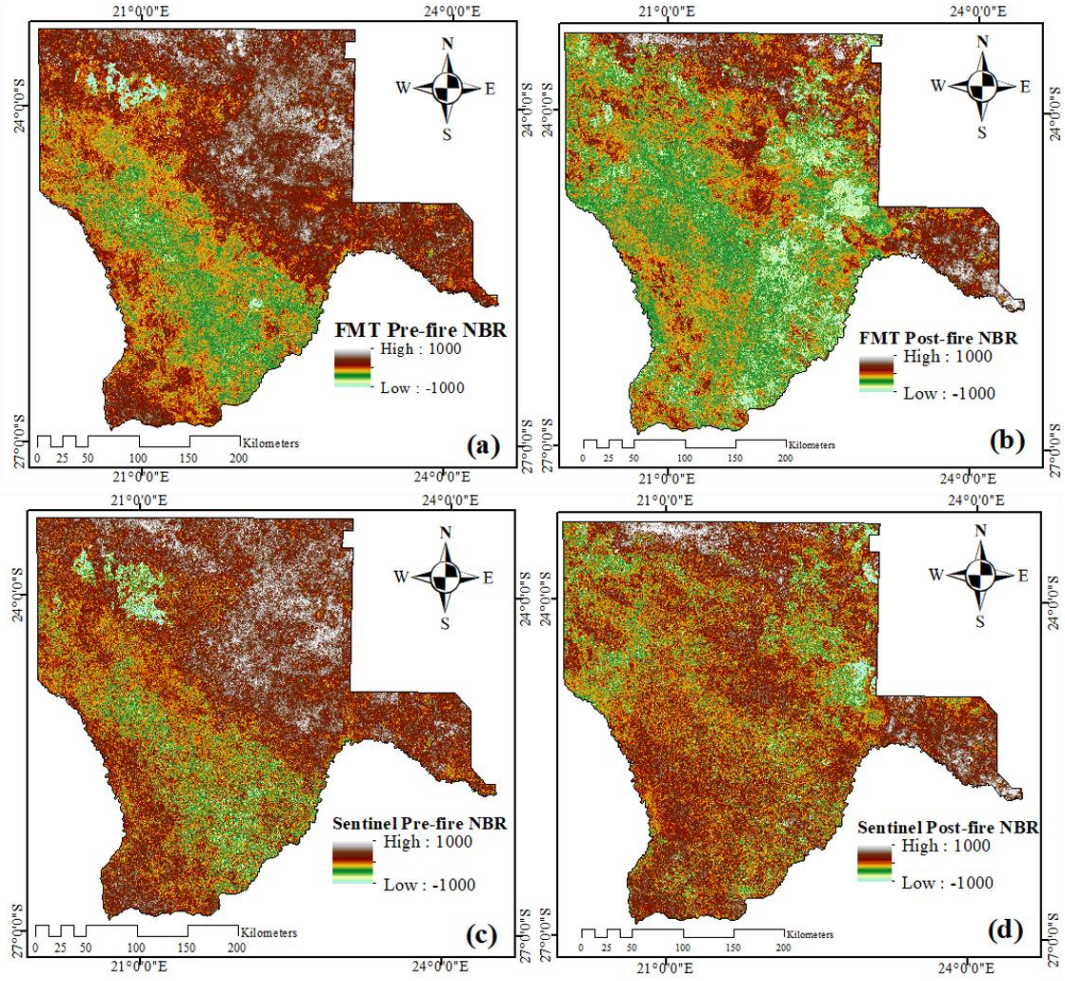

Figure 22: Normalised burn ratio (NBR), (a) pre-fire NBR, and (b) post-fire NBR derived from Landsat images using the QGIS FMT tool. (c) Pre-fire and (d) Post-fire NBR derived from sentinel images

The dNBR for the study area was estimated using the pre-fire and post-fire NBR data in the FMT tool and ArcMap. Images of the resulting dNBR maps are shown in Figure 23. Visual presentation of the images does not show a significant difference between burned and unburned areas. However, there appears to be a clear agreement in dNBR values for both Landsat and Sentinel 2A dNBR images. Results indicated higher values (brown and white) around the burned areas than in unburned areas, which aligned well with high fire probability areas and burned areas

shown in Figure 20. Similar to the Sentinel dNBR, dNBR results from the FMT analysis indicate lower values (green) in the burn area, especially in the western part of the study area.

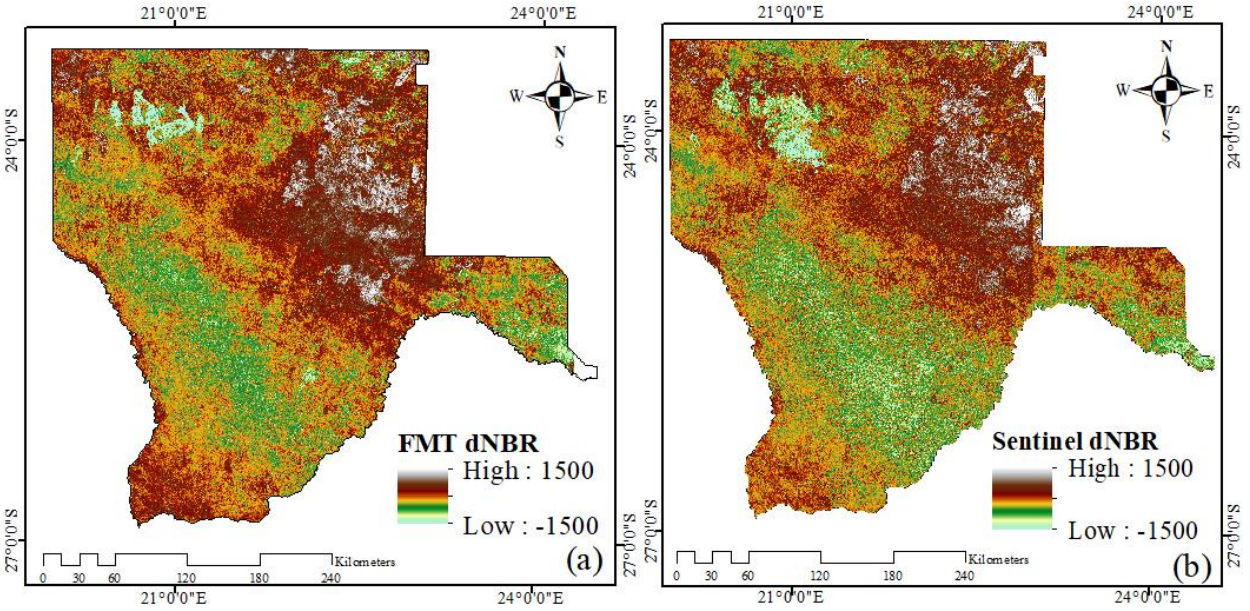

Figure 23: Difference Normalised Burn ratio (dNBR) derived using the FMT from Landsat data (a) and sentinel 2A data (b)

From Figure 22 and Figure 23, results show that NBR and dNBR derived using the FMT contribute to reliable estimation of burn severities of rangelands of the Kgalagadi district. Veraverbeke *et al*. (2011) also earlier reported that NBR and dNBR improve the efficiency of assessing burn severity in a Mediterranean environment. The difference in the results from FMT and sentinel results could be attributed to the differences in resolution, with sentinel having a higher resolution (10m) than Landsat data (30m). A positive significant ($p<0.05$) correlation was also observed between FMT and sentinel 2A dNBR results, further confirming the potential of the FMT in mapping burn severity. This study attributes the lack of discrimination for the burned and unburned areas to the existing environmental factors such as similarity in reflectance from unburned dry vegetation and ashes from the fire. The effect of these environmental factors could result in difficulty in discriminating between burned and unburned regions using dNBR data. Similar to this study, although Sentinel 2A provided a higher potential in mapping burn severity than Landsat 8 OLI FMT estimates, data from the two sensors could complement each other in burn severity mapping (Mallinis *et al*., 2018).

Table 11: Correlation of FMT and Sentinel-2A indices

	FMT INDICES				
Sentinel index	Pre-fire NBRNBR	Post-fire NBR	dNBR	RdNBR	P-value
Pre-fire NBR	0.302694				< 2.2e-16
Post-fire NBR		0.682412			< 2.2e-16
dNBR			0.392162		< 2.2e-16
RdNBR				0.003876	0.7727

This study also estimated RdNBR values from the dNBR data. RdNBR results showed no discrimination between burned and unburned areas. Relative to the sentinel RdNBR, a weak ($r < 0.1$, $P > 0.05$) and non-significant correlation was observed between the Landsat FMT and Sentinel RdNBR values (

Table 11).

Table 11 shows that FMT and Sentinel-based indices have a significant ($P < 0.05$) positive correlation except for RdNBR.

4.2.2 Thematic burn area

The final step of the FMT fire mapping process was creating a thematic map of burn severity using the tool's estimates of the severity thresholds. Figure 24(a) represents the FMT's thematic map. Results indicate that over half (58.6%) of the area within the burn area perimeter is an unburned area (Table 12). Only 39.7% of the burned area vegetation was burned at low severity, and 0.26% of the mapped burn area was mapped as moderate severity. About 0.0001% of the burned area was classed as high severity. For comparison and assessment, the study applied the severity thresholds derived from the FMT to the sentinel 2A dNBR data. Results from the com-

parison indicate significant variation in the areas for the different burn severity classes. About a third of the area (35.1%) in the delineated burn area was classed as Low burn severity, and only 64% of the area was unburned-low severity from the sentinel data. In addition, severity classification using Sentinel data indicated a slightly lower area (0.199% and 0.0001%) as moderate and high severity, respectively, than the FMT Landsat thematic map. Although, Sentinel data is obtained at 10m resolution, results from the FMT tool are within the same range despite the 30m resolution Landsat data used. However, the USGS (2018) recommends using severity thresholds obtained from field measurements. The lack of field-based threshold values could account for the differences in the extent of the severity classes classified from FMT and Sentinel data. Nonetheless, the FMT produced correlating results of burn severity cases making it a promising tool in classifying burn severity in rangeland areas.

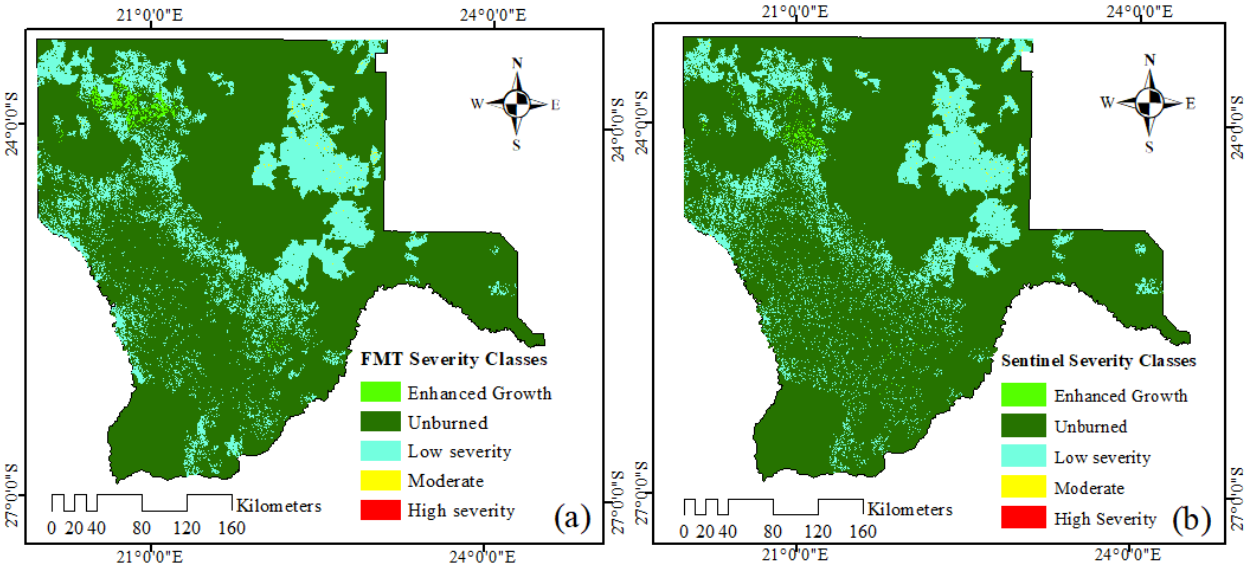

Figure 24: Thematic maps of burn severities derived from Landsat using FMT (a) and from Sentinel data (b)

Overall, there was low burn severity in the Kgalagadi district (Figure 24). These results are typical of grassland fires which have earlier been reported to burn at low severity than shrubland and forest fires. Similar to this study, Argañaraz & Bellis (2021), while evaluating the burn severity of 2020 fires that occurred in the mountains of Córdoba, in central Argentina, found that grasslands and shrubs burned at low to moderate severity compared to forests that burned at moderate to high severity. Fidelis *et al*. (2010) also reported low fire severity in Brazilian Campos grasslands with low residence time and average fire temperatures. Although dead fuel in grasslands

tends to burn completely, the quantity of fuel (biomass) available to burn significantly affects the burn severity in grasslands (Wragg *et al*., 2018). The low burn intensity in the current study for most of the burn area suggests low availability of biomass during the fire season resulting in low severities. The effect of accumulated biomass on burn severity highlights the need to use dry matter productivity in predicting wildfires for the rangelands of the study area.

Table 12: Percentage of the mapped burned area classified under different severity classes

Thresholds	**Landsat FMT area (%)**	**Sentinel area (%)**
Enhanced regrowth	1.437	0.638
Unburned	58.636	64.049
Low severity	39.668	35.114
Moderate severity	0.260	0.199
High severity	0.0001	0.0001

CHAPTER 5: Conclusions and recommendations

5.1 Conclusions

The study sought to understand wildfire occurrence and probability of fire ignition in Kgalagadi District, Botswana, using remote sensed data and machine learning models from 2015 to 2021. The results showed that dry matter productivity and soil moisture were the highest contributors to fire and non-fire point discrimination. In contrast, dead fuel moisture content had the lowest but significant contribution. DMP and SM had a substantial contribution to the classification of fire points, followed by LST, LFMC, and then DFMC. A logistic model was also computed and used to map the wildfire probability of the month before the Kgalagadi 2021 mega-fires. The results indicated that moderate and high chances of fire occurrence were spatially distributed in areas with high dry matter productivity (Shrub and grassland) due to the influence of large fuel quantities available for burning. The spatial and temporal variations of the variables studied also appear to dictate the temporal heterogeneity of wildfire probability of occurrence. Wildfires seem more likely to occur in areas where the very dry biomass has accumulated and at a time when there is very low moisture content to facilitate burning. Overall, 39.12% of the Kgalagadi District for the study period was under high wildfire risk, with 57.35% of the active fire points recorded in the Southern region. The very low probability of fire ignition observed in the Eastern part is basically due to the higher soil moisture and wet fuel accumulated in the area resulting in only 36.47% of the fires. In conclusion, the results of this study avail critical insights needed for planning and implementing fire prevention and mitigation in Botswana.

This study also assessed the ability of the QGIS FMT to map burned areas and severity using Lansat-8 OLI data directly. This study demonstrated how using the FMT tool could improve the timely mapping of rangeland burned areas and severity to overcome the limitations of inaccurate and low-resolution burnt area maps. Using the FMT from Landsat imagery, the burn area perimeter offered promising results correlating with VIIRS data that mapped burnt areas by aggregating active fire points. As such, the FMT could serve as a vital tool for delineating burnt area extent by fire managers in rangeland areas of Botswana, complementing the available methods. In addition, the FMT demonstrated the ability to map large and extended fires, making the tool applicable in delineating frequent mega-fires in rangeland areas in the study area.

The practical application of Landsat data in mapping burn severity using the FMT's NBR and dNBR severity indices to produce thematic burn severity maps offers land managers an oppor-

tunity to plan and implement post-fire interventions. Maps created using the FMT could provide additional information that supports strategic decision-making combined with other burned area data. However, there were significant variations in severity indices from the FMT compared to sentinel indices resulting from differences in spatial resolution of the two datasets.

5.2 Recommendations

Efforts to prevent and control fire are beneficial based on the spatial distribution of fire ignition probability rather than predefined areas in Botswana. This study recommends the use of wildfire risk maps when allocating resources for mitigating wildfires in the study area. In addition, field-validated burnt area maps must be developed by local fire managers to aid effective burnt area management in the study area.

Concerning further developments of this work, this study recommends that;

i. Field-based calibration and validation of fuel moisture contents (FMC) be carried out to improve their contribution to accurate fire prediction. FMC data has been reported to strongly contribute to accurate fire predictions in previous studies.
ii. Studies to develop a fire potential index for the study area using the proposed variables are conducted to minimise disturbances and for optimisation of resources in case of mega-fires.
iii. Field-specific severity thresholds should be determined for application in the FMT. Field-based severity thresholds could improve the accuracy of the FMT's severity maps. Future research should therefore focus on in-situ estimation of field severity thresholds for different land cover types.
iv. The accuracy of the FMT is assessed for other locations to determine its reliability under varying environmental conditions.

References

Abatzoglou, J. T., & Williams, A. P. (2016). Impact of anthropogenic climate change on wildfire across western US forests. *Proceedings of the National Academy of Sciences*, *113*(42), 11770–11775. https://doi.org/10.1073/pnas.1607171113.

Alcaras, E., Costantino, D., Guastaferro, F., Parente, C., & Pepe, M. (2022). Normalized Burn Ratio Plus (NBR+): A New Index for Sentinel-2 Imagery. *Remote Sensing*, *14*(7), 1727. https://doi.org/10.3390/rs14071727.

Alleaume, S., Hély, C., Le Roux, J., Korontzi, S., Swap, R. J., Shugart, H. H., & Justice, C. O. (2005). Using MODIS to evaluate heterogeneity of biomass burning in southern African savannahs: A case study in Etosha. *International Journal of Remote Sensing*, *26*(19), 4219–4237. https://doi.org/10.1080/01431160500113492.

Allen, J. L., Sorbel, B., Allen, J. L., & Sorbel, B. (2008). Assessing the differenced Normalized Burn Ratio's ability to map burn severity in the boreal forest and tundra ecosystems of Alaska's national parks. *International Journal of Wildland Fire*, *17*(4), 463–475. https://doi.org/10.1071/WF08034.

Al-Moustafa, T., Armitage, R. P., & Danson, F. M. (2012). Mapping fuel moisture content in upland vegetation using airborne hyperspectral imagery. *Remote Sensing of Environment*, *127*, 74–83. https://doi.org/10.1016/j.rse.2012.08.034.

Andela, N., Morton, D. C., Giglio, L., Chen, Y., Werf, G. R. van der, Kasibhatla, P. S., DeFries, R. S., Collatz, G. J., Hantson, S., Kloster, S., Bachelet, D., Forrest, M., Lasslop, G., Li, F., Mangeon, S., Melton, J. R., Yue, C., & Randerson, J. T. (2017). A human-driven decline in global burned area. *Science*. https://doi.org/10.1126/science.aal4108.

Andela, N., & van der Werf, G. R. (2014). Recent trends in African fires driven by cropland expansion and El Niño to La Niña transition. *Nature Climate Change*, *4*(9), Article 9. https://doi.org/10.1038/nclimate2313.

Anderson, K., Reuter, G., & Flannigan, M. D. (2007). Fire-growth modelling using meteorological data with random and systematic perturbations. *International Journal of Wildland Fire*, *16*(2), 174–182. Scopus. https://doi.org/10.1071/WF06069.

Andrews, P. L., & Queen, Ll. P. (2001). Fire modeling and information system technology. *International Journal of Wildland Fire*, *10*(4), 343–352. https://doi.org/10.1071/wf01033.

Arevalo-Ramirez, T. A., Castillo, A. H. F., Cabello, P. S. R., & Auat Cheein, F. A. (2021). Single bands leaf reflectance prediction based on fuel moisture content for forestry applications. *Biosystems Engineering*, *202*, 79–95. https://doi.org/10.1016/j.biosystemseng.2020.12.003.

Argañaraz, J. P., & Bellis, L. M. (2021). Evaluation of Burn Severity for the Fires of 2020 in the Mountains of Córdoba: Integration of Field and Remote Sensing Data. *2021 XIX Workshop on Information Processing and Control (RPIC)*, 1–6. https://doi.org/10.1109/RPIC53795.2021.9648471.

Arroyo, L. A., Pascual, C., & Manzanera, J. A. (2008). Fire models and methods to map fuel types: The role of remote sensing. *Forest Ecology and Management*, *256*(6), 1239–1252. https://doi.org/10.1016/j.foreco.2008.06.048

Artés, T., Oom, D., de Rigo, D., Durrant, T. H., Maianti, P., Libertà, G., & San-Miguel-Ayanz, J. (2019). A global wildfire dataset for the analysis of fire regimes and fire behaviour. *Scientific Data*, *6*(1), 296. https://doi.org/10.1038/s41597-019-0312-2.

Barmpoutis, P., Papaioannou, P., Dimitropoulos, K., & Grammalidis, N. (2020). A Review on Early Forest Fire Detection Systems Using Optical Remote Sensing. *Sensors*, *20*(22), 6442. https://doi.org/10.3390/s20226442.

Bartsch, A., Balzter, H., & George, C. (2009). The influence of regional surface soil moisture anomalies on forest fires in Siberia observed from satellites. *Environmental Research Letters*, *4*(4), 045021. https://doi.org/10.1088/1748-9326/4/4/045021.

Benali, A., Ervilha, A. R., Sá, A. C. L., Fernandes, P. M., Pinto, R. M. S., Trigo, R. M., & Pereira, J. M. C. (2016). Deciphering the impact of uncertainty on the accuracy of large wildfire spread simulations. *Science of The Total Environment*, *569–570*, 73–85. https://doi.org/10.1016/j.scitotenv.2016.06.112.

Benali, A., Sá, A. C. L., Ervilha, A. R., Trigo, R. M., Fernandes, P. M., & Pereira, J. M. C. (2017). Fire spread predictions: Sweeping uncertainty under the rug. *Science of The Total Environment*, *592*, 187–196. https://doi.org/10.1016/j.scitotenv.2017.03.106

Bergonse, R., Oliveira, S., Gonçalves, A., Nunes, S., DaCamara, C., & Zêzere, J. L. (2021). Predicting burnt areas during the summer season in Portugal by combining wildfire susceptibility and spring meteorological conditions. *Geomatics, Natural Hazards and Risk*, *12*(1), 1039–1057. https://doi.org/10.1080/19475705.2021.1909664.

Beven, K. (2002). Towards a coherent philosophy for modelling the environment. *Proceedings of the Royal Society A: Mathematical, Physical and Engineering Sciences*, *458*(2026), 2465–2484. Scopus. https://doi.org/10.1098/rspa.2002.0986.

Bisquert, M., Caselles, E., Sánchez, J. M., Caselles, V., Bisquert, M., Caselles, E., Sánchez, J. M., & Caselles, V. (2012). Application of artificial neural networks and logistic regression to the prediction of forest fire danger in Galicia using MODIS data. *International Journal of Wildland Fire*, *21*(8), 1025–1029. https://doi.org/10.1071/WF11105.

Bisquert, M. M., Sánchez, J. M., Caselles, V., Bisquert, M. M., Sánchez, J. M., & Caselles, V. (2011). Fire danger estimation from MODIS Enhanced Vegetation Index data: Application to Galicia region (north-west Spain). *International Journal of Wildland Fire*, *20*(3), 465–473. https://doi.org/10.1071/WF10002.

Bond, W. J., Midgley, G. F., & Woodward, F. I. (2003). What controls South African vegetation—Climate or fire? *South African Journal of Botany*, *69*(1), 79–91. https://doi.org/10.1016/S0254-6299(15)30362-8.

Boschetti, L., Vermote, E., & Wolfe, R. (2015). MODTBGA MODIS/Terra Thermal Bands Daily L2G-Lite Global 1km SIN Grid V006 MODTBGA. *NASA EOSDIS Land Processes DAAC*. https://doi.org/10.5067/MODIS/MODTBGA.006.

Bot, K., & Borges, J. G. (2022). A Systematic Review of Applications of Machine Learning Techniques for Wildfire Management Decision Support. *Inventions*, *7*(1), 15. https://doi.org/10.3390/inventions7010015.

Bowman, D. (2018). Wildfire science is at a loss for comprehensive data. *Nature*, *560*(7716), 7–7. https://doi.org/10.1038/d41586-018-05840-4.

Bowman, D. M. J. S., Balch, J., Artaxo, P., Bond, W. J., Cochrane, M. A., D'Antonio, C. M., DeFries, R., Johnston, F. H., Keeley, J. E., Krawchuk, M. A., Kull, C. A., Mack, M., Moritz, M. A., Pyne, S., Roos, C. I., Scott, A. C., Sodhi, N. S., Swetnam, T. W., & Whittaker, R. (2011). The human dimension of fire regimes on Earth. *Journal of Biogeography*, *38*(12), 2223–2236. https://doi.org/10.1111/j.1365-2699.2011.02595.x.

Briones-Herrera, C. I., Vega-Nieva, D. J., Briseño-Reyes, J., Monjarás-Vega, N. A., López-Serrano, P. M., Corral-Rivas, J. J., Alvarado, E., Arellano-Pérez, S., Jardel Peláez, E. J., Pérez Salicrup, D. R., & Jolly, W. M. (2022). Fuel-Specific Aggregation of Active Fire Detections for Rapid Mapping of Forest Fire Perimeters in Mexico. *Forests*, *13*(1), 124. https://doi.org/10.3390/f13010124.

Briones-Herrera, C. I., Vega-Nieva, D. J., Monjarás-Vega, N. A., Briseño-Reyes, J., López-Serrano, P. M., Corral-Rivas, J. J., Alvarado-Celestino, E., Arellano-Pérez, S., Álvarez-González, J. G., Ruiz-González, A. D., Jolly, W. M., & Parks, S. A. (2020). Near Real-Time Automated Early Mapping of the Perimeter of Large Forest Fires from the Aggregation of VIIRS and MODIS Active Fires in Mexico. *Remote Sensing*, *12*(12), Article 12. https://doi.org/10.3390/rs12122061.

Brunson, M. W., & Tanaka, J. (2011). Economic and Social Impacts of Wildfires and Invasive Plants in American Deserts: Lessons From the Great Basin. *Rangeland Ecology & Management*, *64*(5), 463–470. https://doi.org/10.2111/REM-D-10-00032.1.

Butt, E. W., Conibear, L., Knote, C., & Spracklen, D. V. (2021). Large Air Quality and Public Health Impacts due to Amazonian Deforestation Fires in 2019. *GeoHealth*, *5*(7), e2021GH000429. https://doi.org/10.1029/2021GH000429.

Byer, S., & Jin, Y. (2017). Detecting Drought-Induced Tree Mortality in Sierra Nevada Forests with Time Series of Satellite Data. *Remote Sensing*, *9*(9), Article 9. https://doi.org/10.3390/rs9090929.

Calvão, T., & Palmeirim, J. M. (2004). Mapping Mediterranean scrub with satellite imagery: Biomass estimation and spectral behaviour. *International Journal of Remote Sensing*, *25*(16), 3113–3126. https://doi.org/10.1080/01431160310001654978.

Cantymedia. (2022). *Weatherbase*. Weatherbase. http://www.weatherbase.com/.

Cao, X., Cui, X., Yue, M., Chen, J., Tanikawa, H., & Ye, Y. (2013). Evaluation of wildfire propagation susceptibility in grasslands using burned areas and multivariate logistic regression. *International Journal of Remote Sensing*, *34*(19), 6679–6700. https://doi.org/10.1080/01431161.2013.805280.

Castro, F. X., Tudela, A., & Sebastià, M. T. (2003). Modeling moisture content in shrubs to predict fire risk in Catalonia (Spain). *Agricultural and Forest Meteorology*, *116*(1), 49–59. https://doi.org/10.1016/S0168-1923(02)00248-4.

Cawson, J. G., Nyman, P., Schunk, C., Sheridan, G. J., Duff, T. J., Gibos, K., Bovill, W. D., Conedera, M., Pezzatti, G. B., Menzel, A., Cawson, J. G., Nyman, P., Schunk, C., Sheridan, G. J., Duff, T. J., Gibos, K., Bovill, W. D., Conedera, M., Pezzatti, G. B., & Menzel, A. (2020). Estimation of surface dead fine fuel moisture using automated fuel moisture sticks across a range of forests worldwide. *International Journal of Wildland Fire*, *29*(6), 548–559. https://doi.org/10.1071/WF19061.

CCES. (2021). *Wildfires and Climate Change*. Center of Climate and Energy Solutions. https://www.c2es.org/content/wildfires-and-climate-change/.

Ceccato, P., Flasse, S., & Grégoire, J.-M. (2002b). Designing a spectral index to estimate vegetation water content from remote sensing data: Part 2. Validation and applications. *Remote Sensing of Environment*, *82*(2), 198–207. https://doi.org/10.1016/S0034-4257(02)00036-6.

Ceccato, P., Gobron, N., Flasse, S., Pinty, B., & Tarantola, S. (2002a). Designing a spectral index to estimate vegetation water content from remote sensing data: Part 1: Theoretical approach. *Remote Sensing of Environment*, *82*(2), 188–197. https://doi.org/10.1016/S0034-4257(02)00037-8.

Chang, Y., Zhu, Z., Bu, R., Chen, H., Feng, Y., Li, Y., Hu, Y., & Wang, Z. (2013). Predicting fire occurrence patterns with logistic regression in Heilongjiang Province, China. *Landscape Ecology*, *28*(10), 1989–2004. https://doi.org/10.1007/s10980-013-9935-4.

Chaparro, D., Piles, M., Vall-llossera, M., & Camps, A. (2016b). Surface moisture and temperature trends anticipate drought conditions linked to wildfire activity in the Iberian Peninsula. *European Journal of Remote Sensing*, *49*(1), 955–971. https://doi.org/10.5721/EuJRS20164950.

Chaparro, D., Vall-llossera, M., Piles, M., Camps, A., Rüdiger, C., & Riera-Tatché, R. (2016a). Predicting the Extent of Wildfires Using Remotely Sensed Soil Moisture and Temperature Trends. *IEEE Journal of Selected Topics in Applied Earth Observations and Remote Sensing*, *9*(6), 2818–2829. https://doi.org/10.1109/JSTARS.2016.2571838.

Chavez, P. S. (1988). An improved dark-object subtraction technique for atmospheric scattering correction of multispectral data. *Remote Sensing of Environment*, *24*(3), 459–479. https://doi.org/10.1016/0034-4257(88)90019-3.

Chen, D., Fu, C., Hall, J. V., Hoy, E. E., & Loboda, T. V. (2021). Spatio-temporal patterns of optimal Landsat data for burn severity index calculations: Implications for high northern latitudes wildfire research. *Remote Sensing of Environment*, *258*, 112393. https://doi.org/10.1016/j.rse.2021.112393.

Chen, Y., Lara, M. J., & Hu, F. S. (2020). A robust visible near-infrared index for fire severity mapping in Arctic tundra ecosystems. *ISPRS Journal of Photogrammetry and Remote Sensing*, *159*, 101–113. https://doi.org/10.1016/j.isprsjprs.2019.11.012.

Chuvieco, E., Aguado, I., Jurdao, S., Pettinari, M. L., Yebra, M., Salas, J., Hantson, S., de la Riva, J., Ibarra, P., Rodrigues, M., Echeverría, M., Azqueta, D., Román, M. V., Bastarrika, A., Martínez, S., Recondo, C., Zapico, E., & Martínez-Vega, F. J. (2014). Integrating geospatial information into fire risk assessment. *International Journal of Wildland Fire*. https://doi.org/10.1071/WF12052.

Chuvieco, E., Aguado, I., Salas, J., García, M., Yebra, M., & Oliva, P. (2020). Satellite Remote Sensing Contributions to Wildland Fire Science and Management. *Current Forestry Reports*, *6*(2), 81–96. https://doi.org/10.1007/s40725-020-00116-5.

Chuvieco, E., Cocero, D., Riaño, D., Martin, P., Martínez-Vega, J., de la Riva, J., & Pérez, F. (2004). Combining NDVI and surface temperature for the estimation of live fuel moisture content in forest fire danger rating. *Remote Sensing of Environment*, *92*(3), 322–331. https://doi.org/10.1016/j.rse.2004.01.019.

Chuvieco, E., Englefield, P., Trishchenko, A. P., & Luo, Y. (2008). Generation of long time series of burn area maps of the boreal forest from NOAA–AVHRR composite data. *Remote Sensing of Environment*, *112*(5), 2381–2396. https://doi.org/10.1016/j.rse.2007.11.007.

Chuvieco, E., González, I., Verdú, F., Aguado, I., Yebra, M., Chuvieco, E., González, I., Verdú, F., Aguado, I., & Yebra, M. (2009). Prediction of fire occurrence from live fuel moisture content measurements in a Mediterranean ecosystem. *International Journal of Wildland Fire*, *18*(4), 430–441. https://doi.org/10.1071/WF08020.

Chuvieco, E., Martín, M. P., & Palacios, A. (2002). Assessment of different spectral indices in the red-near-infrared spectral domain for burned land discrimination. *International Journal of Remote Sensing*, *23*(23), 5103–5110. https://doi.org/10.1080/01431160210153129.

Chuvieco, E., Riaño, D., Aguado, I., & Cocero, D. (2002). Estimation of fuel moisture content from multitemporal analysis of Landsat Thematic Mapper reflectance data: Applications in fire danger assessment. *International Journal of Remote Sensing*, *23*(11), 2145–2162. https://doi.org/10.1080/01431160110069818.

Clark, P. E., Williams, C. J., Pierson, F. B., & Hardegree, S. P. (2016). Postfire grazing management effects on mesic sagebrush-steppe vegetation: Spring grazing. *Journal of Arid Environments*, *132*, 49–59. https://doi.org/10.1016/j.jaridenv.2015.10.022.

Clark, R. E., Hope, A. S., Tarantola, S., Gatelli, D., Dennison, P. E., & Moritz, M. A. (2008). Sensitivity Analysis of a Fire Spread Model in a Chaparral Landscape. *Fire Ecology*, *4*(1), 1–13. https://doi.org/10.4996/fireecology.0401001.

Clarke, H., & Evans, J. P. (2019). Exploring the future change space for fire weather in southeast Australia. *Theoretical and Applied Climatology*, *136*(1), 513–527. https://doi.org/10.1007/s00704-018-2507-4

Çolak, E., & Sunar, F. (2020). Evaluation of forest fire risk in the Mediterranean Turkish forests: A case study of Menderes region, Izmir. *International Journal of Disaster Risk Reduction*, *45*, 101479. https://doi.org/10.1016/j.ijdrr.2020.101479.

Çömert, R., Matci, D. K., & Avdan, U. (2019). Object based burned area mapping with random forest algorithm. *International Journal of Engineering and Geosciences*, *4*(2), Article 2. https://doi.org/10.26833/ijeg.455595.

Cruz Núñez, X., Villers Ruiz, L., & Gay García, C. (2014). Black carbon and organic carbon emissions from wildfires in Mexico. *Atmósfera*, *27*(2), 165–172. https://doi.org/10.1016/S0187-6236(14)71107-5.

Dahiru, M. Z., & Hashim, M. (2020). An Approach for the Retrieval of Land Surface Temperature from the Industrial Area Using Landsat-8 Thermal Infrared Sensors. *IOP Conference Series: Earth and Environmental Science*, *540*(1), 012059. https://doi.org/10.1088/1755-1315/540/1/012059.

Danson, F. M., & Bowyer, P. (2004). Estimating live fuel moisture content from remotely sensed reflectance. *Remote Sensing of Environment*, *92*(3), 309–321. https://doi.org/10.1016/j.rse.2004.03.017.

Das, N. N., Entekhabi, D., Dunbar, R. S., Chaubell, M. J., Colliander, A., Yueh, S., Jagdhuber, T., Chen, F., Crow, W., O'Neill, P. E., Walker, J. P., Berg, A., Bosch, D. D., Caldwell, T., Cosh, M. H., Collins, C. H., Lopez-Baeza, E., & Thibeault, M. (2019). The SMAP and Copernicus Sentinel 1A/B microwave active-passive high resolution surface soil moisture product. *Remote Sensing of Environment*, *233*, 111380. https://doi.org/10.1016/j.rse.2019.111380.

Dennison, P. E., Moritz, M. A., Dennison, P. E., & Moritz, M. A. (2009). Critical live fuel moisture in chaparral ecosystems: A threshold for fire activity and its relationship to antecedent precipitation. *International Journal of Wildland Fire*, *18*(8), 1021–1027. https://doi.org/10.1071/WF08055.

DFRR. (2009). *Summary Report of the Fire Season*. Department of Forestry Range Resources, Division of Conservation and Management, Fire Management Section, Ministry of Environment, Wildlife and Tourism.

Dillon, G., Menakis, J., & Fay, F. (2015). Wildland fire potential: A tool for assessing wildfire risk and fuels management needs. *In: Keane, Robert E.; Jolly, Matt; Parsons, Russell; Riley, Karin. Proceedings of the Large Wildland Fires Conference; May 19-23, 2014; Missoula, MT. Proc. RMRS-P-73. Fort Collins, CO: U.S. Department of Agriculture, Forest Service, Rocky Mountain Research Station. p. 60-76.*, *73*, 60–76.

Dimitrakopoulos, A. P., & Papaioannou, K. K. (2001). Flammability Assessment of Mediterranean Forest Fuels. *Fire Technology*, *37*(2), 143–152. https://doi.org/10.1023/A:1011641601076

D'Onofrio, D., Baudena, M., Lasslop, G., Nieradzik, L. P., Wårlind, D., & von Hardenberg, J. (2020). Linking Vegetation-Climate-Fire Relationships in Sub-Saharan Africa to Key Ecological Processes in Two Dynamic Global Vegetation Models. *Frontiers in Environmental Science*, *8*. https://www.frontiersin.org/articles/10.3389/fenvs.2020.00136.

Dougill, A. J., Akanyang, L., Perkins, J. S., Eckardt, F. D., Stringer, L. C., Favretto, N., Atlhopheng, J., & Mulale, K. (2016). Land use, rangeland degradation and ecological changes in the southern Kalahari, Botswana. *African Journal of Ecology*, *54*(1), 59–67. https://doi.org/10.1111/aje.12265.

Duan, S.-B., Li, Z.-L., Li, H., Göttsche, F.-M., Wu, H., Zhao, W., Leng, P., Zhang, X., & Coll, C. (2019). Validation of Collection 6 MODIS land surface temperature product using in situ measurements. *Remote Sensing of Environment*, *225*, 16–29. https://doi.org/10.1016/j.rse.2019.02.020.

Dube, O. P. (2013). Challenges of wildland fire management in Botswana: Towards a community inclusive fire management approach. *Weather and Climate Extremes*, *1*, 26–41. https://doi.org/10.1016/j.wace.2013.08.001.

Dwyer, E., Pinnock, S., Gregoire, J.-M., & Pereira, J. M. C. (2000). Global spatial and temporal distribution of vegetation fire as determined from satellite observations. *International Journal of Remote Sensing*, *21*(6–7), 1289–1302. https://doi.org/10.1080/014311600210182.

Entekhabi, D., Njoku, E. G., O'Neill, P. E., Kellogg, K. H., Crow, W. T., Edelstein, W. N., Entin, J. K., Goodman, S. D., Jackson, T. J., Johnson, J., Kimball, J., Piepmeier, J. R., Koster, R. D., Martin, N., McDonald, K. C., Moghaddam, M., Moran, S., Reichle, R., Shi, J. C., … Van Zyl, J. (2010). The Soil Moisture Active Passive (SMAP) Mission. *Proceedings of the IEEE*, *98*(5), 704–716. https://doi.org/10.1109/JPROC.2010.2043918.

ESA. (2021). *Multi-Decade Global Fire Dataset Set To Support Trend Analysis*. The EUropean Space Agency. ESA Climate Office. https://climate.esa.int/de/news-events/multi-decade-global-fire-dataset-set-support-trend-analysis/.

Escuin, S., Navarro, R., & Fernández, P. (2008). Fire severity assessment by using NBR (Normalized Burn Ratio) and NDVI (Normalized Difference Vegetation Index) derived from LANDSAT TM/ETM images. *International Journal of Remote Sensing*, *29*(4), 1053–1073. https://doi.org/10.1080/01431160701281072.

Estes, B. L., Knapp, E. E., Skinner, C. N., Uzoh, F. C. C., Estes, B. L., Knapp, E. E., Skinner, C. N., & Uzoh, F. C. C. (2012). Seasonal variation in surface fuel moisture between unthinned and thinned mixed conifer forest, northern California, USA. *International Journal of Wildland Fire*, *21*(4), 428–435. https://doi.org/10.1071/WF11056.

Fayiah, M., Xavier, R., & Supe Tulcan, R. (2021). Seasonal Wildfire Outbreak Trend and its Consequences on Forest Biodiversity and the Environment: A Case Study of Sierra Leone. *International Journal of Sustainable Energy and Environmental Research*, *10*(2), 69–84. https://doi.org/10.18488/journal.13.2021.102.69.84.

Fernandes, P. A. M., Loureiro, C. A., & Botelho, H. S. (2004). Fire behaviour and severity in a maritime pine stand under differing fuel conditions. *Annals of Forest Science*, *61*(6), 537–544. https://doi.org/10.1051/forest:2004048.

Ferraz, A., Bretar, F., Jacquemoud, S., & Gonçalves, G. (2009). *The Role of Lidar Systems in Fuel Mapping*. https://doi.org/10.13140/RG.2.2.17984.23048.

Fidelis, A., Delgado-Cartay, M. D., Blanco, C. C., Müller, S. C., Pillar, V. D., & Pfadenhauer, J. (2010). FIRE INTENSITY AND SEVERITY IN BRAZILIAN CAMPOS GRASSLANDS. *Interciencia*, *35*(10), 739–745. https://doi.org/0378-1844/10/10/739-07 $ 3.00/0.

Filella, I., Peñuelas, J., Llorens, L., & Estiarte, M. (2004). Reflectance assessment of seasonal and annual changes in biomass and CO2 uptake of a Mediterranean shrubland submitted to experimental warming and drought. *Remote Sensing of Environment*, *90*(3), 308–318. https://doi.org/10.1016/j.rse.2004.01.010.

Finney, M. A. (1998). FARSITE: Fire Area Simulator-model development and evaluation. *Res. Pap. RMRS-RP-4, Revised 2004. Ogden, UT: U.S. Department of Agriculture, Forest Service, Rocky Mountain Research Station. 47 p.*, *4*. https://doi.org/10.2737/RMRS-RP-4.

Flannigan, M. D., Krawchuk, M. A., de Groot, W. J., Wotton, B. M., & Gowman, L. M. (2009). Implications of changing climate for global wildland fire. In *International Journal of Wildland Fire* (Vol. 18, Issue 5, pp. 483–507).

Flasse, S. P., Trigg, S. N., Ceccato, P. N., Perryman, A. H., Hudak, A. T., Thompson, M. W., Brockett, B. H., Drame, M., Ntabeni, T., Frost, P. E., & Landmann, T. (2004). Remote Sensing Of Vegetation Fires And Its Contribution To A Fire Management Information System. In *Goldammer, J.; de Ronde, C., eds. Fire management handbook for sub-Sahara Africa* (pp. 158–211). Frieburg, Germany: Global Fire Monitoring Center.

Florec, V., Thompson, M. P., & Rodríguez y Silva, F. (2019). Cost of Suppression. In S. L. Manzello (Ed.), *Encyclopedia of Wildfires and Wildland-Urban Interface (WUI) Fires* (pp. 1–11). Springer International Publishing. https://doi.org/10.1007/978-3-319-51727-8_96-1.

Forkel, M., Thonicke, K., Beer, C., Cramer, W., Bartalev, S., & Schmullius, C. (2012). Extreme fire events are related to previous-year surface moisture conditions in permafrost-underlain larch forests of Siberia. *Environmental Research Letters*, *7*, 044021. https://doi.org/10.1088/1748-9326/7/4/044021.

Fox, J., Vandewalle, M., & Alexander, K. (2017). Land Cover Change in Northern Botswana: The Influence of Climate, Fire, and Elephants on Semi-Arid Savanna Woodlands. *Land*, *6*(4), 73. https://doi.org/10.3390/land6040073.

Freeborn, P. H., Jolly, W. M., Cochrane, M. A., & Roberts, G. (2022). Large wildfire driven increases in nighttime fire activity observed across CONUS from 2003–2020. *Remote Sensing of Environment*, *268*, 112777. https://doi.org/10.1016/j.rse.2021.112777.

French, N. H. F., Kasischke, E. S., Hall, R. J., Murphy, K. A., Verbyla, D. L., Hoy, E. E., Allen, J. L., French, N. H. F., Kasischke, E. S., Hall, R. J., Murphy, K. A., Verbyla, D. L., Hoy, E. E., & Allen, J. L. (2008). Using Landsat data to assess fire and burn severity in the North American boreal forest region: An overview and summary of results. *International Journal of Wildland Fire*, *17*(4), 443–462. https://doi.org/10.1071/WF08007.

García, M. J. L., & Caselles, V. (1991). Mapping burns and natural reforestation using thematic Mapper data. *Geocarto International*, *6*(1), 31–37. https://doi.org/10.1080/10106049109354290.

Giglio, L., Csiszar, I., & Justice, C. O. (2006). Global distribution and seasonality of active fires as observed with the Terra and Aqua Moderate Resolution Imaging Spectroradiometer

(MODIS) sensors. *Journal of Geophysical Research: Biogeosciences*, *111*(G2). https://doi.org/10.1029/2005JG000142.

Girona-García, A., Ortiz-Perpiñá, O., & Badía-Villas, D. (2019). Dynamics of topsoil carbon stocks after prescribed burning for pasture restoration in shrublands of the Central Pyrenees (NE-Spain). *Journal of Environmental Management*, *233*, 695–705. https://doi.org/10.1016/j.jenvman.2018.12.057.

Gitelson, A. A., & Merzlyak, M. N. (1998). Remote sensing of chlorophyll concentration in higher plant leaves. *Advances in Space Research*, *22*(5), 689–692. https://doi.org/10.1016/S0273-1177(97)01133-2.

Gomes, L., Miranda, H. S., Silvério, D. V., & Bustamante, M. M. C. (2020). Effects and behaviour of experimental fires in grasslands, savannas, and forests of the Brazilian Cerrado. *Forest Ecology and Management*, *458*, 117804. https://doi.org/10.1016/j.foreco.2019.117804

Gómez, C., White, J. C., Wulder, M. A., & Alejandro, P. (2014). Historical forest biomass dynamics modelled with Landsat spectral trajectories. *ISPRS Journal of Photogrammetry and Remote Sensing*, *93*, 14–28. https://doi.org/10.1016/j.isprsjprs.2014.03.008.

Gonsamo, A., Chen, J. M., Colombo, S. J., Ter-Mikaelian, M. T., & Chen, J. (2017). Global change induced biomass growth offsets carbon released via increased forest fire and respiration of the central Canadian boreal forest: Global Change and Boreal Forest C Budget. *Journal of Geophysical Research: Biogeosciences*, *122*(5), 1275–1293. https://doi.org/10.1002/2016JG003627.

Goode, L. (2019). The New Science of Wildfire Prediction. *Wired*. https://www.wired.com/story/get-wired-podcast-13-fire-science/.

Government of Botswana. (1977). *Act NO. 37 Herbage Preservation (Prevention of fires) 1977*. Laws of Botswana. https://botswanalaws.com/alphabetical-list-of-statutes/herbage-preservation-prevention-of-fires.

Grant, E., & Runkle, J. D. (2022). Long-term health effects of wildfire exposure: A scoping review. *The Journal of Climate Change and Health*, *6*, 100110. https://doi.org/10.1016/j.joclim.2021.100110.

Grömping, U. (2009). Variable Importance Assessment in Regression: Linear Regression versus Random Forest. *The American Statistician*, *63*(4), 308–319. https://doi.org/10.1198/tast.2009.08199.

Guo, F., Su, Z., Tigabu, M., Yang, X., Lin, F., Liang, H., & Wang, G. (2017). Spatial Modelling of Fire Drivers in Urban-Forest Ecosystems in China. *Forests*, *8*(6), Article 6. https://doi.org/10.3390/f8060180.

Guo, F., Su, Z., Wang, G., Sun, L., Lin, F., & Liu, A. (2016). Wildfire ignition in the forests of southeast China: Identifying drivers and spatial distribution to predict wildfire likelihood. *Applied Geography*, *66*, 12–21. https://doi.org/10.1016/j.apgeog.2015.11.014.

GWIS. (2022). *GWIS - Statistics Portal*. Global WIldfire Information System. https://gwis.jrc.ec.europa.eu/apps/gwis.statistics/estimates.

Halofsky, J. E., Peterson, D. L., & Harvey, B. J. (2020). Changing wildfire, changing forests: The effects of climate change on fire regimes and vegetation in the Pacific Northwest, USA. *Fire Ecology*, *16*(1), 4. https://doi.org/10.1186/s42408-019-0062-8

Handmer, J., Honda, Y., Kundzewicz, Z. W., & Mechler, R. (2012). *Changes in impacts of climate extremes: Human systems and ecosystems* (C. B. Field, V. Barros, & T. F. Stocker, Eds.). Cambridge University Press. http://ipcc-wg2.gov/SREX/images/uploads/SREX-Chap4_FINAL.pdf.

Hantson, S., Pueyo, S., & Chuvieco, E. (2015). Global fire size distribution is driven by human impact and climate. *Global Ecology and Biogeography*, *24*(1), 77–86. https://doi.org/10.1111/geb.12246.

Harden, J. W., Trumbore, S. E., Stocks, B. J., Hirsch, A., Gower, S. T., O'neill, K. P., & Kasischke, E. S. (2000). The role of fire in the boreal carbon budget: FIRE IN THE BOREAL CARBON BUDGET. *Global Change Biology*, *6*(S1), 174–184. https://doi.org/10.1046/j.1365-2486.2000.06019.x.

Hawbaker, T. J., Vanderhoof, M. K., Beal, Y.-J., Takacs, J. D., Schmidt, G. L., Falgout, J. T., Williams, B., Fairaux, N. M., Caldwell, M. K., Picotte, J. J., Howard, S. M., Stitt, S., & Dwyer, J. L. (2017). Mapping burned areas using dense time-series of Landsat data. *Remote Sensing of Environment*, *198*, 504–522. https://doi.org/10.1016/j.rse.2017.06.027.

Heisig, J., Olson, E., & Pebesma, E. (2022). Predicting Wildfire Fuels and Hazard in a Central European Temperate Forest Using Active and Passive Remote Sensing. *Fire*, *5*(1), Article 1. https://doi.org/10.3390/fire5010029.

Hiers, J. K., Stauhammer, C. L., O'Brien, J. J., Gholz, H. L., Martin, T. A., Hom, J., & Starr, G. (2019). Fine dead fuel moisture shows complex lagged responses to environmental condi-

tions in a saw palmetto (Serenoa repens) flatwoods. *Agricultural and Forest Meteorology*, *266–267*, 20–28. https://doi.org/10.1016/j.agrformet.2018.11.038.

Hilton, J. E., Miller, C., Sullivan, A. L., & Rucinski, C. (2015). Effects of spatial and temporal variation in environmental conditions on simulation of wildfire spread. *Environmental Modelling & Software*, *67*, 118–127. https://doi.org/10.1016/j.envsoft.2015.01.015.

Howard, S., Picotte, J., & Coan, M. (2014). Utilizing Multi-Sensor Fire Detections to Map Fires in the United States. *The International Archives of the Photogrammetry, Remote Sensing and Spatial Information Sciences*, *XL–1*, 161–166. https://doi.org/10.5194/isprsarchives-XL-1-161-2014.

Huber, K. (2018). Resilience Strategies for wildfire. *Center for Climate and Energy Solutions*, 12.

Huete, A. R. (1988). A soil-adjusted vegetation index (SAVI). *Remote Sensing of Environment*, *25*(3), 295–309. https://doi.org/10.1016/0034-4257(88)90106-X.

Huh, Y., & Lee, J. (2017). Enhanced contextual forest fire detection with prediction interval analysis of surface temperature using vegetation amount. *International Journal of Remote Sensing*, *38*(11), 3375–3393. https://doi.org/10.1080/01431161.2017.1295481.

Hunt, E. R., Li, L., Yilmaz, M. T., & Jackson, T. J. (2011). Comparison of vegetation water contents derived from shortwave-infrared and passive-microwave sensors over central Iowa. *Remote Sensing of Environment*, *115*(9), 2376–2383. https://doi.org/10.1016/j.rse.2011.04.037.

IUFRO. (2018). *Global Fire Challenges in a Warming World. Robinne F.-N., Burns J., Kant P., de Groot B., Flannigan M.D., Kleine M., Wotton D. M. (eds.)* (Occasional Paper No. 32). International Union of Forest Research Organizations. https://www.iufro.org/news/article/2019/01/23/occasional-paper-32-global-fire-challenges-in-a-warming-world/.

Jensen, D., Reager, J. T., Zajic, B., Rousseau, N., Rodell, M., & Hinkley, E. (2018). The sensitivity of US wildfire occurrence to pre-season soil moisture conditions across ecosystems. *Environmental Research Letters: ERL [Web Site]*, *13*(No 1), 014021. https://doi.org/10.1088/1748-9326/aa9853.

Jia, S., Kim, S. H., Nghiem, S. V., & Kafatos, M. (2019). Estimating Live Fuel Moisture Using SMAP L-Band Radiometer Soil Moisture for Southern California, USA. *Remote Sensing*, *11*(13), Article 13. https://doi.org/10.3390/rs11131575.

Jurdao, S., Arevalillo, J. M., Chuvieco, E., & Yebra, M. (2011). *Development of a method to transform Life Fuel Moisture Content into ignition probability*. 3.

Justino, F., Stordal, F., Clement, A., Coppola, E., Setzer, A., & Brumatti, D. (2013). Modelling Weather and Climate Related Fire Risk in Africa. *American Journal of Climate Change*, *2013*. https://doi.org/10.4236/ajcc.2013.24022.

Kahiu, M. N., & Hanan, N. P. (2018). Fire in sub-Saharan Africa: The fuel, cure and connectivity hypothesis. *Global Ecology and Biogeography*, *27*(8), 946–957. https://doi.org/10.1111/geb.12753.

Karimi, A., Abdollahi, S., Ostad-Ali-Askari, K., Eslamian, S., & Singh, V. P. (2021). Predicting fire hazard areas using vegetation indexes, case study: Forests of Golestan Province, Iran. *Journal of Geography and Cartography*, *4*(1), Article 1. https://doi.org/10.24294/jgc.v4i1.451.

Keane, R. E., Burgan, R. E., & Van Wagtendonk, J. W. (2001). Mapping wildland fuels for fire management across multiple scales: Integrating remote sensing, GIS, and biophysical modeling. *International Journal of Wildland Fire*, *10*(4), 301–319. USGS Publications Warehouse. https://doi.org/10.1071/WF01028.

Keane, R. E., Mincemoyer, S. A., Schmidt, K. M., Long, D. G., & Garner, J. L. (2000). Mapping vegetation and fuels for fire management on the Gila National Forest Complex, New Mexico. *Gen. Tech. Rep. RMRS-GTR-46. Ogden, UT: U.S. Department of Agriculture, Forest Service, Rocky Mountain Research Station, 126 p.*, *46*. https://doi.org/10.2737/RMRS-GTR-46.

Keane, R. E., & Reeves, M. (2012). Use of Expert Knowledge to Develop Fuel Maps for Wildland Fire Management. In A. H. Perera, C. A. Drew, & C. J. Johnson (Eds.), *Expert Knowledge and Its Application in Landscape Ecology* (pp. 211–228). Springer. https://doi.org/10.1007/978-1-4614-1034-8_11

Keeley, J. E. (2009). Fire intensity, fire severity and burn severity: A brief review and suggested usage. *International Journal of Wildland Fire*, *18*(1), 116. https://doi.org/10.1071/WF07049.

Kerr, Y. H., Waldteufel, P., Wigneron, J.-P., Delwart, S., Cabot, F., Boutin, J., Escorihuela, M.-J., Font, J., Reul, N., Gruhier, C., Juglea, S. E., Drinkwater, M. R., Hahne, A., Martín-Neira, M., & Mecklenburg, S. (2010). The SMOS Mission: New Tool for Monitoring

Key Elements ofthe Global Water Cycle. *Proceedings of the IEEE*, *98*(5), 666–687. https://doi.org/10.1109/JPROC.2010.2043032.

Key, C. H., & Benson, N. C. (2006). Landscape Assessment (LA). Sampling and Analysis Methods. In *In: Lutes, Duncan C.; Keane, Robert E.; Caratti, John F.; Key, Carl H.; Benson, Nathan C.; Sutherland, Steve; Gangi, Larry J. 2006. FIREMON: Fire effects monitoring and inventory system. Gen. Tech. Rep. RMRS-GTR-164-CD. Fort Collins, CO: U.S. Department of Agriculture, Forest Service, Rocky Mountain Research Station. P. LA-1-55* (Vol. 164). http://www.fs.usda.gov/treesearch/pubs/24066.

Kgosikoma, O. E., & Batisani, N. (2014). Livestock population dynamics and pastoral communities' adaptation to rainfall variability in communal lands of Kgalagadi South, Botswana. *Pastoralism*, *4*(1), 19. https://doi.org/10.1186/s13570-014-0019-0.

Kim, P. (2017). Machine Learning. In P. Kim (Ed.), *MATLAB Deep Learning: With Machine Learning, Neural Networks and Artificial Intelligence* (pp. 1–18). Apress. https://doi.org/10.1007/978-1-4842-2845-6_1.

Kimbrough. (2020, September 4). *Around the world, a fire crisis flares up, fueled by human actions*. Mongabay Environmental News. https://news.mongabay.com/2020/09/around-the-world-a-fire-crisis-flares-up-fueled-by-human-actions/.

Kingma, D. P., & Ba, L. J. (2015). *Adam: A Method for Stochastic Optimization*. 13. https://hdl.handle.net/11245/1.505367.

Kolanek, A., Szymanowski, M., & Raczyk, A. (2021). Human Activity Affects Forest Fires: The Impact of Anthropogenic Factors on the Density of Forest Fires in Poland. *Forests*, *12*(6), 728. https://doi.org/10.3390/f12060728.

Kolden, C. A., & Rogan, J. (2013). Mapping wildfire burn severity in the Arctic Tundra from downsampled MODIS data. In *Arctic, Antarctic, and Alpine Research* (Vol. 45, Issue 1, p. 6476). https://doi.org/10.1657/1938-4246-45.1.64.

Kouassi, J.-L., Wandan, N., & Mbow, C. (2020). Predictive Modeling of Wildfire Occurrence and Damage in a Tropical Savanna Ecosystem of West Africa. *Fire*, *3*(3), Article 3. https://doi.org/10.3390/fire3030042.

Latifah, A. L., Shabrina, A., Wahyuni, I. N., & Sadikin, R. (2019). Evaluation of Random Forest model for forest fire prediction based on climatology over Borneo. *2019 International Conference on Computer, Control, Informatics and Its Applications (IC3INA)*, 4–8. https://doi.org/10.1109/IC3INA48034.2019.8949588.

Le, H. V., Hoang, D. A., Tran, C. T., Nguyen, P. Q., Tran, V. H. T., Hoang, N. D., Amiri, M., Ngo, T. P. T., Nhu, H. V., Hoang, T. V., & Bui, D. T. (2021). A new approach of deep neural computing for spatial prediction of wildfire danger at tropical climate areas. *Ecological Informatics*, *63*, 101300. https://doi.org/10.1016/j.ecoinf.2021.101300.

Leblon, B. (2005). Monitoring Forest Fire Danger with Remote Sensing. *Natural Hazards*, *35*(3), 343–359. https://doi.org/10.1007/s11069-004-1796-3.

Lee, R. J., & Chow, T. E. (2015). Post-wildfire assessment of vegetation regeneration in Bastrop, Texas, using Landsat imagery. *GIScience & Remote Sensing*, *52*(5), 609–626. https://doi.org/10.1080/15481603.2015.1055451.

Lehsten, V., Tansey, K., Balzter, H., Thonicke, K., Spessa, A., Weber, U., Smith, B., & Arneth, A. (2009). Estimating carbon emissions from African wildfires. *Biogeosciences*, *6*(3), Article 3.

Leuenberger, M., Kanevski, M., & Vega Orozco, C. D. (2013). *Forest Fires in a Random Forest*. EGU2013-3238.

Li, S. (2019). Wildfire early warning system based on wireless sensors and unmanned aerial vehicle. *Journal of Unmanned Vehicle Systems*, *7*(1), 76–91. https://doi.org/10.1139/juvs-2018-0022.

Li, Z.-L., & Duan, S.-B. (2018). 5.11—Land Surface Temperature. In S. Liang (Ed.), *Comprehensive Remote Sensing* (pp. 264–283). Elsevier. https://doi.org/10.1016/B978-0-12-409548-9.10375-6.

Liu, Y., Liu, Y., Fu, J., Yang, C.-E., Dong, X., Tian, H., Tao, B., Yang, J., Wang, Y., Zou, Y., Ke, Z., Liu, Y., Liu, Y., Fu, J., Yang, C.-E., Dong, X., Tian, H., Tao, B., Yang, J., … Ke, Z. (2021). Projection of future wildfire emissions in western USA under climate change: Contributions from changes in wildfire, fuel loading and fuel moisture. *International Journal of Wildland Fire*, *31*(1), 1–13. https://doi.org/10.1071/WF20190.

Liu, Z., & Wimberly, M. C. (2016). Direct and indirect effects of climate change on projected future fire regimes in the western United States. *Science of The Total Environment*, *542*, 65–75. https://doi.org/10.1016/j.scitotenv.2015.10.093.

Loehman, R. A., Reinhardt, E., & Riley, K. L. (2014). Wildland fire emissions, carbon, and climate: Seeing the forest and the trees – A cross-scale assessment of wildfire and carbon dynamics in fire-prone, forested ecosystems. *Forest Ecology and Management*, *317*, 9–19. https://doi.org/10.1016/j.foreco.2013.04.014.

Lozano, O. M., Salis, M., Ager, A. A., Arca, B., Alcasena, F. J., Monteiro, A. T., Finney, M. A., Del Giudice, L., Scoccimarro, E., & Spano, D. (2017). Assessing Climate Change Impacts on Wildfire Exposure in Mediterranean Areas. *Risk Analysis*, *37*(10), 1898–1916. https://doi.org/10.1111/risa.12739.

Lu, Y., & Wei, C. (2021). Evaluation of microwave soil moisture data for monitoring live fuel moisture content (LFMC) over the coterminous United States. *Science of The Total Environment*, *771*, 145410. https://doi.org/10.1016/j.scitotenv.2021.145410.

Lundgren, S., Mitchell, W., & Wallace, M. (1995). Status report on NFMAS--an interagency system update project. *Fire Management Notes*. https://scholar.google.com/scholar_lookup?title=status+report+on+NFMAS--an+interagency+system+update+project&author=Lundgren%2C+S.&publication_year=1995.

Lutakamale, A. S., & Kaijage, S. (2017). Wildfire Monitoring and Detection System Using Wireless Sensor Network: A Case Study of Tanzania. *Wireless Sensor Network*, *9*(8), Article 8. https://doi.org/10.4236/wsn.2017.98015.

Luyssaert, S., Ciais, P., Piao, S. L., Schulze, E.-D., Jung, M., Zaehle, S., Schelhaas, M. J., Reichstein, M., Churkina, G., Papale, D., Abril, G., Beer, C., Grace, J., Loustau, D., Matteucci, G., Magnani, F., Nabuurs, G. J., Verbeeck, H., Sulkava, M., … Team, members of the C.-I. S. (2010). The European carbon balance. Part 3: Forests. *Global Change Biology*, *16*(5), 1429–1450. https://doi.org/10.1111/j.1365-2486.2009.02056.x.

Maabong, K. E., & Mphale, K. (2021). Wildfires in Botswana and Their Frequency of Occurrence. *Atmospheric and Climate Sciences*, *11*(04), 689–696. https://doi.org/10.4236/acs.2021.114040.

Mallinis, G., Mitsopoulos, I., & Chrysafi, I. (2018). Evaluating and comparing Sentinel 2A and Landsat-8 Operational Land Imager (OLI) spectral indices for estimating fire severity in a Mediterranean pine ecosystem of Greece. *GIScience & Remote Sensing*, *55*(1), 1–18. https://doi.org/10.1080/15481603.2017.1354803.

Mansoor, S., Farooq, I., Kachroo, M. M., Mahmoud, A. E. D., Fawzy, M., Popescu, S. M., Alyemeni, M. N., Sonne, C., Rinklebe, J., & Ahmad, P. (2022). Elevation in wildfire frequencies with respect to the climate change. *Journal of Environmental Management*, *301*, 113769. https://doi.org/10.1016/j.jenvman.2021.113769.

Marsett, R. C., Qi, J., Heilman, P., Biedenbender, S. H., Watson, M. C., Amer, S., Weltz, M., Goodrich, D., & Marsett, R. (2006). *Remote Sensing for Grassland Management in the Arid Southwest*. 11.

Martín, Y., Zúñiga-Antón, M., & Rodrigues Mimbrero, M. (2019). Modelling temporal variation of fire-occurrence towards the dynamic prediction of human wildfire ignition danger in northeast Spain. *Geomatics, Natural Hazards and Risk*, *10*(1), 385–411. https://doi.org/10.1080/19475705.2018.1526219.

Matthews, S. (2014). Dead fuel moisture research: 1991–2012. *International Journal of Wildland Fire*, *23*(1), 78–92. https://doi.org/10.1071/WF13005.

Mazzeo, G., De Santis, F., Falconieri, A., Filizzola, C., Lacava, T., Lanorte, A., Marchese, F., Nolè, G., Pergola, N., Pietrapertosa, C., & Satriano, V. (2022). Integrated Satellite System for Fire Detection and Prioritization. *Remote Sensing*, *14*(2), 335. https://doi.org/10.3390/rs14020335.

McArthur, A. G. (1967). *Fire behaviour in eucalypt forests. Australian Forestry and Timber Bureau Leaflet, 107*. https://catalogue.nla.gov.au/Record/2275488.

McColl-Gausden, S. C., Bennett, L. T., Ababei, D. A., Clarke, H. G., & Penman, T. D. (2022). Future fire regimes increase risks to obligate-seeder forests. *Diversity and Distributions*, *28*(3), 542–558.

McKenzie, D., Gedalof, Z., Peterson, D. L., & Mote, P. (2004). Climatic Change, Wildfire, and Conservation. *Conservation Biology*, *18*(4), 890–902. https://doi.org/10.1111/j.1523-1739.2004.00492.x.

Meldrum, J. R., Brenkert-Smith, H., Champ, P. A., Falk, L., Wilson, P., & Barth, C. M. (2018). Wildland–Urban Interface Residents' Relationships with Wildfire: Variation Within and Across Communities. *Society & Natural Resources*, *31*(10), 1132–1148. https://doi.org/10.1080/08941920.2018.1456592.

Meredith, G. R., & Brunson, M. W. (2021). Effects of Wildfire on Collaborative Management of Rangelands: A Case Study of the 2015 Soda Fire. *Rangelands*, 10. https://doi.org/10.1016/j.rala.2021.03.001.

Merrill, D. F., & Alexander, M. E. (1987). *Glossary of forest fire management terms.* http://cfs.nrcan.gc.ca/publications?id=35337.

Merzouki, A., & Leblon, B. (2011). Mapping fuel moisture codes using MODIS images and the Getis statistic over western Canada grasslands. *International Journal of Remote Sensing*, *32*(6), 1619–1634. https://doi.org/10.1080/01431160903586773.

Michael, Y., Helman, D., Glickman, O., Gabay, D., Brenner, S., & Lensky, I. M. (2021). Forecasting fire risk with machine learning and dynamic information derived from satellite vegetation index time-series. *Science of The Total Environment*, *764*, 142844. https://doi.org/10.1016/j.scitotenv.2020.142844.

Miller, J. D., Safford, H. D., Crimmins, M., & Thode, A. E. (2009). Quantitative Evidence for Increasing Forest Fire Severity in the Sierra Nevada and Southern Cascade Mountains, California and Nevada, USA. *Ecosystems*, *12*(1), 16–32. https://doi.org/10.1007/s10021-008-9201-9.

Miller, J. D., & Thode, A. E. (2007). Quantifying burn severity in a heterogeneous landscape with a relative version of the delta Normalized Burn Ratio (dNBR). *Remote Sensing of Environment*, *109*(1), 66–80. https://doi.org/10.1016/j.rse.2006.12.006.

Mondal, P., McDermid, S. S., & Qadir, A. (2020). A reporting framework for Sustainable Development Goal 15: Multi-scale monitoring of forest degradation using MODIS, Landsat and Sentinel data. *Remote Sensing of Environment*, *237*, 111592. https://doi.org/10.1016/j.rse.2019.111592.

Monteith, J. L. (1972). Solar Radiation and Productivity in Tropical Ecosystems. *Journal of Applied Ecology*, *9*(3), 747–766. https://doi.org/10.2307/2401901.

Morvan, D. (2013). Numerical study of the effect of fuel moisture content (FMC) upon the propagation of a surface fire on a flat terrain. *Fire Safety Journal*, *58*, 121–131. https://doi.org/10.1016/j.firesaf.2013.01.010.

Moyo, T., Musakwa, W., Nyathi, N. A., Mpofu, E., & Gumbo, T. (2020). MODELLING OF NATURAL FIRE OCCURRENCES: A CASE OF SOUTH AFRICA. *The International Archives of the Photogrammetry, Remote Sensing and Spatial Information Sciences*, *XLIII-B3-2020*, 1477–1482. https://doi.org/10.5194/isprs-archives-XLIII-B3-2020-1477-2020.

Müller, J., Moritz, W., Nörthemann, K., & Bienge, J.-E. (2015). Innovative Forest Fire Early Warning System: *Thünen-Institute of Forest Ecosystems, Alfred-Möller-Strasse 1, 16225 Eberswalde, Germany*, 1.

Naderpour, M., Rizeei, H. M., Khakzad, N., & Pradhan, B. (2019). Forest fire induced Natech risk assessment: A survey of geospatial technologies. *Reliability Engineering & System Safety*, *191*, 106558. https://doi.org/10.1016/j.ress.2019.106558.

NASA, J. (2020). *NASADEM Merged DEM Global 1 arc second V001*. *NASA EOSDIS Land Processes DAAC* [Map]. https://doi.org/10.5067/MEaSUREs/NASADEM/NASADEM_HGT.001.

Neary, D. G., & Leonard, J. M. (2020). Effects of Fire on Grassland Soils and Water: A Review. In *Grasses and Grassland Aspects*. IntechOpen. https://doi.org/10.5772/intechopen.90747.

Nelson Jr, R. M. (2000). Prediction of diurnal change in 10-h fuel stick moisture content. *Canadian Journal of Forest Research*, *30*(7), 1071–1087. https://doi.org/10.1139/x00-032.

Nhongo, E. J. S., Fontana, D. C., Guasselli, L. A., & Bremm, C. (2019). Probabilistic modelling of wildfire occurrence based on logistic regression, Niassa Reserve, Mozambique. *Geomatics, Natural Hazards and Risk*, *10*(1), 1772–1792. https://doi.org/10.1080/19475705.2019.1615559.

Nolan, R. H., Resco de Dios, V., Boer, M. M., Caccamo, G., Goulden, M. L., & Bradstock, R. A. (2016). Predicting dead fine fuel moisture at regional scales using vapour pressure deficit from MODIS and gridded weather data. *Remote Sensing of Environment*, *174*, 100–108. https://doi.org/10.1016/j.rse.2015.12.010.

Nunes, A. N., Lourenço, L., & Meira, A. C. C. (2016). Exploring spatial patterns and drivers of forest fires in Portugal (1980–2014). *Science of The Total Environment*, *573*, 1190–1202. https://doi.org/10.1016/j.scitotenv.2016.03.121.

Ochsner, T. E., Cosh, M. H., Cuenca, R. H., Dorigo, W. A., Draper, C. S., Hagimoto, Y., Kerr, Y. H., Larson, K. M., Njoku, E. G., Small, E. E., & Zreda, M. (2013). State of the Art in Large-Scale Soil Moisture Monitoring. *Soil Science Society of America Journal*, *77*(6), 1888–1919. https://doi.org/10.2136/sssaj2013.03.0093.

Oliva, P., & Schroeder, W. (2015). Assessment of VIIRS 375m active fire detection product for direct burned area mapping. *Remote Sensing of Environment*, *160*, 144–155. https://doi.org/10.1016/j.rse.2015.01.010.

Opitz, T., Bonneu, F., & Gabriel, E. (2020). Point-process based Bayesian modeling of space–time structures of forest fire occurrences in Mediterranean France. *Spatial Statistics*, *40*, 100429. https://doi.org/10.1016/j.spasta.2020.100429.

Ottmar, R. D., Sandberg, D. V., Riccardi, C. L., & Prichard, S. J. (2007). An overview of the Fuel Characteristic Classification System—Quantifying, classifying, and creating fuelbeds for resource planningThis article is one of a selection of papers published in the Special Forum on the Fuel Characteristic Classification System. *Canadian Journal of Forest Research*, *37*(12), 2383–2393. https://doi.org/10.1139/X07-077.

Palmer, T. N., Shutts, G. J., Hagedorn, R., Doblas-Reyes, F. J., Jung, T., & Leutbecher, M. (2005). Representing Model Uncertainty in Weather and Climate Prediction. *Annual Review of Earth and Planetary Sciences*, *33*(1), 163–193. https://doi.org/10.1146/annurev.earth.33.092203.122552.

Parente, J., Amraoui, M., Menezes, I., & Pereira, M. G. (2019). Drought in Portugal: Current regime, comparison of indices and impacts on extreme wildfires. *Science of The Total Environment*, *685*, 150–173. https://doi.org/10.1016/j.scitotenv.2019.05.298.

Parisien, M.-A., Miller, C., Ager, A. A., & Finney, M. A. (2010). Use of artificial landscapes to isolate controls on burn probability. *Landscape Ecology*, *25*(1), 79–93. https://doi.org/10.1007/s10980-009-9398-9.

Parks, S. A., Dillon, G. K., & Miller, C. (2014). A New Metric for Quantifying Burn Severity: The Relativized Burn Ratio. *Remote Sensing*, *6*(3), Article 3. https://doi.org/10.3390/rs6031827.

Parson, A., Robichaud, P. R., Lewis, S. A., Napper, C., & Clark, J. T. (2010). Field guide for mapping post-fire soil burn severity. *Gen. Tech. Rep. RMRS-GTR-243. Fort Collins, CO: U.S. Department of Agriculture, Forest Service, Rocky Mountain Research Station. 49 p.*, *243*. https://doi.org/10.2737/RMRS-GTR-243.

Peng, C.-Y. J., Lee, K. L., & Ingersoll, G. M. (2002). An Introduction to Logistic Regression Analysis and Reporting. *The Journal of Educational Research*, *96*(1), 3–14. https://doi.org/10.1080/00220670209598786.

Pepe, M., & Parente, C. (2018). Burned area recognition by change detection analysis using images derived from Sentinel-2 satellite: The case study of Sorrento Peninsula, Italy. *Journal of Applied Engineering Science*, *16*(2), 225–232. https://doi.org/10.5937/jaes16-17249.

Pereira, J. M. C. (2003). Remote sensing of burned areas in tropical savannas. *International Journal of Wildland Fire*, *12*(4), 259. https://doi.org/10.1071/WF03028.

Pereira, M. G., Parente, J., Amraoui, M., Oliveira, A., & Fernandes, P. M. (2020). 3—The role of weather and climate conditions on extreme wildfires. In F. Tedim, V. Leone, & T. K. McGee (Eds.), *Extreme Wildfire Events and Disasters* (pp. 55–72). Elsevier. https://doi.org/10.1016/B978-0-12-815721-3.00003-5.

Pereira, P., Bogunovic, I., Zhao, W., & Barcelo, D. (2021). Short-term effect of wildfires and prescribed fires on ecosystem services. *Current Opinion in Environmental Science & Health*, *22*, 100266. https://doi.org/10.1016/j.coesh.2021.100266.

Pettinari, M. L., & Chuvieco, E. (2020). Fire Danger Observed from Space. *Surveys in Geophysics*, *41*(6), 1437–1459. https://doi.org/10.1007/s10712-020-09610-8.

Pew, K. L., & Larsen, C. P. S. (2001). GIS analysis of spatial and temporal patterns of human-caused wildfires in the temperate rain forest of Vancouver Island, Canada. *Forest Ecology and Management*, *140*(1), 1–18.

Picotte, J. J. (2020). Development of a New Open-Source Tool to Map Burned Area and Burn Severity. In *In: Hood, Sharon; Drury, Stacy; Steelman, Toddi; Steffens, Ron, tech. Eds. The fire continuum—Preparing for the future of wildland fire: Proceedings of the Fire Continuum Conference. 21-24 May 2018, Missoula, MT. Proc. RMRS-P-78. Fort Collins, CO* (pp. 182–195). U.S. Department of Agriculture, Forest Service, Rocky Mountain Research Station.

Piles, M., Sánchez, N., Vall-llossera, M., Camps, A., Martínez-Fernández, J., Martínez, J., & González-Gambau, V. (2014). A Downscaling Approach for SMOS Land Observations: Evaluation of High-Resolution Soil Moisture Maps Over the Iberian Peninsula. *IEEE Journal of Selected Topics in Applied Earth Observations and Remote Sensing*, *7*(9), 3845–3857. https://doi.org/10.1109/JSTARS.2014.2325398.

Pinty, B., & Verstraete, M. M. (1992). GEMI: A non-linear index to monitor global vegetation from satellites. *Vegetatio*, *101*(1), 15–20. https://doi.org/10.1007/BF00031911.

Probst, P., & Boulesteix, A.-L. (2017). *To tune or not to tune the number of trees in random forest?* (arXiv:1705.05654). arXiv. https://doi.org/10.48550/arXiv.1705.05654.

Probst, P., Wright, M., & Boulesteix, A.-L. (2019). Hyperparameters and Tuning Strategies for Random Forest. *WIREs Data Mining and Knowledge Discovery*, *9*(3). https://doi.org/10.1002/widm.1301.

Pulvirenti, L., Squicciarino, G., Fiori, E., Fiorucci, P., Ferraris, L., Negro, D., Gollini, A., Severino, M., & Puca, S. (2020). An Automatic Processing Chain for Near Real-Time

Mapping of Burned Forest Areas Using Sentinel-2 Data. *Remote Sensing*, *12*(4), 674. https://doi.org/10.3390/rs12040674.

Qi, J., Chehbouni, A., Huete, A. R., Kerr, Y. H., & Sorooshian, S. (1994). A modified soil adjusted vegetation index. *Remote Sensing of Environment*, *48*(2), 119–126. https://doi.org/10.1016/0034-4257(94)90134-1

Quan, X., He, B., Yebra, M., Yin, C., Liao, Z., & Li, X. (2017). Retrieval of forest fuel moisture content using a coupled radiative transfer model. *Environmental Modelling & Software*, *95*, 290–302. https://doi.org/10.1016/j.envsoft.2017.06.006.

Quintiere, J. G. (2006). *Fundamentals of fire phenomena*. Wiley & Sons. https://scholar.google.com/scholar_lookup?title=Fundamentals%20of%20Fire%20Phenomena&author=J.G.%20Quintiere&publication_year=2006.

Radeloff, V. C., Helmers, D. P., Kramer, H. A., Mockrin, M. H., Alexandre, P. M., Bar-Massada, A., Butsic, V., Hawbaker, T. J., Martinuzzi, S., Syphard, A. D., & Stewart, S. I. (2018). Rapid growth of the US wildland-urban interface raises wildfire risk. *Proceedings of the National Academy of Sciences of the United States of America*, *115*(13), 3314–3319. https://doi.org/10.1073/pnas.1718850115.

Raiesi, F., & Pejman, M. (2021). Assessment of post-wildfire soil quality and its recovery in semi-arid upland rangelands in Central Iran through selecting the minimum data set and quantitative soil quality index. *CATENA*, *201*, 105202. https://doi.org/10.1016/j.catena.2021.105202.

Rakhmatulina, E., Stephens, S., & Thompson, S. (2021). Soil moisture influences on Sierra Nevada dead fuel moisture content and fire risks. *Forest Ecology and Management*, *496*, 119379. https://doi.org/10.1016/j.foreco.2021.119379.

Rao, K., Williams, A. P., Flefil, J. F., & Konings, A. G. (2020). SAR-enhanced mapping of live fuel moisture content. *Remote Sensing of Environment*, *245*, 111797. https://doi.org/10.1016/j.rse.2020.111797.

Rau, B. M., Chambers, J. C., Blank, R. R., & Johnson, D. W. (2008). Prescribed Fire, Soil, and Plants: Burn Effects and Interactions in the Central Great Basin. *Rangeland Ecology & Management*, *61*(2), 169–181. https://doi.org/10.2111/07-037.1.

Raviv, O., Zemah-Shamir, S., Izhaki, I., & Lotan, A. (2021). The effect of wildfire and land-cover changes on the economic value of ecosystem services in Mount Carmel Biosphere

Reserve, Israel. *Ecosystem Services*, *49*, 101291. https://doi.org/10.1016/j.ecoser.2021.101291.

Ribeiro, N., Ruecker, G., Govender, N., Macandza, V., Pais, A., Machava, D., Chauque, A., Lisboa, S. N., & Bandeira, R. (2019). The influence of fire frequency on the structure and botanical composition of savanna ecosystems. *Ecology and Evolution*, *9*(14), 8253–8264. https://doi.org/10.1002/ece3.5400.

Rodrigues, M., de la Riva, J., & Fotheringham, S. (2014). Modeling the spatial variation of the explanatory factors of human-caused wildfires in Spain using geographically weighted logistic regression. *Applied Geography*, *48*, 52–63. https://doi.org/10.1016/j.apgeog.2014.01.011

Romps, D. M., Seeley, J. T., Vollaro, D., & Molinari, J. (2014). Projected increase in lightning strikes in the United States due to global warming. *Science*, *346*(6211), 851–854. https://doi.org/10.1126/science.1259100.

Rothermel, R. C. (1972). A mathematical model for predicting fire spread in wildland fuels. *Res. Pap. INT-115. Ogden, UT: U.S. Department of Agriculture, Intermountain Forest and Range Experiment Station. 40 p., 115*. http://www.fs.usda.gov/treesearch/pubs/32533.

Roznik, M., Brock Porth, C., Porth, L., Boyd, M., & Roznik, K. (2019). Improving agricultural microinsurance by applying universal kriging and generalised additive models for interpolation of mean daily temperature. *The Geneva Papers on Risk and Insurance - Issues and Practice*, *44*(3), 446–480. https://doi.org/10.1057/s41288-019-00127-9

Ruffault, J., Martin-StPaul, N., Pimont, F., & Dupuy, J.-L. (2018). How well do meteorological drought indices predict live fuel moisture content (LFMC)? An assessment for wildfire research and operations in Mediterranean ecosystems. *Agricultural and Forest Meteorology*, *262*, 391–401. https://doi.org/10.1016/j.agrformet.2018.07.031.

Running, S. W., Nemani, R. R., Townshend, J. R. G., & Baldocchi, D. D. (2009). Next-Generation Terrestrial Carbon Monitoring. In *Carbon Sequestration and Its Role in the Global Carbon Cycle* (pp. 49–69). American Geophysical Union (AGU). https://doi.org/10.1029/2006GM000526.

Sá, A. C. L., Benali, A., Fernandes, P. M., Pinto, R. M. S., Trigo, R. M., Salis, M., Russo, A., Jerez, S., Soares, P. M. M., Schroeder, W., & Pereira, J. M. C. (2017). Evaluating fire growth simulations using satellite active fire data. *Remote Sensing of Environment*, *190*, 302–317. https://doi.org/10.1016/j.rse.2016.12.023.

Saefuddin, A., Setiabudi, N. A., & Fitrianto, A. (2012). On comparison between logistic regression and geographically weighted logistic regression: With application to Indonesian poverty data. *World Applied Sciences Journal*, *19*(2), 205–210. Scopus. https://doi.org/10.5829/idosi.wasj.2012.19.02.528.

Salvador, R., Piñol, J., Tarantola, S., & Pla, E. (2001). Global sensitivity analysis and scale effects of a fire propagation model used over Mediterranean shrublands. *Ecological Modelling*, *136*(2), 175–189. https://doi.org/10.1016/S0304-3800(00)00419-1.

Samran, S., Woodard, P. M., & Rothwell, R. L. (1995). The Effect of Soil Water on Ground Fuel Availability. *Forest Science*, *41*(2), 255–267. https://doi.org/10.1093/forestscience/41.2.255.

Sánchez-Ruiz, S., Piles, M., Sánchez, N., Martínez-Fernández, J., Vall-llossera, M., & Camps, A. (2014). Combining SMOS with visible and near/shortwave/thermal infrared satellite data for high resolution soil moisture estimates. *Journal of Hydrology*, *516*, 273–283. https://doi.org/10.1016/j.jhydrol.2013.12.047

Santos, E. E. dos, Sena, N. C., Balestrin, D., Fernandes Filho, E. I., Costa, L. M. da, & Zeferino, L. B. (2020). Prediction of Burned Areas Using the Random Forest Classifier in the Minas Gerais State. *Floresta e Ambiente*, *27*. https://doi.org/10.1590/2179-8087.011518

Santos, F. L. M., Libonati, R., Peres, L. F., Pereira, A. A., Narcizo, L. C., Rodrigues, J. A., Oom, D., Pereira, J. M. C., Schroeder, W., & Setzer, A. W. (2020). Assessing VIIRS capabilities to improve burned area mapping over the Brazilian Cerrado. *International Journal of Remote Sensing*, *41*(21), 8300–8327. https://doi.org/10.1080/01431161.2020.1771791.

Saura-Mas, S., & Lloret, F. (2007). Leaf and Shoot Water Content and Leaf Dry Matter Content of Mediterranean Woody Species with Different Post-fire Regenerative Strategies. *Annals of Botany*, *99*(3), 545–554. https://doi.org/10.1093/aob/mcl284.

Scasta, J. D., Weir, J. R., & Stambaugh, M. C. (2016). Droughts and Wildfires in Western U.S. Rangelands. *Rangelands*, *38*(4), 197–203. https://doi.org/10.1016/j.rala.2016.06.003.

Schroeder, W., Oliva, P., Giglio, L., & Csiszar, I. A. (2014). The New VIIRS 375m active fire detection data product: Algorithm description and initial assessment. *Remote Sensing of Environment, 143*, 85–96. https://doi.org/10.1016/j.rse.2013.12.008.

Shaffer, L. J. (2010). Indigenous Fire Use to Manage Savanna Landscapes in Southern Mozambique. *Fire Ecology*, *6*(2), Article 2. https://doi.org/10.4996/fireecology.0602043.

Shahdeo, A., Shahdeo, A., & Reddy, P. S. (2020). Wildfire Prediction and Detection using Random Forest and Different Color Models. *International Research Journal of Engineering and Technology*, *07*(06), 7326–7332.

Shang, C., Wulder, M. A., Coops, N. C., White, J. C., & Hermosilla, T. (2020). Spatially-Explicit Prediction of Wildfire Burn Probability Using Remotely-Sensed and Ancillary Data. *Canadian Journal of Remote Sensing*, *46*(3), 313–329. https://doi.org/10.1080/07038992.2020.1788385.

Sharma, A., Sohi, B. S., & Chandra, S. (2019). SN Based Forest Fire Detection and Early Warning System. *International Journal of Innovative Technology and Exploring Engineering*, *8*(9), 209–214. https://doi.org/10.35940/ijitee.H6733.078919

Sharma, S., & Dhakal, K. (2021). Boots on the Ground and Eyes in the Sky: A Perspective on Estimating Fire Danger from Soil Moisture Content. *Fire*, *4*(3), Article 3. https://doi.org/10.3390/fire4030045.

Sharma, S., & Pant, H. (2017). Vulnerability of Indian Central Himalayan forests to fire in a warming climate and a participatory preparedness approach based on modern tools. *Current Science*, *112*(10), 2100–2105.

Shekede, M. D., Mupandira, I., & Gwitira, I. (2021). Spatio-temporal clustering of active wildfire pixels over a 19-year period in a southern African savanna ecosystem of Zimbabwe. *South African Geographical Journal*, *103*(3), 283–302. https://doi.org/10.1080/03736245.2020.1786442.

Shoshany, M., & Karnibad, L. (2011). Mapping shrubland biomass along Mediterranean climatic gradients: The synergy of rainfall-based and NDVI-based models. *International Journal of Remote Sensing*, *32*(24), 9497–9508. https://doi.org/10.1080/01431161.2011.562255

Slijepcevic, A., Anderson, W. R., Matthews, S., & Anderson, D. H. (2015). Evaluating models to predict daily fine fuel moisture content in eucalypt forest. *Forest Ecology and Management*, *335*, 261–269. https://doi.org/10.1016/j.foreco.2014.09.040.

Smit, I. P. J., Asner, G. P., Govender, N., Kennedy-Bowdoin, T., Knapp, D. E., & Jacobson, J. (2010). Effects of fire on woody vegetation structure in African savanna. *Ecological Applications*, *20*(7), 1865–1875.

Snyman, H. A. (2015a). Short-Term Responses of Southern African Semi-Arid Rangelands to Fire: A Review of Impact on Plants. *Arid Land Research and Management*, *29*(2), 237–254. https://doi.org/10.1080/15324982.2014.960625

Snyman, H. A. (2015b). Short-Term Responses of Southern African Semi-Arid Rangelands to Fire: A Review of Impact on Soils. *Arid Land Research and Management*, *29*(2), 222–236. https://doi.org/10.1080/15324982.2014.944244.

Srivas, T., de Callafon, R. A., Crawl, D., & Altintas, I. (2017). Data Assimilation of Wildfires with Fuel Adjustment Factors in farsite using Ensemble Kalman Filtering * *This work is funded by NSF 1331615 under CI, Information Technology Research and SEES Hazards programs. *Procedia Computer Science*, *108*, 1572–1581. https://doi.org/10.1016/j.procs.2017.05.197.

Statistics Botswana. (2018a). *Botswana Demographic Survey Report 2017* (pp. 12–14). Stastistics Botswana. https://www.statsbots.org.bw/sites/default/files/publications/Botswana%20Demographic%20Survey%20Report%202017.pdf

Statistics Botswana. (2018b). *Botswana Environment Statistics Natural Disasters Digest 2017*. Statistics Botswana, Gaborone, Botswana. https://www.statsbots.org.bw/sites/default/files/publications/Botswana%20Environment%20Natural%20Disaster%20Digest_2017.pdf.

Stavi, I. (2019). Wildfires in Grasslands and Shrublands: A Review of Impacts on Vegetation, Soil, Hydrology, and Geomorphology. *Water*, *11*(5), 1042. https://doi.org/10.3390/w11051042.

Stavi, I., Barkai, D., Knoll, Y. M., Glion, H. A., Katra, I., Brook, A., & Zaady, E. (2017). Fire impact on soil-water repellency and functioning of semi-arid croplands and rangelands: Implications for prescribed burnings and wildfires. *Geomorphology*, *280*, 67–75. https://doi.org/10.1016/j.geomorph.2016.12.015

Stevens-Rumann, C. S., Hudak, A. T., Morgan, P., Arnold, A., & Strand, E. K. (2020). Fuel Dynamics Following Wildfire in US Northern Rockies Forests. *Frontiers in Forests and Global Change*, *3*, 51. https://doi.org/10.3389/ffgc.2020.00051.

Stratton, R. D. (2006). Guidance on spatial wildland fire analysis: Models, tools, and techniques. *Gen. Tech. Rep. RMRS-GTR-183. Fort Collins, CO: U.S. Department of Agriculture, Forest Service, Rocky Mountain Research Station. 15 p., 183*. https://doi.org/10.2737/RMRS-GTR-183.

Su, Z., Hu, H., Wang, G., Ma, Y., Yang, X., & Guo, F. (2018). Using GIS and Random Forests to identify fire drivers in a forest city, Yichun, China. *Geomatics, Natural Hazards and Risk*, *9*(1), 1207–1229. https://doi.org/10.1080/19475705.2018.1505667.

Sungmin, O., Hou, X., & Orth, R. (2020). Observational evidence of wildfire-promoting soil moisture anomalies. *Scientific Reports*, *10*(1), 11008. https://doi.org/10.1038/s41598-020-67530-4.

Swinnen, E., & Toté, C. (2022). *Algorithm Theoretical Basis Document Normalized Difference Vegetation Index (NDVI) Col-lection 300m Version 2*. Copernicus Global Land Operations. https://land.copernicus.eu/global/sites/cgls.vito.be/files/products/CGLOPS1_ATBD_NDVI300m-V2_I1.20.pdf.

Swinnen, E., Toté, C., & Van Hoolst, R. (2021a). *Algorithm Theoretical Basis Document Dry Matter Productivity (DMP) Gross Dry Matter Productivity (GDMP) Collection 300 M Version 1.1 Issue 1.10*. Copernicus Global Land Operations "Vegetation and Energy" "CGLOPS-1" Framework Service Contract. https://land.copernicus.eu/global/sites/cgls.vito.be/files/products/CGLOPS1_ATBD_DMP300m-V1.1_I1.10.pdf.

Swinnen, E., Toté, C., & Van Hoolst, R. (2021b). *Quality Assessment Report, Dry Matter Productivity (DMP) Collection 300m, Version 1.1*. Copernicus Global Land Operations "Vegetation and Energy" "CGLOPS-1" Framework Service Contract. https://land.copernicus.eu/global/sites/cgls.vito.be/files/products/CGLOPS1_QAR_S3_DMP300m_V1.1_I1.00.pdf

Tacheba, B., Segosebe, E., Vanderpost, C., & Sebego, R. (2009). Assessing the impacts of fire on the vegetation resources that are available to the local communities of the seasonal wetlands of the Okavango, Botswana, in the context of different land uses and key government policies. *African Journal of Ecology*, *47*, 71–77. https://doi.org/10.1111/j.1365-2028.2008.01052.x.

Tehrany, M. S., Jones, S., Shabani, F., Martínez-Álvarez, F., & Tien Bui, D. (2019). A novel ensemble modeling approach for the spatial prediction of tropical forest fire susceptibility using LogitBoost machine learning classifier and multi-source geospatial data. *Theoretical and Applied Climatology*, *137*(1–2), 637–653. https://doi.org/10.1007/s00704-018-2628-9.

Teodoro, A., & Amaral, A. (2019). A Statistical and Spatial Analysis of Portuguese Forest Fires in Summer 2016 Considering Landsat 8 and Sentinel 2A Data. *Environments*, *6*(3). https://doi.org/10.3390/environments6030036.

Thomas, H. S. (2006). Rangeland Wildfires Can Be Good or Bad. *Rangelands*, *28*(2), 12–16. https://doi.org/10.2111/1551-501X(2006)28.2[12:RWCBGO]2.0.CO;2.

Tihay-Felicelli, V., Santoni, P. A., Gerandi, G., & Barboni, T. (2017). Smoke emissions due to burning of green waste in the Mediterranean area: Influence of fuel moisture content and fuel mass. *Atmospheric Environment*, *159*, 92–106. https://doi.org/10.1016/j.atmosenv.2017.04.002.

Tonini, M., D'Andrea, M., Biondi, G., Degli Esposti, S., Trucchia, A., & Fiorucci, P. (2020). A Machine Learning-Based Approach for Wildfire Susceptibility Mapping. The Case Study of the Liguria Region in Italy. *Geosciences*, *10*(3), Article 3. https://doi.org/10.3390/geosciences10030105.

Tran, B., Tanase, M., Bennett, L., & Aponte, C. (2018). Evaluation of Spectral Indices for Assessing Fire Severity in Australian Temperate Forests. *Remote Sensing*, *10*(11), 1680. https://doi.org/10.3390/rs10111680

Tucker, C. J. (1979). Red and photographic infrared linear combinations for monitoring vegetation. *Remote Sensing of Environment*, *8*(2), 127–150. https://doi.org/10.1016/0034-4257(79)90013-0.

Turco, M., von Hardenberg, J., AghaKouchak, A., Llasat, M. C., Provenzale, A., & Trigo, R. M. (2017). On the key role of droughts in the dynamics of summer fires in Mediterranean Europe. *Scientific Reports*, *7*(1), 1–10.

Turner, M. G. (2010). Disturbance and landscape dynamics in a changing world. *Ecology*, *91*(10), 2833–2849. https://doi.org/10.1890/10-0097.1.

Urbanski, S. (2014). Wildland fire emissions, carbon, and climate: Emission factors. *Forest Ecology and Management. 317: 51-60.*, 51–60. https://doi.org/10.1016/j.foreco.2013.05.045

USGS. (2018). *QGIS Fire Mapping Tool (FMT) user guide version 1*. MTBS. https://www.mtbs.gov/qgis-fire-mapping-tool.

USGS. (2022). *Wildland Fire Science*. U.S. Geological Survey. https://www.usgs.gov/special-topics/wildland-fire-science.

Valdez, M. C., Chang, K.-T., Chen, C.-F., Chiang, S.-H., & Santos, J. L. (2017). Modelling the spatial variability of wildfire susceptibility in Honduras using remote sensing and geographical information systems. *Geomatics, Natural Hazards and Risk*, *8*(2), 876–892. https://doi.org/10.1080/19475705.2016.1278404

van Etten, E. J. B. (2010). Fire in Rangelands and its Role in Management. In *Range and Animal Sciences and Resources Management* (Vol. 2, p. 9).

Van Wagner, C. E., & Pickett, T. L. (1985). *Equations and FORTRAN program for the Canadian Forest Fire Weather Index System* (Vol. 33). http://cfs.nrcan.gc.ca/publications?id=19973.

Veraverbeke, S., Lhermitte, S., Verstraeten, W. W., & Goossens, R. (2011). Evaluation of pre/post-fire differenced spectral indices for assessing burn severity in a Mediterranean environment with Landsat Thematic Mapper. *International Journal of Remote Sensing*, *32*(12), 3521–3537. https://doi.org/10.1080/01431161003752430.

Verhegghen, A., Eva, H., Ceccherini, G., Achard, F., Gond, V., Gourlet-Fleury, S., & Cerutti, P. O. (2016). The Potential of Sentinel Satellites for Burnt Area Mapping and Monitoring in the Congo Basin Forests. *Remote Sensing*, *8*(12), Article 12. https://doi.org/10.3390/rs8120986.

Vicente-Serrano, S. M., Quiring, S. M., Peña-Gallardo, M., Yuan, S., & Domínguez-Castro, F. (2020). A review of environmental droughts: Increased risk under global warming? *Earth-Science Reviews*, *201*, 102953. https://doi.org/10.1016/j.earscirev.2019.102953.

Viegas, D. X., Piñol, J., Viegas, M. T., & Ogaya, R. (2001). Estimating live fine fuels moisture content using meteorologically-based indices. *International Journal of Wildland Fire*, *10*(2), 223–240. https://doi.org/10.1071/wf01022.

Vinodkumar, & Dharssi, I. (2019). Evaluation and calibration of a high-resolution soil moisture product for wildfire prediction and management. *Agricultural and Forest Meteorology*, *264*, 27–39. https://doi.org/10.1016/j.agrformet.2018.09.012

Vinodkumar, V., Dharssi, I., Yebra, M., & Fox-Hughes, P. (2021). Continental-scale prediction of live fuel moisture content using soil moisture information. *Agricultural and Forest Meteorology*, *307*, 108503. https://doi.org/10.1016/j.agrformet.2021.108503.

Vlassova, L., Pérez-Cabello, F., Mimbrero, M. R., Llovería, R. M., & García-Martín, A. (2014). Analysis of the Relationship between Land Surface Temperature and Wildfire Severity in

a Series of Landsat Images. *Remote Sensing*, *6*(7), Article 7. https://doi.org/10.3390/rs6076136.

Wan, Z. (2013). *Collection-6 MODIS Land Surface Temperature Products Users' Guide*. ERI, University of California, Santa Barbara. https://lpdaac.usgs.gov/documents/118/MOD11_User_Guide_V6.pdf

Wan, Z., Hook, S., & Hulley, G. (2021). *MODIS/Terra Land Surface Temperature/Emissivity Daily L3 Global 1km SIN Grid V061 [Data set]* [Map]. NASA EOSDIS Land Processes DAAC. https://doi.org/10.5067/MODIS/MOD11A1.061.

Wang, J., & Zhang, X. (2020). Investigation of wildfire impacts on land surface phenology from MODIS time series in the western US forests. *ISPRS Journal of Photogrammetry and Remote Sensing*, *159*, 281–295. https://doi.org/10.1016/j.isprsjprs.2019.11.027

Wang, M., He, G., Zhang, Z., Wang, G., Wang, Z., Yin, R., Cui, S., Wu, Z., & Cao, X. (2019). A radiance-based split-window algorithm for land surface temperature retrieval: Theory and application to MODIS data. *International Journal of Applied Earth Observation and Geoinformation*, *76*, 204–217. https://doi.org/10.1016/j.jag.2018.11.015.

Weisshaupt, B. R., Jakes, P. J., Carroll, M. S., & Blatner, K. A. (2007). Northern Inland West Land/Homeowner Perceptions of Fire Risk and Responsibility in the Wildland-Urban Interface. *Human Ecology Review*, *14*(2), 177–187.

Williams, J., Albright, D., Hoffmann, A. A., Eritsov, A., Moore, P. F., Morais, J. C. M. de, Leonard, M., San Miguel-Ayanz, J., Xanthopoulos, G., & Lierop, P. van. (2011). Findings and implications from a coarse-scale global assessment of recent selected mega-fires. *Findings and Implications from a Coarse-Scale Global Assessment of Recent Selected Mega-Fires.*, 19.

Won, M. S., Koo, K. S., Lee, M. B., & Lee, S. Y. (2006). Fuel Type Classification and Fuel Loading in Central Interior, Korea: Uiseong-Gun. *In: Andrews, Patricia L.; Butler, Bret W., Comps. 2006. Fuels Management-How to Measure Success: Conference Proceedings. 28-30 March 2006; Portland, OR. Proceedings RMRS-P-41. Fort Collins, CO: U.S. Department of Agriculture, Forest Service, Rocky Mountain Research Station. p. 305-319*, *041*. http://www.fs.usda.gov/treesearch/pubs/25957.

Wragg, P. D., Mielke, T., & Tilman, D. (2018). Forbs, grasses, and grassland fire behaviour. *Journal of Ecology*, *106*(5), 1983–2001. https://doi.org/10.1111/1365-2745.12980

Xie, C., Zhang, X., Zhuang, L., Zhu, R., & Guo, J. (2022). Analysis of surface temperature variation of lakes in China using MODIS land surface temperature data. *Scientific Reports*, *12*(1), Article 1. https://doi.org/10.1038/s41598-022-06363-9.

Yang, H. (2021, April 23). *Land Surface Temperature Anomalies and Fire Occurrence*. ArcGIS StoryMaps. https://storymaps.arcgis.com/stories/06a6acff8a544fb187b2cb4ce262e614

Yang, S. (2021). *The Relationship between Land Surface Temperature Anomalies and Fire Occurrence in Cariboo Region in 2017*. http://dx.doi.org/10.14288/1.0396751.

Yang, X., Yu, Y., Hu, H., & Sun, L. (2018). Moisture content estimation of forest litter based on remote sensing data. *Environmental Monitoring and Assessment*, *190*(7), 421. https://doi.org/10.1007/s10661-018-6792-2.

Yebra, M., Aguado, I., García, M., Nieto, H., Chuvieco, E., & Salas, J. (2007). Fuel moisture estimation for fire ignition mapping. In *Wildfire*.

Yebra, M., Chuvieco, E., & Riaño, D. (2008). Estimation of live fuel moisture content from MODIS images for fire risk assessment. *Agricultural and Forest Meteorology*, *148*(4), 523–536. https://doi.org/10.1016/j.agrformet.2007.12.005.

Yebra, M., Dennison, P. E., Chuvieco, E., Riaño, D., Zylstra, P., Hunt, E. R., Danson, F. M., Qi, Y., & Jurdao, S. (2013). A global review of remote sensing of live fuel moisture content for fire danger assessment: Moving towards operational products. *Remote Sensing of Environment*, *136*, 455–468. https://doi.org/10.1016/j.rse.2013.05.029.

Yebra, M., Quan, X., Riaño, D., Rozas Larraondo, P., van Dijk, A. I. J. M., & Cary, G. J. (2018). A fuel moisture content and flammability monitoring methodology for continental Australia based on optical remote sensing. *Remote Sensing of Environment*, *212*, 260–272. https://doi.org/10.1016/j.rse.2018.04.053.

Yool, S. (2009). Broad-Scale Monitoring of Live Fuel Moisture. *Geography Compass*, *3*(5), 1703–1716. https://doi.org/10.1111/j.1749-8198.2009.00267.x.

Yu, Y., Mao, J., Thornton, P. E., Notaro, M., Wullschleger, S. D., Shi, X., Hoffman, F. M., & Wang, Y. (2020). Quantifying the drivers and predictability of seasonal changes in African fire. *Nature Communications*, *11*(1), Article 1. https://doi.org/10.1038/s41467-020-16692-w.

Yu, Y., Mao, J., Wullschleger, S. D., Chen, A., Shi, X., Wang, Y., Hoffman, F. M., Zhang, Y., & Pierce, E. (2022). Machine learning–based observation-constrained projections reveal el-

evated global socioeconomic risks from wildfire. *Nature Communications*, *13*(1), Article 1. https://doi.org/10.1038/s41467-022-28853-0.

Zanaga, D., Van De Kerchove, R., De Keersmaecker, W., Souverijns, N., Brockmann, C., Quast, R., Wevers, J., Grosu, A., Paccini, A., Vergnaud, S., Cartus, O., Santoro, M., Fritz, S., Georgieva, I., Lesiv, M., Carter, S., Herold, M., Li, L., Tsendbazar, N.-E., … Arino, O. (2021). *ESA WorldCover 10 m 2020 v100* [Data set]. Zenodo. https://doi.org/10.5281/zenodo.5571936.

Zdeborová, L. (2017). New tool in the box. *Nature Physics*, *13*(5), 420–421. https://doi.org/10.1038/nphys4053.

Zeiler, M. D. (2012). ADADELTA: An Adaptive Learning Rate Method. *ArXiv:1212.5701 [Cs]*. http://arxiv.org/abs/1212.5701.

Zhang, Y., Lim, S., & Sharples, J. J. (2016). Modelling spatial patterns of wildfire occurrence in South-Eastern Australia. *Geomatics, Natural Hazards and Risk*, *7*(6), 1800–1815. https://doi.org/10.1080/19475705.2016.1155501

Zhang, Z., & He, G. (2013). Generation of Landsat surface temperature product for China, 2000–2010. *International Journal of Remote Sensing*, *34*(20), 7369–7375. https://doi.org/10.1080/01431161.2013.820368.

Zhao, L., Yebra, M., van Dijk, A. I. J. M., Cary, G. J., Matthews, S., & Sheridan, G. (2021). The influence of soil moisture on surface and sub-surface litter fuel moisture simulation at five Australian sites. *Agricultural and Forest Meteorology*, *298–299*, 108282. https://doi.org/10.1016/j.agrformet.2020.108282.

Zhu, L., Webb, G. I., Yebra, M., Scortechini, G., Miller, L., & Petitjean, F. (2021). Live fuel moisture content estimation from MODIS: A deep learning approach. *ISPRS Journal of Photogrammetry and Remote Sensing*, *179*, 81–91. https://doi.org/10.1016/j.isprsjprs.2021.07.010.

Zormpas, K., Vasilakos, C., Athanasis, N., Soulakellis, N., & Kalabokidis, K. (2017). Dead fuel moisture conetent estimation using remote sensing. *European Journal of Geography*, *8*(5), 17–32.

APPENDICES

Appendix 1: Multi-collinearity graph